Miia John

SEPARATION EFFICIENCIES OF FREEZE CRYSTALLIZATION IN WASTEWATER PURIFICATION

ACTA UNIVERSITATIS LAPPEENRANTAENSIS 906

Miia John

SEPARATION EFFICIENCIES OF FREEZE CRYSTALLIZATION IN WASTEWATER PURIFICATION

Dissertation for the degree of Doctor of Science (Technology) to be presented with due permission for public examination and criticism in the Auditorium 1316 at Lappeenranta-Lahti University of Technology LUT, Lappeenranta, Finland on the 25th of June, 2020, at noon.

Acta Universitatis
Lappeenrantaensis 906

Supervisors Docent Marjatta Louhi-Kultanen
LUT School of Engineering Science
Lappeenranta-Lahti University of Technology LUT
School of Chemical Engineering
Aalto University
Finland

Professor Satu-Pia Reinikainen
LUT School of Engineering Science
Lappeenranta-Lahti University of Technology LUT
Finland

Professor Antti Häkkinen
LUT School of Engineering Science
Lappeenranta-Lahti University of Technology LUT
Finland

Reviewers Professor Alison Lewis
Chemical Engineering Department
University of Cape Town
South Africa

Professor Jukka Tuhkuri
Department of Mechanical Engineering
Aalto University
Finland

Opponent Professor Alison Lewis
Chemical Engineering Department
University of Cape Town
South Africa

ISBN 978-952-335-515-6
ISBN 978-952-335-516-3 (PDF)
ISSN-L 1456-4491
ISSN 1456-4491

Lappeenranta-Lahti University of Technology LUT
LUT University Press 2020

Abstract

Miia John
Separation efficiencies of freeze crystallization in wastewater purification
Lappeenranta 2020
71 pages
Acta Universitatis Lappeenrantaensis 906
Diss. Lappeenranta-Lahti University of Technology LUT
ISBN 978-952-335-515-6, ISBN 978-952-335-516-3 (PDF), ISSN-L 1456-4491, ISSN 1456-4491

In a changing world, it is of paramount importance to ensure the sufficiency of clean water for all. Wastewater purification will face unprecedented challenges as a result of growing human population and accelerating industrialisation. Thus, novel methods and applications are needed to manage multifarious pollutants and increasing wastewater volumes. The new generation of the wastewater treatment should focus on developing techniques that allow efficient water and material reclamation for recycling and reuse.

The freeze crystallization method possesses the main features required for sustainable wastewater purification, i.e. the potential for the simultaneous separation of water (ice) and material, and the high separation efficiency of impurities of all kinds – energy efficiently without added chemicals. Freeze crystallization has previously been the subject of rather extensive research in various fields of application, i.e. the food industry, desalination, and wastewater purification. However, much of the research has been done on a laboratory scale and using model solutions, as the pioneering research interests have focused on the phenomenon of freeze separation and the theoretical models to explain them. Thus, real wastewaters have rarely been used for research, and the overall impurity removal efficiencies of freeze purification are still incompletely known.

The research of this thesis aimed to demonstrate the purification efficiencies of freeze crystallization in wastewater treatment by appraising the freezing conditions and the wastewater characteristics affecting the process performance. Freeze crystallization in the separation of impurities was studied through experiments based on convenient engineering practices and using wastewaters from various origins, i.e. a municipal wastewater treatment plant, landfill, peat production lands, and the mining industry. The experiments were implemented both in laboratories and on naturally frozen ice layers in wastewater basins. In addition, the design and functionality testing of a pilot-scale suspension freeze crystallizer was presented.

Based on the experiments, freeze crystallization was found to be a suitable purification method for all wastewaters tested. Highly efficient impurity removal, even close to 100%, was achieved with low ice growth rates in the freezing of municipal wastewater. The increased ice growth rate was found to decrease the separation efficiency. The decrease in separation efficiency was much stronger in more concentrated wastewater, even though no substantive differences in ice growth rates could be noticed between the wastewaters of different concentrations under the same freezing conditions. The exploration of ice

layers in wastewater basins showed separation efficiencies of 65-90%, which can be consider high under unpredictable water and weather conditions. The pilot-crystallizer achieved over 95% purification efficiencies determined by an extensive impurity analysis when landfill leachate was used in tests. These promising results of high efficiencies achievable by the freeze purification of wastewaters are an important motivator for further development of energy-efficient water treatment applications with an option for material recovery.

Keywords: freeze crystallization, freezing point depression, ice purity, impurity removal, landfill leachate, mine wastewater, municipal wastewater, natural freeze crystallization, purification efficiency, wastewater treatment

Acknowledgements

This work was carried out in the LUT School of Engineering Science at Lappeenranta-Lahti University of Technology LUT, Finland, between 2016 and 2019. The funding received from the Academy of Finland (WINICE project) and the Business Finland (The JÄPÄ project) is truly acknowledged. The grant given by the Research Foundation of Lappeenranta University of Technology is greatly appreciated.

Foremost, I would like to convey my deepest gratitude to my supervisors, Docent Marjatta Louhi-Kultanen, Professor Satu-Pia Reinikainen and Professor Antti Häkkinen, for their support and shared knowledge. I am grateful for the precious advice offered whenever most needed. I wish to give special thanks to my first supervisor Marjatta for the research idea and the opportunity to carry out this work.

I wish to thank Professor Alison Lewis and Professor Jukka Tuhkuri for reviewing the manuscript. I am pleased with the constructive comments that helped me to realign and deepen the different perspectives around the topic.

I would like to pay my regards to all the co-authors and co-workers on the freeze crystallization projects; Tuhin Choudhury, Roman Filimonov, Mehdi Hasan, Pentti Kujala, Emil Kurvinen, Aki Mikkola, Mika Mänttäri, Muhammad Saeed, Otto-Ville Sormunen and Mikko Suominen. It has been a privilege to work with a multidisciplinary team that owned such a dedication to the scientific research and shared a strong vision to see the common goal. I wish to thank especially Emil, not only for all the encouragement, but also for the positive attitude at work and the maintaining of good team spirit from day to day.

I am grateful to all the people at LUT's academic crew who supported me during this study. I would like to thank my current and former research group members, all colleagues and technical and support personnel for all the invaluable professional advice and help with laboratory set-ups. I wish to express my thanks to Peter Jones, Scott Semken and Tiina Väisänen for their efforts in the language revisions of the papers and this thesis. Especially I want to recognise the importance of the emotional intelligence and the social support provided by so many people. Thank you, Matti, Mikko, Paula, Teemu and many others for rational reassuring, every so often, when I was getting (nearly) nervous and overexcited.

At the end of the day, I wish to thank my great family, kinsfolk and old friends, who have encouraged me throughout the endeavours and struggles of my life. Without their support, this project would not have been succeeded either.

Miia John
May 2020
Lappeenranta, Finland

Dedicated to all human beings who feel eco-anxiety when flushing the toilet with potable water.

Contents

List of publications

This dissertation is based on the following papers. The publishers granted the right to include the papers in this dissertation.

I. John, M., Suominen, M., Kurvinen, E., Hasan, M., Sormunen, O.-V., Kujala, P., Mikkola, A. and Louhi-Kultanen, M. (2019). Separation efficiency and ice strength properties in simulated natural freezing of aqueous solutions. *Cold Regions Science and Technology*, 158, pp. 18-29.

II. John, M., Häkkinen, A. and Louhi-Kultanen, M. (2020). Purification efficiency of natural freeze crystallization for urban wastewaters. *Cold Regions Science and Technology*, 170, 102953.

III. John, M., Suominen, M., Sormunen, O.-V., Hasan, M., Kurvinen, E., Kujala, P., Mikkola, A. and Louhi-Kultanen, M. (2018). Purity and mechanical strength of naturally frozen ice in wastewater basins. *Water Research*, 145, pp. 418-428.

IV. John, M., Choudhury, T., Filimonov, R., Kurvinen, E., Saeed, M., Mikkola, A., Mänttäri, M. and Louhi-Kultanen, M. (2020). Impurity separation efficiency of multi-component wastewater in a pilot-scale freeze crystallizer. *Separation and Purification Technology*, 236, 116271.

Author's contribution

Miia John is the principal author and investigator in papers I–IV. The author has done most of the writing and corresponded with the journals about the submissions. The author planned the experiments, analysed the data and results, and conducted most of the experimental work in paper II. In papers I, III and IV, the experiments were planned, the experimental work conducted and the experimental data post-processed with co-authors.

Related publications

Hasan, M., Filimonov, R., John, M., Sorvari, J. and Louhi-Kultanen, M. (2018). Influence and CFD analysis of cooling air velocity on the purification of aqueous nickel sulfate solutions by freezing. *AIChE Journal*, 64, pp. 200–208.

Hasan, M., Rotich, N., John, M. and Louhi-Kultanen, M. (2017). Salt recovery from wastewater by air-cooled eutectic freeze crystallization. *Chemical Engineering Journal*, 326, pp. 192-200.

Kurvinen, E., John, M. and Mikkola, A. (2020). Measurement and evaluation of natural frequencies of bulk ice plate using Scanning Laser Doppler Vibrometer. *Measurement*, 150, 107091.

Nomenclature

C_i	impurity concentration in the ice	mg/L
C_w	impurity concentration in the water	mg/L
E	purification efficiency	%
G	linear ice growth rate	m/s
G_m	ice mass growth rate	kg/h
K	effective distribution coefficient	-
K_f	cryoscopic constant	K kg/mol
m	molality of the solution	mol/kg
t	time	s
v_{air}	air flow velocity	m/s
T	temperature	°C, K
ΔT	undercooling temperature	°C, K

Abbreviations

CFD	computational fluid dynamics
COD	chemical oxygen demand
EC	electrical conductivity
EFC	eutectic freeze crystallization
FC	freeze crystallization
FPD	freezing point depression
IC	inorganic carbon
TC	total carbon
TN	total nitrogen
TOC	total organic carbon

1 Introduction

1.1 Background

1.1.1 New direction in wastewater treatment

Wastewater treatment is closely connected with fresh water resources. The sustainable development of advanced water and wastewater treatment technologies is important in solving local water management problems as well as the global water crisis. The scarcity of fresh water or challenges in sanitation and adequate hygiene cannot be thought of as problems of merely the developing world and humanitarian work. Urbanization and increasing industrial activity due to the human population growth cause universal challenges for wastewater purification. Since the need for material production, food and goods is constantly increasing, the volumes of industrial wastewater, in addition to municipal wastewater, will be greater and the treatment plants larger. Therefore, the developing of advanced treatment technologies for water saving, recovery and recycling are of economic interest, especially in industrial processes. This has a direct impact on the energy consumption and cost of wastewater management and purification.

However, the main issue is not the huge volumes of wastewater alone. The composition of wastewaters makes the problem solving more complicated. Wastewaters originating from modern living are loaded with micro sized pollutants and plastics in addition to ordinary organic and inorganic matter. These small pollutants, called emerging contaminants, cannot be sufficiently separated from wastewater by conventional treatment processes and thus remain in the effluents. Over time, these pollutants become enriched in the aquatic ecosystems and cause harm to the health of flora, fauna and humans (Prasse et al., 2015; Rodriguez-Narvaez et al., 2017). Accordingly, universal health and environmental issues require more efficient wastewater treatment methods and technologies.

Instead of harmful impurities only, wastewaters may be considered to contain valuable materials like nutrients in municipal wastewater or salts and metals in industrial wastewater. Wastewaters should no longer be considered as an obligation to meet the legislative requirements of water purification but rather a source of water and valuable material. Such renewal of thinking has already started, as this objective is clearly stated in the World Water Assessment Programme by the 2030 Agenda for Sustainable Development of the United Nations (WWAP, 2017). This brings a fresh and interesting aspect to the development of water treatment technology, that is, material recovery from wastewater. Consequently, it is of environmental and economic interest to study and develop alternative wastewater treatment methods which can remove impurities from wastewater for the reclamation of the by-products desired.

1.1.2 Freeze purification

The new optimistic thinking about the prospects of wastewater treatment being in the recovery of wastewater as a raw material (or clean water) motivates also the research around the utilization of freeze crystallization (FC) in water purification (Randall et al., 2014; Hasan et al., 2017). The concept of a holistic wastewater treatment system implemented with freeze crystallization technology is illustrated in Figure 1.1. In freeze purification, pure ice crystals begin to form when an aqueous solution is cooled to its freezing point. Ice crystals are naturally intolerant to impurities and reject them. The impurities thus remain in the solution and the concentration of impurities increases, i.e. they form a concentrated solution called concentrate. After the clean ice and the concentrate are separated, the concentrate can be further processed e.g. by evaporative crystallization, and material can be reclaimed even from dilute wastewaters. A more sophistic separation process can be implemented with eutectic freeze crystallization (EFC) under eutectic conditions (temperature and concentration) for certain salt compounds. In this way, the ice and salt can be crystallized at the same time and then separated (Randall et al., 2011). Because FC can be used as a concentration method, freezing technology may enable sustainable selective material recovery in the future.

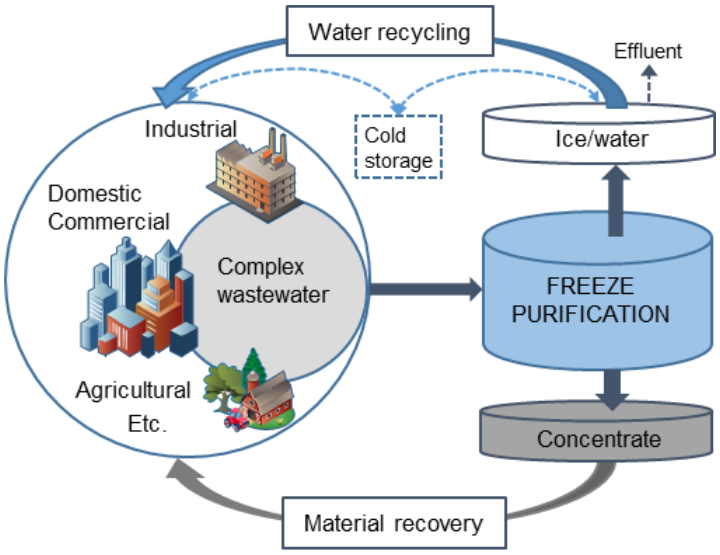

Figure 1.1: Conceptual freeze purification process enabling water and material reclamation.

For the most part, previous freeze crystallization studies have focused on other than wastewater purification applications, including the concentration of juices in the food industry or desalination of seawater for potable water production (Williams et al., 2015). Consequently, the main benefits of the freezing of aqueous solutions are well known. Compared with traditional treatment methods, freeze crystallization can be considered a sustainable and environmentally friendly method because the process does not need any pre-treatment in form of additive materials like chemicals (Lorain et al., 2001) or a

medium which will generate waste. The efficiencies of conventional purification methods are often limited by concentration, pH or another wastewater character. For instance, the high toxicity of wastewater may make the biological treatment difficult (Shirai et al. 1998). These factors have not been noticed to affect the performance of freeze crystallization.

Wastewater purification by freeze crystallization has not been extensively studied using real wastewaters but rather with model solutions or specific industrial waters or brines. In general, FC is considered an energy and cost-efficient method in addition to high efficiencies in the separation of impurities from solutions (Hasan and Louhi-Kultanen, 2015; Yin et al., 2017). This strongly motivates studies concerning the utilization of FC technology for wastewater purification since FC may be suitable for the treatment of wastewaters containing a very broad mixture of different impurities (Lorain et al., 2001). In terms of energy efficiency, the possibility for the exploitation of natural cooling energy in Arctic regions is a strong additional motivator for freeze crystallization studies (Zhang et al., 2011). In addition, studies have presented the possibility of utilizing produced ice for a cold heat storage system (Shirai et al., 1998).

Despite the prominent motivation and very promising results of previous studies, some challenges still hinder the development of application and thus also the utilization of freezing technology for wastewater treatment. This thesis assessed these challenges and aimed to find answers to important questions in implementing freezing technology.

1.2 **Research questions**

The main question of the thesis was: How efficiently can impurities be removed from wastewaters by freeze crystallization? The hypothesis was that high purification efficiencies can be achieved by freeze crystallization, but freezing conditions and the type of wastewater affect the degree of efficiency.

In general, wastewaters are rather complex mixtures of water and infinite quantities of different impurities dissolved and suspended, both organic and inorganic substances. Hence, the modelling of a freezing process (e.g. by solid-liquid phase equilibrium) or establishing theoretical and phenomenological interpretations based on the characteristics of a multicomponent composition is challenging. Therefore, it was of interests to investigate if the generally definable quality of wastewater affects the thermodynamics and kinetics of the freezing process, i.e. the ice growth. This was implemented in two different laboratory scale experiments. First, the separation efficiency and properties (structure and mechanical strength) of ice formed was studied by simulating the natural freezing of different model solutions. The second freezing study was carried out using municipal wastewater and landfill leachate in different concentrations in a winter simulator. The setup enabled the evaluation of separation performance and ice mass growth in different freezing conditions; the velocity and temperature of cooling air flow.

To the author's best knowledge, the wastewater treatment system based on natural freezing is not yet utilized on a full industrial scale. Therefore, an exploration was carried out in natural ice-covered water and wastewater environments, which were not initially designed for freeze purification, i.e. in a freshwater lake, peatlands and mining site basins (Figure 1.2). The study aimed to find out how efficiently wastewater can be treated by freeze separation in basins under natural weather conditions. Since the harvesting of ice is generally known to cause challenges in the utilization of natural freezing, the mechanical strength properties of the ice were investigated to understand better the forces needed for ice breaking.

Figure 1.2: Part of the experimental setup in open pit water basin in mining site.

In practical terms, the simple natural freezing technology in basins could be utilized (almost exclusively) in geographical regions with a sufficient number of freezing degree days per year. To expand the proof of concept to a practical application usable in wider areas, an energy source independent system needed to be developed. Such a prototype crystallizer (Figure 1.3) with an external cooling unit was designed within the project implemented at LUT University. The purification efficiency of the suspension freeze crystallizer and the suitability of the freeze separation method for multicomponent wastewater treatment were demonstrated using landfill leachates and extensive water quality analysis.

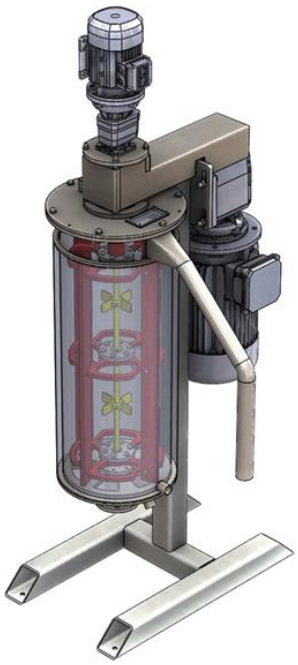

Figure 1.3: A prototype freeze crystallizer for wastewater purification. Figure modified from Figure 1 in *Publication IV*.

More detailed energy or economic evaluations of the freeze crystallization methods or applications were not carried out at this stage of the study. The fate of the concentrate formed due to freeze crystallization was not particularly considered during this study either. However, these would be highly interesting subjects for future research. The potential of freeze purification needed to be solved first, i.e. how effectively various contaminants can be separated from wastewater to produce (ice) water clean enough for water recycling and recovery or for discharge back to the water environment.

1.3 Outline of the thesis

This thesis comprises four international journal publications and consists of five chapters. The first chapter introduces the purpose and motivation for the research and gives an overview of freeze crystallization in wastewater treatment. It presents the universal state of wastewater treatment, demands for sustainable water use and challenges that purification technology will face in the future. Chapter 2 provides the theoretical background of ice crystallization and impurity separation by freezing and presents commonly used freeze crystallization methods. The chapter focuses more closely on natural freeze crystallization and suspension freeze crystallization.

Chapter 3 presents the experimental work conducted for this thesis in four rather different experimental setups and procedures. Three of the experiments employed natural freezing. Two of those experiments were conducted by simulated freezing, using model water in the first one and real wastewaters in the second. The third exploration was carried out under natural weather conditions in real wastewater basins. The fourth experiment represented the pilot freeze crystallizer developed for wastewater treatment. Analysed test results and a discussion are presented in chapter 4 and concluding remarks in chapter 5.

2 Freeze crystallization

The freezing of water, as simple it sounds, is a complicated and still rather unsolved natural phenomena. The theories for ice crystallization and particularly for impurity freeze separation are multifarious, as the research objectives ordinarily depend upon the discipline and the environment in question. In nature environments, in water systems such as lakes (Figure 2.1) and seas, and in the soil and air, freezing generally happens when the temperature drops below the freezing point of water. In the atmosphere, the freezing of water is of interest to meteorologists and climate scientists who study and model the weather. Similarly, the water frozen in permafrost and glaciers has motivated explorations of geoscientists – just to name some examples in natural sciences. In the field of engineering sciences, the areas of interest are as versatile. For instance, the mechanical properties of lake or sea ice are an important factor in ice breaker design in marine technology, and ice adhesion studies in the frost protection of windmill blades in energy production technology (Ryzhkin and Petrenko, 1997). An application where the ice growth and ice characteristics studies have great importance is freeze crystallization technology in wastewater purification.

Figure 2.1: On the ice cover of Lake Saimaa, Finland. Scientists at work or ice fishing?

2.1 Ice nucleation and crystallization

In freeze purification, it is important to be familiar with the physical and chemical properties of water and ice, as these affect the behaviour of the material treated during the

freezing. For instance, water reaches its maximum density at 4 °C. As ice is less dense (916.7 kg/m^3 at 0 °C) than water (999.8 7 kg/m^3 at 0 °C), water expands as it freezes and may cause problems, such as breaking containers (Petrenko and Whitworth, 2002). However, ice floats, which will help the separation of ice from liquid in the freeze purification process. Consequently, water is a complex material with exceptional properties, such as thermodynamic and volumetric anomalies, in both liquid and solid (ice) form. These abnormal properties are studied extensively and are explained and modelled in the molecular structure of water, i.e. through hydrogen bonds and the hydrogen-hydrogen (H-H) bonding network (Brini et al., 2017; Gallo et al., 2016).

The transition of water from liquid to solid is called ice crystallization. To date, about 16-17 crystalline phases of ice have been discovered (Shultz et al., 2014; Brini et al., 2017). The different crystalline forms occur under different temperature and pressure conditions. The most familiar phase, which is the one that can be found on Earth at normal atmospheric pressure, is ice I_h. "Ice crystal" or "ice" discussed in this study are referred to this ice I_h with hexagonal crystal structure at the basal plane (Brini et al., 2017).

One of the peculiarities of water is that it can supercool to an extreme even though the freezing point of pure water is 0 °C. Water has cooled near the temperature of 232 K (-41 °C) until it has crystallized, i.e. homogeneous ice nucleation occurred (Moore and Molinero, 2011; Gallo et al., 2016). The homogeneous ice nucleation can be defined as ice nucleation without any other foreign substance (Vali et al., 2015). The supercooling of water has been the basis for many resent ice crystallization studies when addressing the reasons for the ice nucleation and crystallization processes at the molecular level, i.e. how ice crystallization initiates.

The nucleation and growth of an ice crystal are studied particularly in the atmospheric sciences. Koop et al. (2000) present that in aqueous solutions the homogeneous nucleation depends on water activity, but not on the properties of the solute. The water activity criterion, under certain conditions, was defined as the water vapor pressure ratio between the solution and pure water. The simulation of ice nucleation and crystallization is difficult because of the disordered hydrogen bonds of the water molecule network and numerous network configurations. Matsumoto et al. (2002) have simulated the molecular dynamics of freezing in supercooled water. They state that an initial nucleus begins to form when a sufficient number of hydrogen bonds have lived a relatively long time (~2 ns) in the same region and start spontaneously to form a compact nucleus. This nucleus continues slowly changing in size and shape until it rapidly expands and results in crystallization. Similarly, in molecular dynamics simulations of supercooled water, Moore and Molinero (2011) have found the ice crystallization rate to be controlled by structural transformations in liquid water and the homogeneous ice nucleation to be dependent on the thermodynamics of water.

After nucleation and primary crystallization, the growth of ice crystal continues leading to the formation of a certain crystal size and structure. The appearance and structure of the formed ice can vary greatly. Figure 2.2 shows the formation of different shapes in the

ice layer. The driving force for further crystal growth is the supercooling or supersaturation of the solution, depending on the freezing conditions and the solution in question. For instance, Shibkov et al. (2005) have studied the dendritic growth of ice in a pure water film by measuring e.g. the tip speed and position. They found the growth to be diffusion-limited in low supercooling (2 - 4°C) but kinetic-limited in higher supercooling. Shultz et al. (2014) and Brumberg et al. (2017) have studied the stability of ice crystal faces and ice-growth inhibition in the ice-water interface with crystallographic methods. They linked the macroscopic ice crystal faces to the microscopic, i.e. the molecular hexagonal, structure of I_h ice. They found that the primary prism and basal faces dominate the surface (due to the surface free energy) at the solid–vapor interface. At the solid-liquid interface, the surface is dominated by the secondary prism (Brumberg et al., 2017).

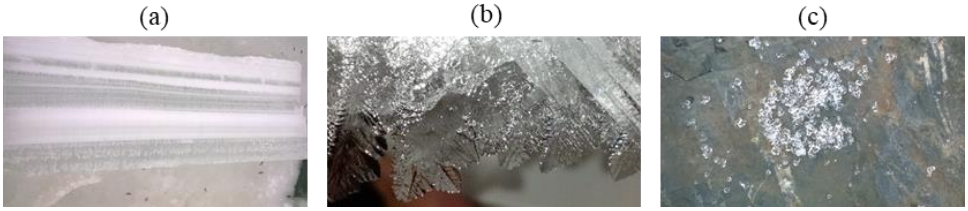

Figure 2.2: Different shapes of ice studied in the present research: (a) layered lake ice, (b) dendritic platelets formed from an ethanol solution and (c) ice hails formed on the ice cover of a mine pit pond.

The waters in nature environments are hardly impurity-free, and hence, the ice nucleation occurs heterogeneously, i.e. through the presence of a foreign substance. The impurities suspended or dissolved in water are known to promote the ice nucleation and prevent strong supercooling – compared to the process in pure water. However, heterogeneous ice nucleation is not yet well understood and has been described as stochastic (Koop et al., 2000; Randall et al., 2012). The mechanisms behind the effects of solutes and/or different nucleators on ice nucleation are still somewhat unsolved. The water activity may not necessarily explain the heterogeneous nucleation, as solutes even in low concentrations are known to affect the ice nucleation temperature (Whale et al., 2018).

In wastewaters in general, the number of different impurities, which may influence ice nucleation, may be high. Substances that are known to induce ice nucleation can be found among many organic compounds, minerals and alkali metal halides. Acknowledged nucleators include e.g. silver iodide AgI, kaolin and quartz (Gao et al., 1999; Whale et al., 2018). Not only material substances but also several bacteria can act as ice nucleators and reduce supercooling. The most studied of these microbes seems to be *Pseudomonas syringae* (Widehem and Cochet, 2003), also called leaf-deriver nuclei LDN. As these pathogens originate from woody plants in general, they might be found in wastewaters. The ice nucleation and supercooling in wastewaters has rarely been studied, probably due to the diversity of wastewater. For instance, Gao et al. (1999) have studied the spray

freezing of industrial wastewaters and ice nucleus concentrations in frozen droplets derived by the nucleus spectra model. Their main results show that the freezing temperatures of different wastewaters are different, and the freezing points somewhat correspond to the impurity concentration as the nucleus content in different wastewater drops varies.

However, in practical freeze purification with miscellaneous types of wastewater, the actual heterogeneous nucleation mechanism is difficult to control. The most efficient way to influence ice nucleation is to use ice seeds (as secondary nucleation) for a kick-start of crystallization. In this manner, the important process parameters can be slightly adjusted to control the undercooling (supercooling) temperature and induction time. The control of further ice growth during the freeze purification process can be considered a great concern – especially when the effect of nucleation on ice growth is yet unknown.

2.2 Temperature profile of freezing process

The clearly distinguishable effect of impurities in water can be seen in the freezing point of an aqueous solution. When water contains impurities like electrolytes, the freezing point is depressed, i.e. the ice crystals begin forming at a lower temperature than 0 °C, which is the freezing point of pure water. This temperature difference is called freezing point depression (FPD).

The FPD (K) can be calculated for dilute, ideal solutions by the colligative property equation:

$$FPD = mK_f, \tag{2.1}$$

where m is the molal concentration of the solute in the solvent (mol/kg) and K_f is the cryoscopic constant (K kg/mol), a characteristic property of solvent (Mullin, 2001). Thus, the FPD corresponds with the concentration to some extent, i.e. the higher the solute concentration is in a solution, the greater the freezing point depression is.

The FPDs of all common electrolyte solutions, such as NaCl and KCl, have been fundamentally studied. Data on the freezing point depressions of aqueous solutions in different concentrations of electrolytes is comprehensively available in literature, i.e. in chemistry handbooks. The FPD data can be used in determining and modelling other thermodynamic properties of solutions, for instance in the determination of the Pitzer interaction parameters (Hasan et al., 2014). Although electrolyte modelling is rather far advanced, calculation models are not yet entirely utilized to process the extremely complex mixtures of electrolytes in an aqueous solution. Similarly, calculation models will hardly be usable with real wastewaters in the near future, as they are much more complex.

The FPD determination has been commonly used in the food industry, and FPD data is available for dilute solutions such as milk, juices and coffee extracts (Chen and Chen,

1996; Chen et al., 1996). FPD measurement could be used in the evaluation of the solute concentration in a solution as well – at least when measuring relative changes. Surprisingly, the freezing point depression of wastewater has rarely been studied.

The FPD can be determined with, for instance, a simple cooling curve method, i.e. by measuring the temperature of the solution during cooling in a vessel with appropriate agitation. The measurement will result in a freezing curve, temperature against time (*t*,*T*), where the temperature differences for the FPD and supercooling are displayed, as Figure 2.3 shows. The simple curve illustrates the thermodynamics of the freezing process. When the solution is cooled at a constant rate, it will be supercooled until heterogeneous nucleation initiates spontaneously at the lowest point of the curve. The vertical jump from the lowest point to the freezing point shows the heat of fusion, which is released due to the ice crystallization (Kapembwa et al., 2014). The temperature then plateaus to the freezing point for a while if the cooling is kept constant.

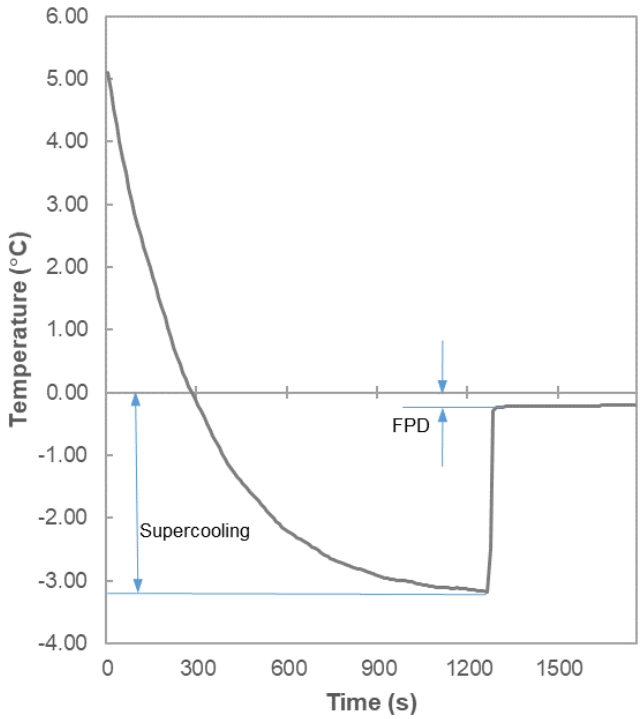

Figure 2.3: An example of a freezing curve (*t*,*T*), the supercooling temperature and freezing point depression FPD. Measured using landfill leachate and a cooling rate of 1 °C/min.

With a simple electrolyte solution of one or a few solutes in suitable concentrations and continuing cooling, a eutectic point can be seen as a little leap in the curve when the solute crystallizes (Rahman et al., 2002). Consequently, ice and solute crystallize concurrently

at the eutectic point (temperature and concentration) of a certain electrolyte. This process is called eutectic freeze crystallization (EFC). Wastewaters are mainly rather dilute, and thus, it is not possible to utilize EFC as such, but after concentration by pre-freezing and particularly with industrial brines, the potential is much higher.

The determination of the FPD temperature of wastewaters is of importance in freeze purification experiments and in the development of devices because this temperature sets the baseline for the cooling required. The ice nucleation and crystal growth rate can primarily be influenced by the cooling temperature used for freezing, as the driving force is the temperature difference. The undercooling level selected for one of the process parameters not only influences ice productivity but also the total energy consumption.

2.3 Impurity separation by freezing

2.3.1 Fundamentals

In the freezing process of an aqueous solution, the ice crystals can be thought to be naturally intolerant to impurities (Bogdan et al., 2014). When ice crystals are forming, they tend to reject impurities. As a result of these interactions between ice and impurities, two different components form, i.e. rather pure bulk ice and a concentrated solution enriched by impurities. For instance, Bogdan and Molina (2017) have found that the freeze concentrated solution covered the ice core when micrometer-scaled droplets of an aqueous sulfuric acid solution were frozen. However, the mechanism of separation, at the macroscopic and particularly the microscopic level, is still incompletely understood.

The movement of a particle in the interface between ice and liquid during the freezing has been studied in terms of the critical velocity of the freezing front (Körber et al., 1985). The repulsion or the capture of the particle depends on this critical velocity (Azouni et al., 1990). Several theoretical models have been presented concerning the particle–front interactions, but they have not been validated for a wide variety of materials or conditions (Asthana and Tewari, 1993).

It has been proposed that the ice crystal lattice has such small dimensions that impurities cannot be included in the lattice, but with only a few exceptions such as HF and HCl (Lorain et al., 2001; Petrenko, 1993). This would, to some extent, explain why ice does not incorporate any other solid compounds. A more comprehensive explanation for the repulsion of impurities may be found in the hydrogen bonding network of water, which solutes affect (Koop et al., 2000). The investigation of the water-solid interface is challenging, as the measurement of ice is difficult (Lovering et al., 2017).

Because the mechanism of impurity separation phenomena at the microscopic or molecular level has been rather obscure until recently, it has been more meaningful to concentrate on studying the freeze crystallization process. Freezing conditions and ice growth mechanisms define how ice crystals grow and form (the size and morphology)

and how the structure and purity of the bulk ice forms (Kapembwa et al., 2014). As wastewater can contain miscellaneous impurities – soluble and non-soluble, organics and inorganics – the influence of the whole freezing process on the main outcomes (the ice production and separation efficiency) is the most significant indicator when evaluating the functionality of the freezing process.

2.3.2 Freezing methods in wastewater treatment

There are many different research trends in freeze separation techniques, and the terminology is somewhat confusing. Freeze separation methods used (or studied) in wastewater treatment can be categorized into three main groups based on the ice growth process or mechanism. First is the ice crystal growth from water droplets in vapour, called *spray freezing*. In this process, wastewater is sprayed into cold air, where droplets freeze, forming ice or snow, and impurities concentrate in the liquid phase. This method has been examined in field conditions by, for instance, Gao et al. (2004) using industrial wastewaters from pulp mill and oil sands, and by Biggar et al. (2005) using mining tailing water. The second freeze crystallization method is *ice growth in a layer*. When the water surface is cooled by air flow, the layer ice growth method is called natural freezing, as in this thesis. The third freeze crystallization method is *ice growth in suspension*, called suspension freezing. The process is usually operated in a vessel, a crystallizer, where ice particles form in water suspension. This thesis focuses more closely on the natural freezing method and suspension freeze crystallization in wastewater purification.

2.4 Natural freeze crystallization

The natural freeze crystallization of wastewater in a basin comprises several interesting aspects for research. Traditionally, the natural freezing of lakes or seas in arctic regions has been studied in geosciences, particularly glaciology, and in marine technology. These research areas have focused more closely on the structural analysis and other properties of ice formed during the freezing process (Timco and Weeks, 2010). However, the impurity separation or purification performances of the natural freezing process have not been in the research focus.

2.4.1 Natural freezing process

Material sciences or crystallization research have usually focused on sub-processes or interfaces of ice layer growth instead of the comprehensive freezing process. This section gives an overview of the natural wastewater freezing process with different sub-processes and interactions in the interfaces (air-ice and ice-water) and parts (air, ice, and wastewater). Figure 2.4 illustrates the conceptual overall process. For simplification, the bottom and walls of the basin are assumed to be heat insulated. Furthermore, the wastewater flow, the external agitation of wastewater, and the effect of sunlight and precipitation are excluded from this review. Nevertheless, these factors have been

examined e.g. by Launiainen and Cheng (1998) in the thermodynamics of a natural water system in modelling or simulating the natural ice growth.

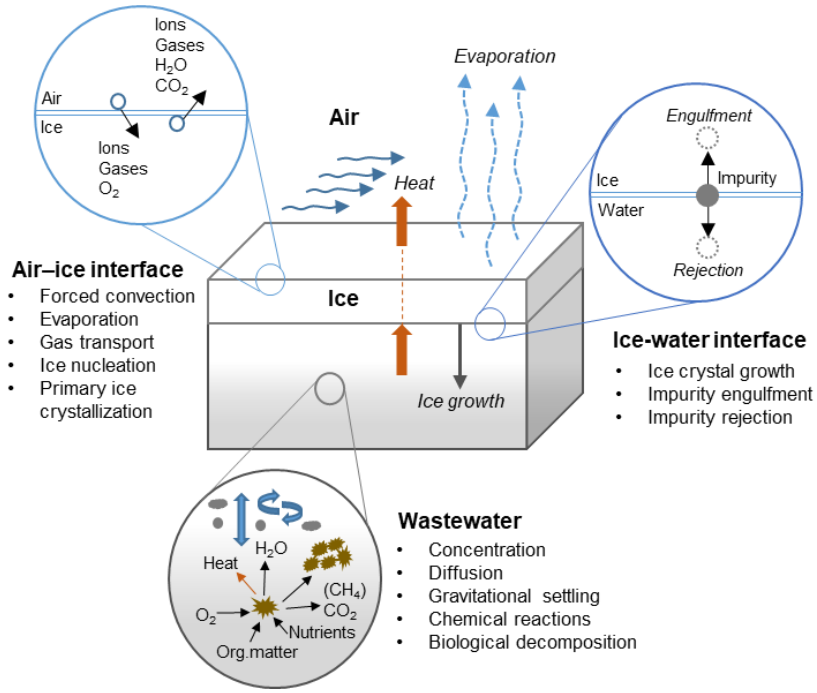

Figure 2.4: Process principle of natural freeze crystallization in wastewater basin.

Air-ice interface

In natural freezing, the water surface is first cooled by cold flowing air, i.e. via forced convection in heat transfer. The temperature of the water surface decreases due to the heat flux from water to air. Therefore, it is likely that the upper water is supercooled slightly before the nucleation takes place. Depending mostly on the temperature gradient and the mixing effect of airflow, crystals first form on the liquid water surface in the shapes of platelets or needles (Petrenko and Withworth, 2002; Leppäranta, 2015). After the water surface is covered by ice crystals and with sufficient undercooling, ice keeps growing downwards and forms an ice layer.

When the cooling of the ice surface continues, the heat transfer from liquid water to ice and through the interface further into the air remains. It could be assumed that some mass transfer occurs through the air-ice interface as well. However, the evaporation or sublimation of water from the ice surface, or other gas (e.g. CO_2) transfer during the freezing process has been ignored in ice research and freeze separation studies.

Ice-water interface

Heat and mass transfer are the main factors that determine the ice crystal growth mechanism, i.e. what polycrystalline structure of the ice is formed and how the ice layer grows. First, when the primary ice crystallization occurs, the heat of crystallization, here heat from the fusion of water 6.01 kJ/mol (Rumble, 2019), is released and transferred to the surroundings of the interface – both to the solid ice and to the liquid (Kapembwa et al., 2014). It is proposed that the boundary layers for thermal and mass diffusion are formed in the ice–solution interface, which enables the theoretical modelling of ice layer growth in electrolyte solutions. When ice crystal grows due to the temperature gradient, the concentration of the solute increases in the boundary layer (Hasan and Louhi-Kultanen, 2015). Thereby the local temperature and concentration gradients are coupled to each other by interactions and consequently determine the supersaturation, nucleation and ice crystal growth (Kapembwa et al., 2014).

In the case of a single ice crystal, it is known that when the crystal growth rate is low, the solute (impurity) is able to diffuse away from the boundary layer surrounding the ice crystal. Accordingly, the impurity is engulfed at a high ice crystal growth rate (Butler, 2002). The generation of impurity inclusions in the polycrystalline ice layer follows a similar principle; at a low ice growth rate, impurities are diffused to the concentrate, and high-purity ice can be produced (Hasan and Louhi-Kultanen, 2016). At higher ice growth rates, the impurities do not diffuse out as efficiently, and some are thus entrapped between ice crystals. This results in a lower separation efficiency of impurities.

In addition to the cooling air temperature, the air velocity (i.e. wind) substantially affects freezing and the ice layer growth rate (m/s) (Hasan et al., 2018). Obviously, the higher air velocity enhances the heat transfer from the ice surface. The ice growth rate can be expected to slow down as the ice layer thickens. Due to the low thermal conductivity of ice, the ice layer begins to act as a heat insulation when the heat resistance of the ice layer increases, and thus the heat transfer through the ice layer is reduced (Hasan and Louhi-Kultanen, 2016). Consequently, the lower parts of the ice layer could be expected to be cleaner than the upper ones. However, this is not straightforward because the concentration of impurities increases during the process and can affect the separation efficiency.

The structure of polycrystalline ice in the ice layer has been extensively investigated in glaciology. The impurities (i.e. salt, chemicals, and gas) in ice have been mainly of interest when studying the effect of impurity inclusions on the physical properties of ice, such as the mechanical strength (Hammonds and Baker, 2016; 2018). The impurities are trapped inside the bulk ice in pockets, veins, tubes and bubbles (Light et al., 2003; Iliescu and Baker, 2007). The size, shape and orientation of ice crystals vary in the natural ice layer. The smallest dimension can be less than 1 mm and the largest a gigantic 1 m, and the main shapes are classified as granular or columnar (Leppäranta, 2015), depending mostly on ice growth conditions.

Wastewater under the ice cover

When real wastewaters are treated by the natural freeze crystallization in a basin, the possible effect of wastewater under the ice layer on the ice growth process should be taken into consideration to some extent. Traditionally, natural pond systems such as stabilization or oxidation ponds have been utilized for municipal, industrial and agricultural wastewater treatment in many countries. In addition to long-term practical experience, scientific research has recently focused on the design and development of various processing techniques under different conditions and the modelling of complex biochemical reactions (Butler et al., 2017; Ho et al., 2019). However, to the author's best knowledge, research on the behaviour of wastewater under the ice cover has not been reported in context of freeze purification.

Usually, the heavier suspended solids of wastewater will slowly settle at the bottom of the basin when the water is undisturbed and still. Thus, the wastewater closer to the growing ice surface would contain mostly dissolved solids. It is generally acknowledged that organic matter decomposes in wastewater because of the involvement of microorganisms. When the organic matter breaks down either aerobically or anaerobically, decomposition gases (like CO_2, CH_4) and heat from exothermic reactions are released into the water (e.g. Tchobanoglous, 2003). In addition, the composition of wastewater changes simultaneously, i.e. the concentration of compounds undergoes changes as well. The temperature of wastewater and the load of the organic matter might determine the activity of reactions taking place. The lower temperatures slow down the internal processes of wastewater since the settling velocity of solids presumably decreases the activity of microbes. Nonetheless, the effect of microbes on the freezing of wastewater has rarely been studied even though microbes are known to be frost resistant (Parker and Martel, 2002) and some influence on ice nucleation has been proven, as section 2.1 presented.

Consequently, the heat and mass balance of the freezing process can be assumed to be more complex with wastewater than with simpler electrolyte solutions, and the effect of internal mass and heat transfer processes of wastewater on ice growth is more or less unpredictable. However, the influence of wastewater on the overall process efficiency can be expected to depend greatly on the process design. The forced convection driven mass and heat transfers, such as flow rates and water circulation caused by pumping, may be more significant for the freezing kinetics.

2.4.2 Natural freezing technology

The ice layer growth method in natural freezing can also be called progressive freezing (Yin et al., 2017) or unidirectional downward freezing (Gao et al., 2009). Alternatively, an ice layer can form on a cooling surface (e.g. heat exchanger) while water is flowing over it (Wakisaka et al., 2001). Some freezing apparatuses have been named after the techniques they employ, as the bubble-flow circulator (Shirai et al., 1999) and the falling film system (Shirai et al., 1998; Belén et al., 2012). In the latter methods, the mechanism

of freezing differs somewhat from natural freezing, where cooling is caused by a cold air flow. This study does not focus more closely on these non-air cooling methods in this natural freezing context. Natural freezing rather takes place in open-air wastewater basins in geographical regions where weather conditions are suitable for freezing, i.e. in the Arctic region.

Previous studies on layer freezing and its purification efficiency have been conducted using mainly model waters such as electrolyte solutions. In addition to purification efficiency evaluation, these laboratory-scale studies have focused on the modelling of freezing by ice crystallization kinetics (Hasan and Louhi-Kultanen, 2015). Hasan and Louhi-Kultanen (2016) have found the lower ice growth rates to result in higher separation efficiencies, when experiments were conducted using different freezing conditions (the temperatures, air flow velocities and concentrations of electrolyte solutions) in simulated air-cooled layer crystallization experiments. This is an important basis also for research with real wastewaters and on the development of new technologies.

The separation efficiencies of natural or layer freezing using real wastewaters has rarely been studied – only a few studies related to this topic can readily be found. In addition, the multiplicity of compounds in wastewaters poses challenges in separation efficiency evaluation and the comparison of studies, as there is no single meter for measuring the purity of water or ice. In general, chemical oxygen demand (COD, mg/L) or total organic carbon (TOC, mg/L) are used to define the organic matter in wastewater. For instance, Shirai et al. (1998) have studied dairy and rice cracker wastewaters by layer freezing on a plate heat exchanger and have reported very high ice purity (close to 100% impurity removal). Similarly, Gao et al. (2009) have studied pulp mill and refinery effluents by layer freezing, which resulted in 90-96% COD and TOC (i.e. organic contaminants) reduction. COD and TOC have been used also as gross parameters for specific organic compounds. For instance, Gao and Shao et al. (2009) have studied freezing of model solutions including pharmaceuticals (ibuprofen and antibiotic sulfamethoxazole) and they found the COD content reduced by 99% when two-stage layer freezing was applied. Similarly, Yin et al. (2017) have studied the layer freezing of wastewater from the pharmaceutical industry (containing tetrahydrofuran). They found the COD removal efficiency to be over 90%.

Several engineering challenges and open research questions still require solving before natural freezing can be utilized in wastewater purification. Ice harvesting, i.e. ice breaking, collecting, and transporting, is one of these unsolved issues. The mechanical strength properties of ice formed from wastewater will define the force needed for ice breaking. The influence of wastewater ice impurity on the mechanical strength of ice is still poorly known. In addition, it is necessary to solve the melting of ice collected after freezing. What these sub-processes have in common is that the surface area needed is large and energy consumption may be significant. Therefore, they influence the capital costs and operating costs, affecting the profitability of the entire treatment process, and are important to investigate further.

2.5 Suspension freeze crystallization

2.5.1 Suspension freezing process

In suspension freeze crystallization, ice crystals are formed in an aqueous solution (Figure 2.5). After the freezing point of the solution is reached due to cooling (and probably some degree of supercooling), ice nucleation and crystallization take place (Hasan et al., 2017), and therefore, growing ice crystals are dispersed throughout the liquid. Impurities are rejected from the forming ice crystal surfaces, and thus, the remaining solution concentrates with impurities (Feng et al., 2018).

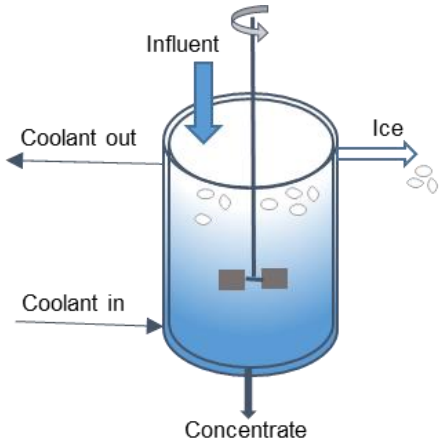

Figure 2.5: Principal process of suspension freeze crystallizer.

The separation efficiency is the result of the interactions between the growing ice crystal surfaces and impurities. The slow crystal growth rate favours the separation of impurities. In addition, fewer impurities adhere to the surfaces of large ice crystals (Shirai et al., 1987), as smaller crystals in higher quantities have an undesirably large surface area. The larger quantity of impurities loosely adhering to ice crystal surfaces will require more effective post-treatment (e.g. ice washing) when the ice and concentrated solution are separated after the freezing process. Gravitational ice separation is simple because ice floats, as section 2.1 highlighted.

Heat and mass transfer are important design parameters for controlling the ice crystal growth in the suspension freeze crystallizer, as the driving force for ice crystallization is the temperature difference (Hasan et al., 2017). Therefore, the solution is mixed to maintain an adequate rate of cooling throughout the solution and to affect the ice crystal growth.

2.5.2 Suspension freezing technology

Many technical solutions have been utilized in studies of suspension freeze crystallization, but mainly on a laboratory or small prototype scale. Some companies have developed commercial systems based on suspension freezing technology, but they are rarely reported in a scientific manner. For instance, the freeze concentration process by GEA Messo PT can be utilized to process all aqueous food products at capacities from 10 to 5 000 kg/h (GEA, 2020). Similarly, Sulzer Chemtech Ltd supplies freeze concentration plants of various sizes for food processing (Sulzer, 2020).

Generally, suspension freezing is carried out in a crystallizer, i.e. a vessel or reactor, which cools the solution usually indirectly with an external cooling unit. Very often a simple vessel with cooled wall has been used as a crystallizer. This usually causes ice formation on the heat transfer surfaces, i.e. on the inner wall. As this ice scaling reduces heat transfer, mechanisms for ice scaling removal (i.e. scraper) have been developed for different reactor configurations (Hasan et al., 2017; Rodriguez Pascual et al., 2010).

Suspension freeze crystallization has been much studied through eutectic freeze crystallization (EFC), where ice and salt can be crystallized and separated simultaneously in the same reactor. The process enables the desalination of salty water and salt recovery from industrial brines or solutions (Rodriguez Pascual et al., 2010; van Spronsen et al., 2010). This method has been rarely studied with real wastewaters other than industrial brines, and reports of achievable purification efficiencies are scarce. For instance, Randall et al. (2011) have conducted EFC tests using reverse osmosis brines from mine wastewater, and Randall et al. (2014) have used textile industry wastewater for such tests. Separation efficiencies were not reported, but ice purity was with one or two indicators. Clear purification efficiencies have not been presented in seawater freeze desalination studies either (Erlbeck et al., 2017; Chang et al., 2016), as their focus is on ice purity in terms of the salinity limits of potable water.

As in the case of natural freezing, suspension freeze crystallization has also been rarely investigated using real wastewaters, and the studies have reported only a few purification efficiencies. Yin et al. (2017) have studied the layer freezing of wastewater from the pharmaceutical industry (containing tetrahydrofuran) and conducted suspension freezing experiments. They found a COD removal efficiency of over 90%. Feng et al. (2018) have also reported a COD removal efficiency of more than 90% using the waste cutting fluid of a machinery factory in EFC tests.

The development of a continuous crystallization process is as challenging in freeze crystallization as in conventional crystallization techniques. However, in addition to studying the separation process mechanisms in the reactor and the effect of operation conditions on ice growth (Shirai et al., 1987; Chivavava et al., 2014), the current areas of development in suspension freeze crystallization techniques could focus more on the control of process operation, energy efficiency and the polishing of ice. The first two require a higher automation level, which might be possible through the holistic design of

prototype or pilot-scale apparatuses. On the other hand, many studies (Chang et al., 2016; Lemmer et al., 2001; Randall et al., 2011;2014) have reported the importance of ice polishing and its effect on the complete separation efficiency of the process. Usually, ice washing has been used for ice polishing, but studies have been initiated on alternative methods. For instance, Erlbeck et al. (2019) have included an ice pressing screw conveyer in the desalination crystallizer and have reported high separation efficiencies as well as reasonable energy consumption for optimized process conditions.

3 Experimental work

The experimental part of the wastewater purification study outlines three experimental and measurement setups based on natural freezing (*Publications I-III*) and an experimental system based on suspension freeze crystallization (*Publication IV*). The detailed experimental design and setups are described in the publication in question. The first experimental system (*Publication I*) was operated with an aqueous solution to ensure the comparability of separation efficiencies and mechanical properties between known molalities in steady state freezing conditions. The rest of the experiments were carried out using real wastewaters. The second experimental system *(Publication II)* focused on studying the effect of different freezing conditions on ice growth and separation efficiencies using urban origin wastewaters. The third experimental system (*Publication III*) explored the ice purity and properties of naturally frozen wastewater basins and a lake by taking in-situ measurements. The fourth experimental system (*Publication IV*) validated the separation performance of a pilot-scale suspension freeze crystallizer developed for wastewater purification.

3.1 Freezing of model solutions

This freezing experimental system used aqueous solutions of known molalities to study both separation efficiencies and the mechanical properties of ice. The aim was to evaluate the effect of impurity inclusions formed during freezing on the mechanical strength of ice. The information gained can be utilized in designing a freeze purification apparatus.

Five different aqueous solutions of sodium chloride (NaCl) and ethanol (EtOH, C_2H_5OH), each with molalities of 0.1 and 0.3 mol/kg, and tap water for comparison were prepared for the freezing experiments. The studied solutions are referred to here as tap water, EtOH 0.1m, EtOH 0.3m, NaCl 0.1m and NaCl 0.3m.

Solution samples, roughly 24 kg each, were frozen from the surface in 20 heat isolated boxes in a walk-in freezing room at temperatures of -5 °C (for the first 60 hours), -15 °C (13 hours) and -10 °C (2 hours). The boxes were placed in four rows so that each five solution types had four replicas with different freezing times (Figure 3.1). The temperature of each solution type in the first row was measured with PT100 thermometers and monitored with PicoLog PT-104 data loggers and a laptop. Figures 2 and 5 in *Publication I* illustrate the arrangements of the freezing room and freezing time profiles in detail. After freezing tests, the formed ice layers were lifted from the box for further measurements and to slice the ice into thinner layers for mechanical measurements and samples for chemical analysis.

Figure 3.1: Experimental setup in freezing room.

The separation efficiencies of the process were further determined by comparing the molalities of the initial solutions and formed ice (melt). Molal concentrations (mol/kg) were calculated based on values reported in literature and the measured results of the electrical conductivity (EC, mS/cm) of salt solutions, the density (g/m^3) of salt, and ethanol solutions. The molalities of the ethanol solutions were calculated based on an analysis of the total organic carbon concentration (TOC, mg/L).

The experiments included natural frequency measurements of ice samples and ice strength tests based on mechanical flexural strength. The masses and dimensions of the formed ice layers were measured to evaluate the growth rate and mechanical properties of the ice. The crystalline structure of the formed ice layers was visually observed with a cross polarized light method for comparison between ice from different solutions (compounds and concentrations). The cross polarized light method was accomplished by placing a thin section of ice between polarizing films over a planar light source.

3.2 Freezing of urban wastewaters in winter simulator

The objectives of the experiment were to evaluate the effect of different freezing conditions (air flow velocity and temperature) on ice mass growth and achievable purification efficiencies with real wastewaters. The natural (air-cooled) freezing tests were conducted using municipal wastewater and landfill leachate with variable

concentrations. Similar freezing tests were conducted with ultrapure water for comparison. Formed ice and initial wastewater samples were analysed using the water quality indicators commonly used in the evaluation of the purification performance of wastewater treatment plants.

The freezing tests were conducted with an experimental setup, i.e. the winter simulator apparatus in Figure 3.2(b). The freezing conditions, air flow velocity (0.5 to 3 m/s) and temperature (approx. -0.5 to -10°C), were carefully controlled with a blower and a thermostat. The freezing point depression temperatures of different wastewaters were measured with a separate experimental setup (Figure 3.2(a)) to ensure the comparability i.e. to set the right undercooling temperature (ΔT). Wastewater samples of 500 ml were frozen on the upper surface for a freezing time of 24 hours. The water temperature in each vessel was measured with PT100 thermometers and monitored with a data logger and computer. The mass and thickness of the formed ice layer were measured for determining the ice growth rate. *Publication II* presents the detailed design of the experiments and describes the experimental procedure.

Figure 3.2: Experimental setups. (a) Freezing point depression determination. (b) Winter simulator.

As the studied wastewaters contained a great variety of different impurities – both organic and inorganic matter with soluble and non-soluble pollutants – conventional water quality measurements such as chemical oxygen demand (COD) and electrical conductivity can be considered to indicate total purification efficiency rather comprehensively. Turbidity (FTU), colour (PtCo), pH and in some cases total solids (TS, mg/L) were determined as well. The microscopic characteristics of formed ice were obtained for the comparison of possible differences between wastewater origins.

3.3 Ice formed naturally due to seasonal variation in wastewater basins

The objective of the wastewater basin studies was to discover how natural freezing works under changing weather conditions in currently existing wastewater basins. Three very different water and ice environments – a lake, peat bogs and a mining site – were selected to compare achievable impurity separation efficiencies (i.e. ice purity) and to evaluate formed ice characteristics, including mechanical strength properties. This knowledge is of interest for future natural freezing technology development.

Ice and water samples were collected from a lake, two settling basins of a peat production area (Peat I and Peat II) and three wastewater basins (Pond, Pit, and Gypsum) of a mining site. Figure 3.3 shows an example of a measurement site, a water settling basin in a peatland. In the laboratory analyses, basic water quality indicators were determined: electrical conductivity (mS/cm), pH, apparent colour (PtCo), turbidity (FTU) and chemical oxygen demand (COD, mg/L). For a more comprehensive evaluation of the ice impurity content, the concentrations of the main anions (sulphate, nitrite, nitrate and chloride) were analysed with ion chromatography and elements (Ag, As, Ca, Cd, Co, Cr, Fe, Hg, K, Mg, Mn, Mo, Na, Ni, Pb, Se, Tl, U, V, Zn) with inductively coupled plasma mass spectrometry. The comprehensive choice of analyses enabled the comparison of different wastewaters with varied contents.

Figure 3.3: Ice sampling in the water settling basin of peatland.

In this experiment, ice strength measurements were conducted in-situ in natural ice-covered environments at the same time but next to a location where ice and water samples were collected for chemical analysis. *Publication III* presents detailed descriptions of the water systems at six measurement sites and experimental procedures including ice strength measurements.

3.4 Suspension freeze crystallizer

This experimental system was used to study the purification performance of a suspension freeze crystallizer developed and tested with real wastewater, landfill leachate. Scaling up a crystallization process to pilot-scale is commonly expected to be challenging.

The freeze purification tests of the suspension freeze crystallizer were conducted with highly concentrated landfill leachates. The leachates contained a great variety of organic and inorganic impurities, including heavy metals. The freezing tests were conducted with a pilot-scale freeze crystallizer. *Publication IV* describes the development of the crystallizer and the experimental setup (Figure 3.4), which includes the cooling unit.

Figure 3.4: Experimental setup in the testing environment; the suspension freeze crystallizer and the cooling unit.

In the experiments, the freeze crystallization process took place in a jacketed reactor with a 120 litre batch of wastewater and 60 minutes residence time. Two different ice seeding

temperatures were used and marked as the series C1 ~0 °C and the series C2 -0.4 °C. With both ice seeding temperatures, five tests were conducted with different combinations of the rotational speed of the ice scraper (7 or 10 rpm) and the agitator (150, 200 or 250 rpm). In every test, the temperature of the coolant was -3 °C.

Immediately after the freezing process, the formed ice was collected from the water surface, washed with water and drained in a funnel. The separation performance of the crystallizer was evaluated by analysing common water quality indicators: COD (mg/L), electrical conductivity (mS/cm), pH, turbidity (FTU) and colour (PtCo). The elements Au, Ag, Al, As, Bi, Ca, Cd, Co, Cu, Cr, Fe, Hg, K, Mg, Mn, Mo, Na, Ni, Pb, Sb, Se, Te, U, V, and Zn were analysed with inductively coupled plasma mass spectrometry.

4 Results and discussion

This chapter combines and discusses the results of the studied four experimental systems. The measured temperature profiles of the freezing processes and determined average ice growth rates were used for the process comparison. To ensure an adequate comparison between freezing experiments, separation efficiencies were determined in a similar manner for water samples based on commonly employed water quality indicators.

The supplementary materials of *Publication II, Publication III and Publication IV* present the measurement data of the second experimental system (winter simulator), the third experimental system (wastewater basins) including some more detailed analysis results, and the fourth experimental system (suspension freeze crystallizer).

4.1 Thermodynamics and kinetics of crystallization

4.1.1 Temperature profile and nucleation

Model solutions

In the freezing test with model solutions, the targeted temperature of the walk-in freezing room, i.e. the freezing temperature, was at first -5°C. The solution samples were similarly precooled, but temperatures varied between 4.7 and 8.3°C when the experiment started (Figure 5. *Publication I*). This led to average cooling rates varying between 0.12 and 0.35 °C/h, the lowest being with tap water and the highest with a NaCl 0.3m solution. The temperatures of water and NaCl solutions levelled close to known freezing points in literature (Haynes, 2017): water 0 °C, NaCl 0.1m -0.34 °C and NaCl 0.3m -1.02 °C. Slight undercooling (~0.1 °C) was noticed in the EtOH 0.1m solution; -0.28 °C (cf. -0.17 °C), but the EtOH 0.3m solution levelled at a warmer temperature of -0.42°C (cf. -0.54 °C). In these model solution experiments, the freezing happened spontaneously in tap water samples and in EtOH 0.1m solutions. Ice seeding was used in all NaCl solutions and in two of four EtOH 0.3m solutions. Thus, no conclusions can be drawn concerning the ice nucleation process in different solutions, as it seemed to occur more randomly and in a disordered manner.

Urban wastewaters

In the second freezing test, the freezing point depression temperatures of real wastewaters were noticed to vary, as expected. The differences between the temperature values were minor (at their greatest 0.185 °C between studied wastewaters), but the value correlates with the purity of wastewater. The closer the temperature was to 0 °C (the freezing point of pure water) the fewer impurities the water contained. *Publication II* presents the determination of the freezing point depression temperatures of different wastewaters in more detail. In winter simulator tests, different combinations of freezing conditions (the temperature and air flow velocity) were studied. All water samples were precooled in a

freezer room. In this manner, it was possible to generate the initial seed ice from the water, and no seed ice crystals were needed. This procedure prevented the subcooling of the wastewater at the beginning of the freezing test and promoted controlled ice nucleation. The cooling rates obtained in the tests were between 0.4 to 0.8 °C/h and varied randomly with all water types (*Publication II*, Figure 4). The measured temperatures of the wastewater samples during the freezing plateaued close to the freezing points, or very minor subcooling occurred in some cases.

Water basins

In the explorations conducted in real wastewater basins, it was possible to determine the average freezing conditions based on methodological data collected during the winter season by weather stations, i.e. freezing degree days and average temperatures. Table 1 in *Publication III* presents the data from six experiment sites. During the in-situ measurements, the water temperature just under the ice cover was below 0 °C in all wastewater basins, but about 0 °C in the lake. The water was slightly undercooled in the wastewater basins where the freezing point of water is likely depressed as well. The influence of the weather in northern locations can be seen clearly, as the average air temperature was 1.5 °C lower in Sotkamo, Northern Finland, than in Lappeenranta, Southern Finland. Northern regions have more freezing degree days during the winter (i.e. the winter period is longer), and ice covers there are thicker compered to ice covers in southern regions. However, a thick ice cover acts as a heat insulator, and the air temperature will not have such a significant effect on the ice layer growth. As the wastewater basins were used for water treatment, the heat balance was influenced by the water temperature of incoming and circulating flows, which further complicated the thermodynamics assessments due to a lack of continuous monitoring.

Suspension freeze crystallizer

The suspension freeze crystallization tests were conducted using landfill leachates. The freezing point depression varied slightly between wastewaters received from two barrel containers. The freezing temperatures were -0.06 °C and -0.1 °C. The average cooling rate in the experiments was close to 0.052 °C/min (i.e. 3.12 °C/h), which was much higher than could have been achieved in any natural freezing tests. Figure 2.4 shows an example of the cooling curve obtained from the freeze crystallizer process near freezing temperature. The shape of the curve is similar to the curve which can be obtained in freezing point depression tests, as, for instance, Figure 3 in *Publication II* presents. Typically, the water first undercooled slightly after ice seeding. Then, the temperature suddenly increased (a vertical leap in the curve) and finally plateaued at the freezing temperature. However, the degree of undercooling and the induction times varied rather randomly in tests, and the effect of ice seeding timing e.g. on nucleation or other mechanisms in ice crystallization could not be clearly explained.

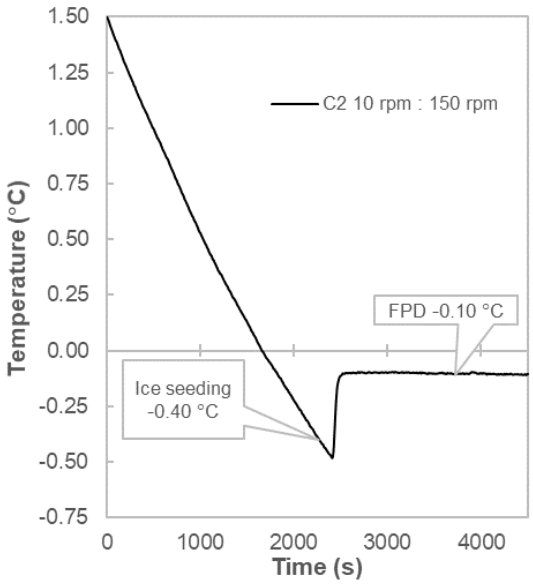

Figure 4.1: Cooling curve of the freezing process with a scraper rotational speed of 10 rpm and an agitator speed of 150 rpm.

4.1.2 **Ice characteristics**

The characteristics of ice formed in the freezing experiments were measured or visualized using various methods. The appearance of ice was assessed in in-situ observations, i.e. colour, transparency, shape, cracks, gas and brine bubbles and possible patterns. The properties of ice samples – the dimensions and mass – were measured in-situ as well. For closer observation of the ice layer structure (crystal or grain size and crystal growth orientation), the ice needed to be sliced in thin sections and visualized under a polarized light. The cross polarized light method is generally used in ice mechanics studies because of known interactions between the polycrystalline ice structure and mechanical properties. For an even more accurate view of ice structure, for instance to visualize clearer impurity inclusions in polycrystalline ice, a microscopic observation was needed.

Model solutions

In the first experimental system with model solutions, the vertical and horizontal structure of ice layers formed in experiments was examined with the cross polarized light method in addition to physical visualization. Ice layers formed under freezing conditions in all five solutions (tap water, EtOH 0.1m and 0.3m solutions, and NaCl 0.1m and 0.3m solutions) were identified to have different structures, as expected. Figure 6 in *Publication I* shows detailed pictures of the ice layers. The tap water ice was smooth-faced and the most homogeneous with a columnar but irregular ice structure of 10-40 mm ice grains.

The ice appeared transparent and clear and contained no bubbles. The ethanol solution ice seemed to be formed of dendritic crystal platelets (*Publication I*, Figure 7) of up to 100 mm and a thickness of 5 mm, which were partly connected irregularly, forming bridges and gaps. This porous ice likely contained entrapped solution inclusions as well. The NaCl ice appeared cloudy and was almost opaque. The bottom of the ice was rough, but the top surface smooth. The NaCl ice was formed of platelets similarly to the ethanol ice, but the platelets were much smaller and less porous.

Based on the measurement results, the ice structure observations were in relation to the mechanical strength of ice. The irregularly structured ethanol ice had lower strength than the less irregular NaCl ice, whereas the most regularly structured tap water ice had the highest strength. Based on the measurements and observations, it can be concluded that different compounds in aqueous solutions have different effects on ice growth mechanisms.

Urban wastewaters

The ice layers formed in winter simulator tests from real wastewaters were visually observed mainly during the other measurements of freezing tests. Some observations were made under a cross polarized light or microscope, but the small ice samples were mainly analysed chemically. In addition, the cross polarized light gave no significant information about the ice structure, as the samples were so small that single horizontal crystals could not be seen. Thus, the ice crystals were assumed to be rather large.

The wastewater ice was mainly transparent but appeared yellow in some light and brownish particularly in landfill leachate ice. The ice surfaces were mostly smooth and planar but with some thin veins and bubbles inside the ice pieces. The ice formed at higher growth rates contained some small needles at the bottom, but no clear patterns were detected. Some of the ice layers were wedge-shaped, as in Figure 4.2(b). After ice pieces were melted, the melt water colour was not usually similar to the ice colour observed after freezing, as seen in Figure 4.2(c) although the ice layer over the concentrated wastewater does not look as transparent in photographs, e.g. Figure 4.2(a), as it actually was. Microscopic pictures (*Publication II*, Figure 6) clearly show the structural differences between ice samples. In pictures of clean ice (formed from ultrapure water), ice crystal boundaries are clearly distinguishable from the blank spaces. Impure municipal wastewater ice contained clear inclusions, and landfill leachate ice additionally included solid particles.

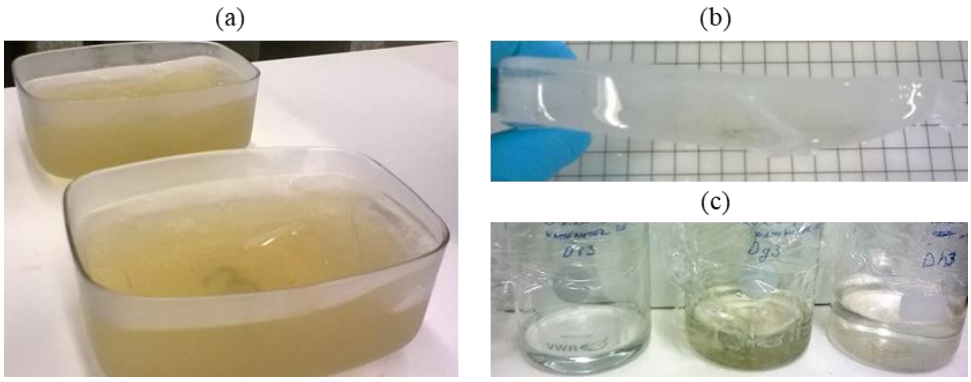

Figure 4.2: Municipal pre-treated wastewater after freezing. (a) Ice layers in crystallizer vessel. (b) Wedge-shaped ice piece. (c) Melted ice samples.

Water basins

The characteristics of ice layers in the third set of experiments were visually observed in-situ during the ice sampling and mechanical measurements. The differences in ice (water) sources can be clearly seen even though all natural ice seemed to be formed or grown in layers, as Figure 4.3 displays. The layered ice growth was likely the result of changes in freezing conditions or the water system. In the lake ice, the layers constructed different ice structures, such as pearls in line (bubbles) or changes in transparency. The ice layers in the peatlands appeared in different brownish colours (humus) and with liquid inclusions, Figure 4.3(b) and (c). The ice layers at the mine site looked different in all three basins. Common to all was the layered growth and very low strength. The ice broke easily into smaller pieces (ice hails), as in Figure 4.3(d).

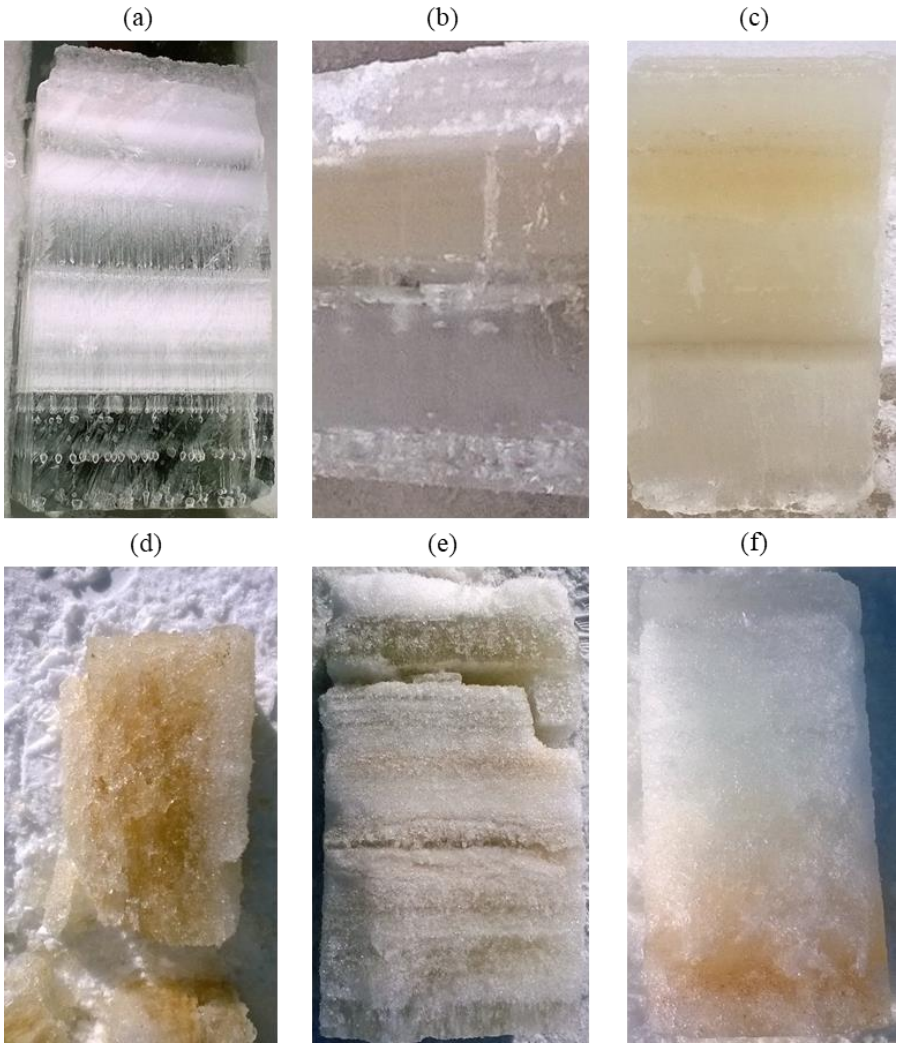

Figure 4.3: Ice layers formed in water basins. Vertical ice cross-sections from: (a) Lake, (b) Peat I, (c) Peat II; (d) broken ice pieces from Pond, and vertical ice cross-sections from (e) Pit and (f) Gypsum.

Suspension freeze crystallizer

When the ice crystals grew in wastewater during the freezing process, frazil ice plates floated freely on the solution surface. Ice started to form on the cooling surface of the reactor only until during the last 10 minutes of the batch time. The size of crystals was rather large, over 500 µm, and mainly thin and plate-like. The washing of the collected ice samples was found to be important in terms of ice purity, as expected. Figure 4.4 compares the colors of washed and unwashed ice samples, showing clear differences.

Impurities were clearly loosely attached to the ice crystal surface and can easily be rinsed away with water.

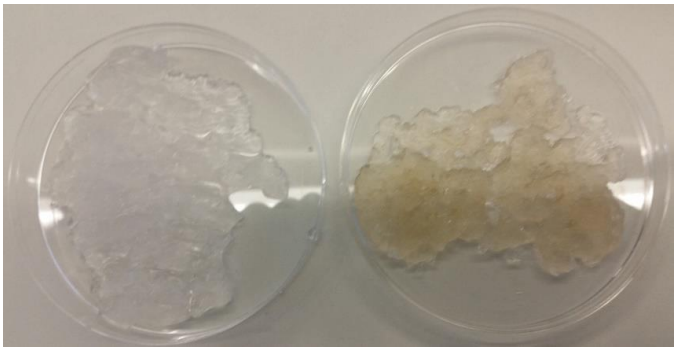

Figure 4.4: Colour differences in ice samples photographed after storing in a freezer. On the left is washed ice and on the right unwashed ice.

4.1.3 **Ice growth**

Ice growth can be determined using two different measures. The ice growth rate G (m/s), also called the liner growth rate, is based on the thickness (m) of the ice layer formed during the freezing time (s). The thickness based measure gives an appropriate approximation of the freezing process, but it ignores the formed ice structure (irregular shape, volume, porosity, etc.). In the evaluation of the ice production rate or yield, the ice mass growth rate G_m (g/s, kg/h) gives more accurate results. In layer freezing, ice mass growth can be calculated per freezing area, kg/(h·m^2), and in suspension freezing per volume, kg/(h·m^3), for the comparison of freezing processes of different sizes.

Model solutions

In the first experimental freezing system with model solutions, the ice layer growth rate was evaluated based on both thickness and mass (*Publication I*, Table 1). Despite the fact that irregular shapes of ice layers (i.e. ice crystals in the form of dendritic platelets) formed especially from ethanol solutions, the average linear growth rates after full-time tests were rather similar to other solutions, as Figure 4.5 shows. Tap water with the ice growth rate of $2.34 \cdot 10^{-7}$ m/s, the EtOH 0.1m solution of $2.45 \cdot 10^{-7}$ m/s and the EtOH 0.3m solution of $2.60 \cdot 10^{-7}$ m/s showed the highest values. The growth rate was lowest, $2.13 \cdot 10^{-7}$ m/s, with the NaCl 0.3m solution, but slightly higher with the NaCl 0.1m solution, $2.27 \cdot 10^{-7}$ m/s. The average ice layer growth rate of all studied solutions was $2.36 \cdot 10^{-7}$ m/s (at freezing temperature -5…-15 °C).

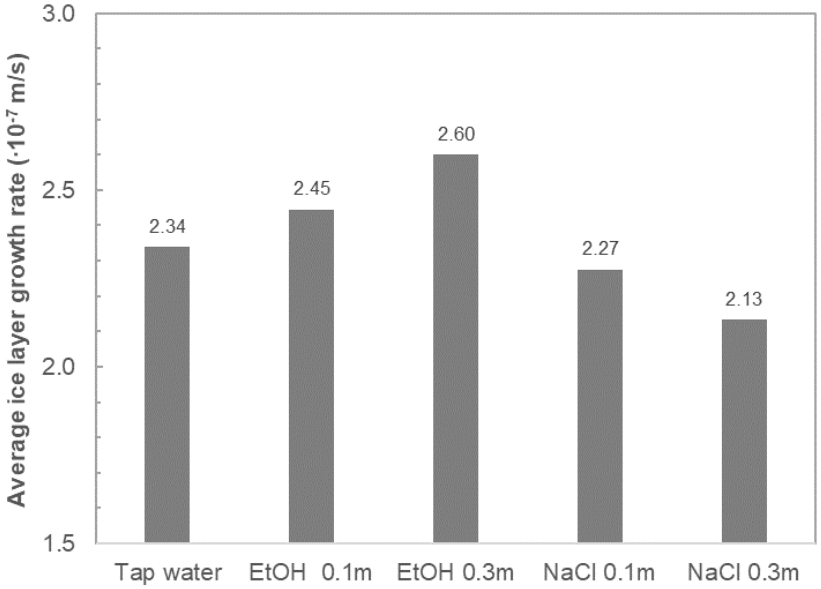

Figure 4.5: Average ice layer growth rates (m/s) of different aqueous solutions and concentrations.

Similarly, the evaluation of average mass growth rates showed the NaCl 0.3m solution gave the lowest 710 g/(h·m^2) value, but the NaCl 0.1m solution gained a slightly higher value of 769 g/(h·m^2). The tap water achieved the highest value of 780 g/(h·m^2). The growth was moderate with ethanol solutions: 748 g/(h·m^2) with the EtOH 0.1 m solution and 731 g/(h·m^2) with the EtOH 0.3m solution. The average ice mass growth rate of all studied solutions was 748 g/(h·m^2), the resulting differences in ice mass growth rates being rather minor, below 5%, as Figure 4.6 indicates. The concentration of the solution may have had an effect on the ice growth rate in this study, i.e. the ice growth rate is lower in concentrated solutions. Nevertheless, conclusions of this kind cannot be presumed, as the difference is rather minor in comparison with the accuracy of the sampling of three replicates.

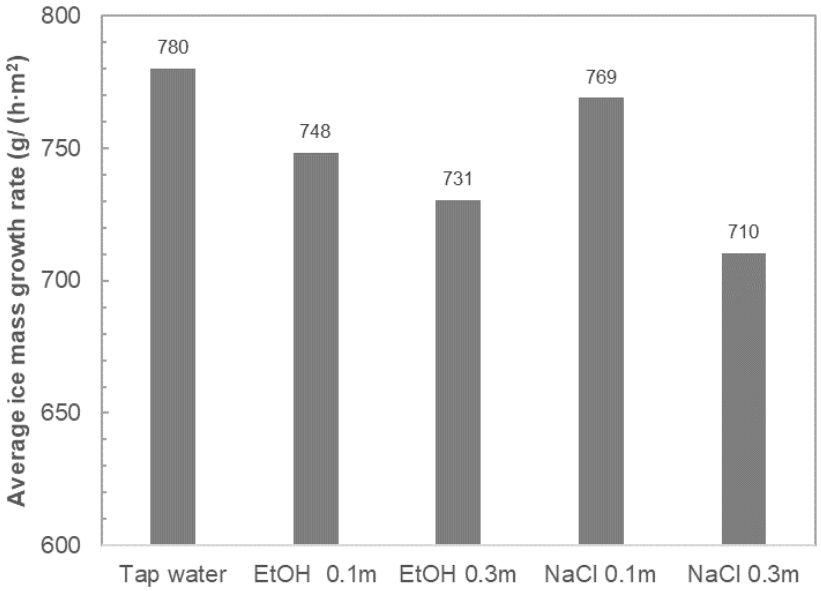

Figure 4.6: Average ice mass growth rates (g/h·m^2) of different aqueous solutions and concentrations.

Urban wastewaters

The second experimental system, equipped with a winter simulator, focused on studying the ice growth rates primarily based on mass but also on the ice layer from different concentrations of wastewaters in different freezing conditions (undercooling temperature ΔT, K and air flow velocity m/s). Table 4.1 presents the ice growth of different wastewaters in different freezing conditions. *Publication II* (Supplementary data, Table A.1, A.2 and A.3) introduces the measurement data of the freezing experiment.

Table 4.1: Average ice layer growth rates in different freezing conditions.

Wastewater	ΔT (K)	v_{air} (m/s)	**Ice layer growth rate** ($\cdot 10^{-7}$m/s)	**Ice mass growth rate** (g/(h·m^2))
Municipal effluent	0.5	3	1.77	548
	1	1	1.25	412
	1	2	1.82	597
	1	3	2.47	780
	2	1	2.03	631
	2	2	2.97	895
	2	3	3.39	992
	3	1	2.62	798
	3	2	3.96	1194
	3	3	4.39	1286
Municipal pretreated	0.5	0.5	1.25	216
	0.5	1	1.90	523
	0.5	2	2.98	910
	1	0.5	0.75	156
	1	1	1.53	431
	1	2	2.10	612
	2	0.5	1.71	415
	2	1	2.31	699
	2	2	3.20	989
	2	3	3.33	993
	5	1	3.47	767
	10	0.5	3.71	807
	10	1	6.69	1838
Landfill leachate	1	1	1.15	384
	1	1.5	2.02	592
	1	2	2.24	654
	1	3	2.86	905
	1.5	1	2.04	542
	1.5	1.5	2.37	676
	1.5	2	2.81	826
	2	1	2.50	721
	2	1.5	2.76	898
	2	2	3.34	998
	2	3	4.38	1288

In this study, the ice mass growth was found to correlate almost linearly with the undercooling temperatures and air flow velocities. A simple linear regression model fitting showed that the lower the freezing temperature and the higher the air velocity were, the higher the ice mass growth rate was, as Figure 4.7 shows. The combined results of municipal and landfill wastewater freezing (at undercooling temperatures of 1 and 2 K and air flow velocities of 0.5–3 m/s) showed that a 1 K change in temperature caused a change of approximately 300 g/(h·m^2) in the mass growth rate. In contrast, when the air flow was changed by 1 m/s, the ice mass growth rate changed by approximately 230 g/(h·m^2). Figure 7 in *Publication II* shows the detailed linear fittings. Due to the high uncertainty, linear fitting was applied to interpret the phenomena in general. *Publication II* also discussed the influence of the experimental setup on R^2 values and deviation (as Figure 4.7 displays).

The quality or concentration of the studied wastewaters had only a minor – if any – effect on ice growth. The lowest average ice mass growth rates of roughly 200 g/(h·m^2) were attained in freezing conditions of an undercooling temperature of 1 K or 0.5 K and an air flow velocity of 0.5 m/s. The highest average ice mass growth rate of 1200 g/(h·m^2) was achieved with 3 K and 3 m/s. Similarly, the lowest average ice layer growth rate of approximately 1 ·10^{-7} m/s was obtained with 1 K and 0.5 m/s, and the highest of roughly 4 ·10^{-7} m/s with 1 or 3 K and 3 m/s.

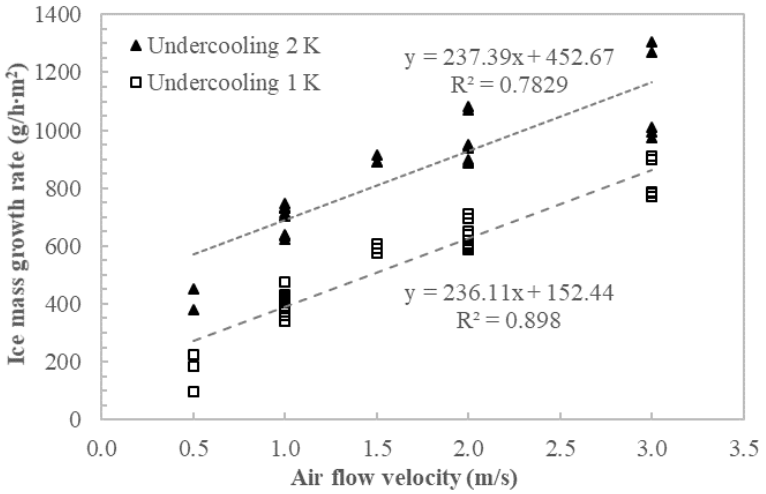

Figure 4.7: Combined linear fitting results: ice mass growth rates (g/h·m^2) and air flow velocities (m/s) with undercooling temperatures 1 and 2 K of municipal and landfill wastewaters. Modified figure from *Publication II*, Figure 7(d).

Water basins

In the third experimental system, the average ice growth rate (m/s) of natural ice layers (ice covers in basins) during the past winter period can be approximated on the basis of measured ice layer thicknesses and freezing degree days (*Publication III*, Table 1). The growth rates are remarkably (approx. 80%) lower in natural basins compared with ice growth rates in simulated freezing tests. The values vary between the highest $5.6 \cdot 10^{-8}$ m/s of Gypsum pond and the lowest $4.7 \cdot 10^{-8}$ m/s of Pond, both at the mining site (see Figure 4.8). This difference likely resulted from the long freezing time and the heat insulating effect of the thick ice layer, which decelerated the ice growth. Warmer water flows under the ice may have an impact as well. Otherwise, greater ice growth could be expected with higher average wind velocities and colder weather.

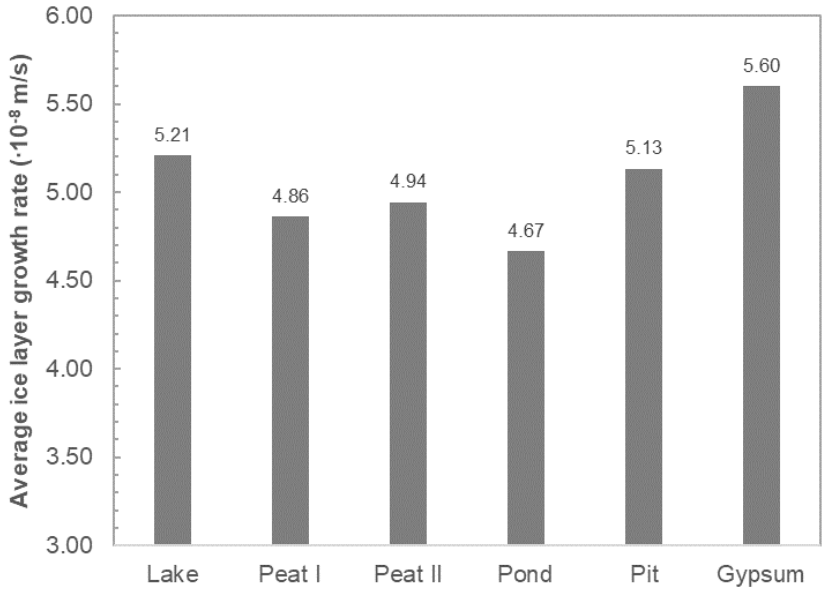

Figure 4.8: Average ice layer growth rates (m/s) in different water basins.

Suspension freeze crystallizer

The ice mass growth during the freezing process in the crystallizer was roughly evaluated based on the total mass production measurements of 11-12 kg batches. The average mean ice growth rate was thereby 96 kg/(h·m^3). The process parameters (i.e. rotational speeds of the agitator and scraper) did not demonstrably affect the ice mass production rate even though the coolant temperature was a constant -3 °C in every test. The large crystal size (>500 µm) may have resulted from Ostwald ripening (melting of smaller ice crystals simultaneously with further growth of larger ice crystals), or less likely, from the agglomeration of ice crystals, which was not observed.

4.2 Impurity removal efficiencies

The efficiency of the water purification process can be presented in two ways. Both methods were used in *Publications I, II and III*. The effective distribution coefficient *K* (-) indicates the impurity ratio between the ice and initial synthetic solution or wastewater, i.e. it characterizes the quantity of impurity that remains in the ice. *K* can be determined by $K = C_i/C_w$, where C_i is the measured value in the ice and C_w the measured value in the initial wastewater. The purification efficiency *E* better characterizes the functionality of the process, i.e. it indicates how rigorously impurities are removed and how well the process performs. *E* can be determined as

$$E = 100 \cdot \left(\frac{C_w - C_i}{C_w}\right). \quad (4.1)$$

The purification efficiencies achieved with different wastewaters in all three experimental freezing systems are presented in the impurity removal efficiencies section of this dissertation. Common analysis methods enable a direct comparison between wastewater purification requirements in current environmental legislation, concentration limits, and achieved water purity.

4.2.1 Model solutions

In the freezing experiments with model solutions (the sodium chloride and ethanol solutions of 0.1 and 0.3 molalities) the purification efficiencies were determined in terms of average molalities (mol/ kg H_2O) of three replicate samples in rows 1, 2 and 3. The purification efficiency for tap water was determined by TOC (mg/L) values. The values of samples in row 4 were not included in this calculation because of a considerably different freezing time but were assessed separately. Tables 1, 4 and 5 in *Publication I* introduce the calculated average values for molalities. Figure 4.9 presents the average purification (or here, separation) efficiencies for each model solution. The results clearly show that the tap water, with a very dilute concentration of impurities, achieved the highest relative removal efficiency of over 80%. EtOH 0.3m, NaCl 0.1m and NaCl 0.3m are at quite a similar level, close to 70%, but the more dilute organic EtOH 0.1m solution could not reach 50% impurity removal efficiency.

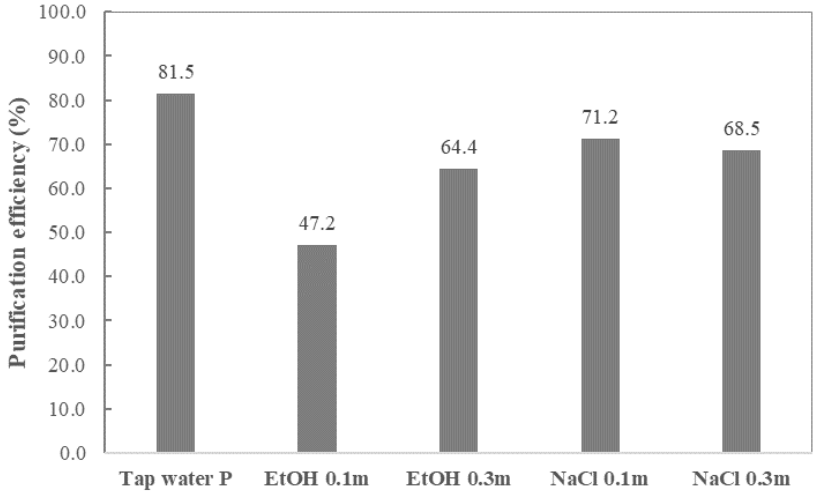

Figure 4.9: The average purification efficiencies (%) of different model solutions.

A closer review of the results of ice layers in different rows revealed variation in the removal efficiencies between all ice samples. The *K* values of all samples in row 4 were below 0.3 (i.e. >70%), and even 0.144 (86%) with NaCl 0.1m. These better efficiencies occurred at a higher freezing temperature (-5 °C), leading to lower ice growth rates, as expected. The impurity removal seemed to be vaguer between different ethanol solution samples than in sodium chloride solutions. This finding confirms the previous observations and explanation about the effect of different compounds in solutions on ice growth mechanisms and different ice structures with impurity inclusions. The irregular ice growth in ethanol solutions led to irregular ice structures and thus to incoherence in impurity removal.

During the experiments, the formed ice layers were sliced horizontally into two (i.e. top and bottom) or three (i.e. top, centre and bottom) approximately 4 cm thick sections for mechanical strength measurements. The impurities remaining in these layers were analysed, and the average concentration results were determined based on these analyses. NaCl solutions seemed to form less impure ice in the top sections, as expected due to lower ice growth rates at a higher freezing temperature. However, the bottom ice sections contained more impurities than the centre ice sections. This was contrary to the assumption that the ice would be less impure in the bottom layer since the thickness of the layer would slow down the ice growth (i.e. heat insulating effect). Nonetheless, the efficiencies are similarly formed in every sample. On the contrary, there is no pattern in ethanol solution *K* values in different layers or samples. Hence, no universal conclusions could be drawn about the effect of different freezing temperatures (i.e. ice growth rates and mechanisms) on impurity removal efficiencies between different layers during the freezing process with such a small number of samples. Therefore, *Publication I* reported no results between ice sections.

4.2.2 **Urban wastewaters**

In this freezing study, the purification efficiencies of different wastewaters in various freezing conditions were determined in terms of COD, colour, turbidity and electrical conductivity. The results showed that the purification efficiency correlates clearly with the ice growth rate; the higher the ice growth rate is, the more impure the ice is and the lower the purification efficiency. This was observed in wastewaters of different concentrations, but the effect was more intense in concentrated wastewater. *Publication II* presents more detailed purification efficiency results.

Figure 4.10 gives an example of the differences in efficiency tendencies between landfill leachate and more dilute pre-treated municipal wastewater with COD reduction. An increase in the ice growth rate caused a much stronger decrease in purification efficiency in landfill leachate than in more dilute municipal wastewater. Similar behaviour has also been reported in previous freeze separation studies, e.g. by Hasan et al. (2018), with salt solutions of different concentrations. Thus, the impurity concentration of wastewater has a certain effect on the impurity rejection during the freezing process.

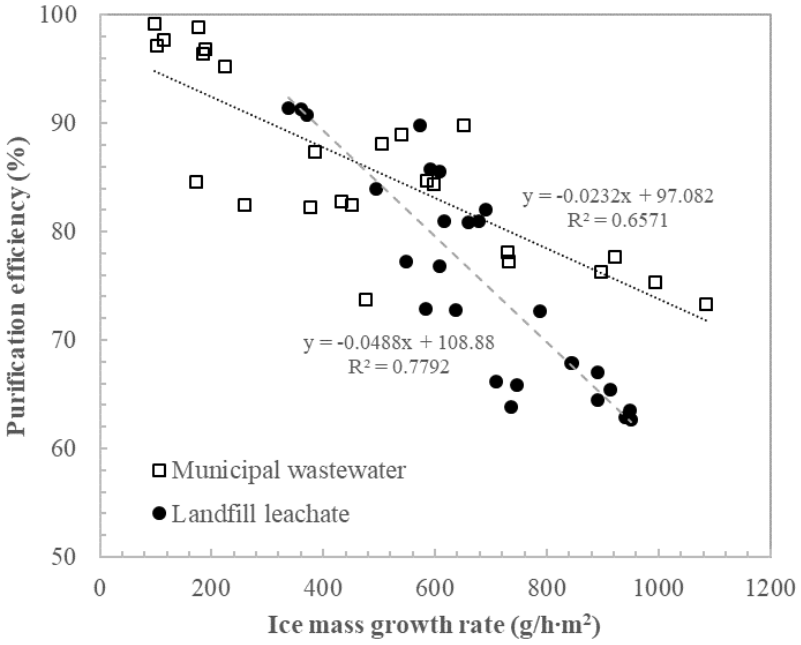

Figure 4.10: Purification efficiencies (%) based on obtained chemical oxygen demand COD results and ice mass growth rates (g/h·m^2) with municipal wastewater and landfill leachate. Combined results modified from Figures 8a and 9 in *Publication II*.

The effect of concentration can be explained by the coupled transfer of heat and mass in the ice-solution interface, i.e. in the boundary layer where ice crystals grow. Since the

concentration of the wastewater had a minor influence on the rate of ice growth, the heat transfer can be assumed to control the ice growth, as the mass transfer coefficient is low with the wastewater of higher impurity concentration. Hence, the impurities accumulated near the interface are not effectively diffused out and are entrapped in the ice. The entrapment rate is directly proportional to the bulk impurity concentration and ice growth rate. However, the effect is difficult to predict when the real wastewaters with a complex mixture of compounds in different concentrations are in question.

The purification efficiencies of all studied wastewaters were at a sufficient level, near or over 90%, when the ice growth rate was low, i.e. 400 g/(h·m^2). In this context, it should be acknowledged that the initial landfill wastewater was 30 times more concentrated than the initial effluent, i.e. 638 vs. 21 mg/L of COD, respectively. Efficiencies near 100% were achieved when freezing municipal pre-treated wastewater at the undercooling temperature of 1 K and the air flow velocity of 0.5 m/s, which led to a very low ice growth rate, below 200 g/(h·m^2).

The limitations of the experimental setup precluded very low or high air flow velocities or undercooling temperatures. The freezer clearly became unstable, which caused deformations in the ice layers, i.e. wedge-shaped ice pieces and deviations in ice masses of replica samples, as discussed in section 4.1.3. High uncertainty and deviation in the ice mass growth rates also affected the purification efficiencies. The influence of the experimental setup can be seen for instance in Figure 4.11, which illustrates the average results of landfill leachate freezing in different experimental conditions. In addition to experimental conditions, the changes in initial wastewater concentrations possibly caused deviations in results.

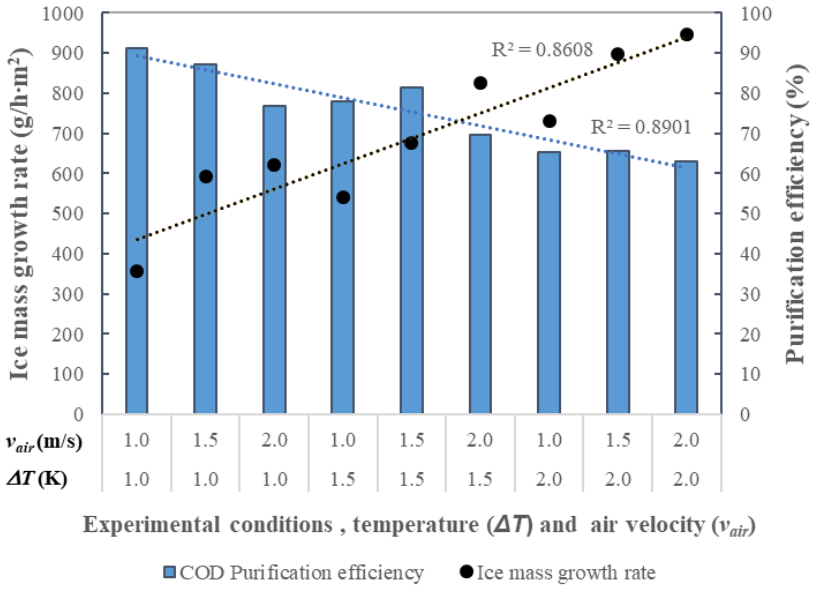

Figure 4.11: Average COD purification efficiency (%) and ice mass growth rate (g/h·m^2) under different freezing conditions with landfill leachate.

4.2.3 **Wastewater basins**

The separation efficiencies of different waters or wastewaters in naturally frozen basins were evaluated by comparing the impurities in the formed ice with water underneath. This gave an overview of average separation efficiency even though the water flow fluctuated under the ice during the winter period and could cause some variation in concentrations. The Supplementary material of *Publication III* presents detailed measurement results. Figure 4.12 shows the levels of calculated average separation efficiencies for comparison. Even though the contents and concentrations of waters were very different, the ice was considerably cleaner than the initial water in every basin. The highest purification efficiencies, nearly 90%, were obtained in Lake and in Pit, which contained completely different quantities of impurities. The lake water was the cleanest of the studied waters, as expected, but differed only slightly from peatland waters. The highly concentrated Pond and more moderate Gypsum achieved almost the same efficiencies (65 and 73%) as dilute Peat II and I (68 and 77%).

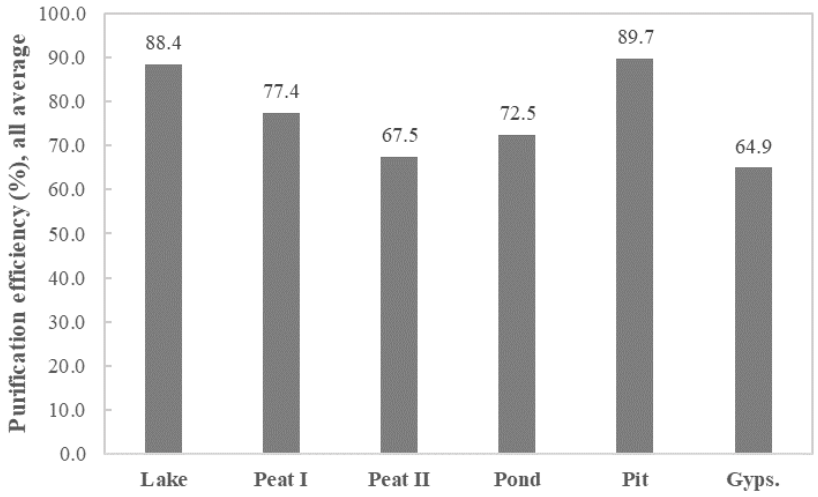

Figure 4.12: Average separation efficiencies (%) calculated for all impurities in the ice of different water and wastewater basins.

A closer study of the different sites revealed variations in water constitutions and differences in impurity removal. Figures 8 and 9 in *Publication II* display more detailed results of effective distribution coefficients for relevant constituents. No conclusions on the mechanisms of impurity inclusions in the ice could be drawn, as the water basins were not designed for freeze purification and the influence of the varying weather and other conditions could not have been taken into account. However, based on the results, it can be deduced that natural freezing can purify water of low impurity concentrations and highly concentrated wastewaters with quite similar efficiencies.

4.2.4 Suspension freeze crystallizer

As section 4.1.2 shows, the washing procedure with ice samples produced by the suspension freeze crystallizer had a significant influence on ice purity. This can be seen in the purification efficiencies as well. Figure 4.13 presents the average purification efficiencies of various water quality measures and Figure 4.14 those of various elements. Without washing, the efficiency of 50% could hardly be achieved, whereas with it, the efficiency rose to an adequate level. The calculated average purification efficiency of all water quality measures was slightly higher for washed ice samples of series C2, 97.3%, than for washed ice samples of series C1, 89.0%. Similarly, the calculated average purification efficiency of all elements was 95% for series C2 and 83% for series C1. *Publication IV* reviews the purification results in more detail. In series C2, the variation in efficiencies between different tests and impurities was minor in comparison with series C1. Therefore, it can be deduced that the process was better balanced in series C2 tests, which involved lower undercooling. Other process parameters, i.e. changes in the rotational speeds of the agitator or scraper, were not found to have a significant effect.

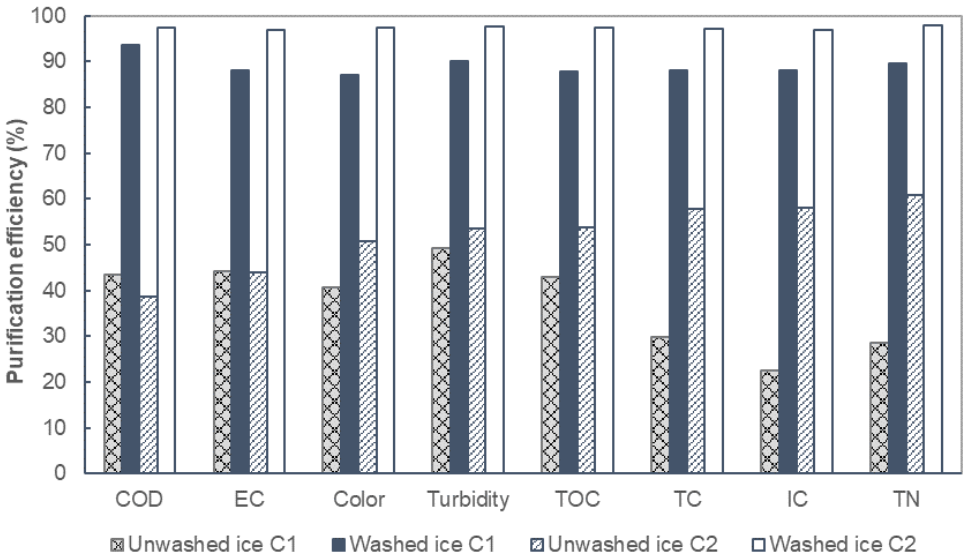

Figure 4.13: Purification efficiencies (%) of chemical oxygen demand COD, electrical conductivity EC, colour, turbidity, total organic carbon TOC, total carbon TC, inorganic carbon TC and total nitrogen TN. Determined on an average for washed and unwashed ice samples of series C1 and C2 tests.

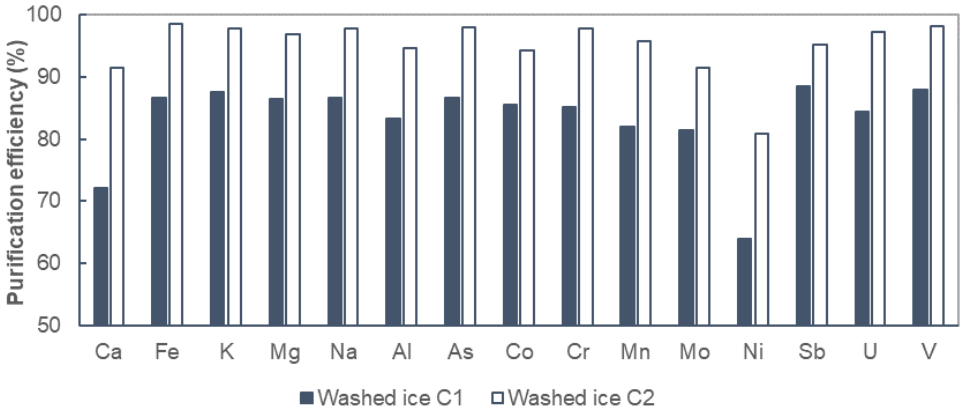

Figure 4.14: Purification efficiencies (%) of elements determined on an average for washed ice samples of series C1 and C2 tests.

4.3 Further remarks

4.3.1 Ice strength vs. impurities

Previously, section 4.1 described how freezing conditions influence the ice growth mechanisms and structure of the ice layer formed from (waste)water. In the freezing process, impurities are either rejected from or engulfed in the ice structure as veins and pockets. The mechanical properties of ice, e.g. strength, are influenced by impurity inclusions in the ice structure and are of interest to study for ice breaking device design. In the freezing experiments of model solutions and wastewater basins, the mechanical properties of ice layers formed were evaluated in terms of flexural and/or compressive strength.

In the experiment with model solutions (*Publication I*), tap water ice (the cleanest one) was found the strongest, ethanol ice the weakest and NaCl ice between the two, even with rather similar molal concentrations. However, organic ethanol seemed to have a tendency to weaken the ice more effectively during the ice growth process. The effect of ethanol on ice forming was also noticed in observations of irregularly structured ice (section 4.1.2).

The experiment with wastewater basins (*Publication III*) demonstrated a straightforward correlation between impurities and ice strength: the less the ice contained impurities, the stronger it was. The strongest ice in Lake with the flexural strength value of 1469 kPa was almost six times stronger than the weakest at the mine site Pond, 239 kPa. These sites were noticed to be the cleanest and the most concentrated with various impurities, respectively. Electrical conductivity, which indicates the overall quality of water containing ionic species, was found to correlate strongly with the mechanical strength of ice. This knowledge is of importance in future applications, e.g. in designing ice harvesting devices and operations where the required force and energy for ice breaking needs to be estimated quickly and simply.

4.3.2 Evaporation and changes in pH

Many previous freezing studies have ignored the evaporation of water during the freezing process or at least considered the impacts negligible. Consequently, in the experimental system with real wastewaters (*Publication II*), the loss of water mass was measured during air-cooled freezing. Significant mass loss, i.e. evaporation, was observed: 7–15% of the formed ice mass depending on the freezing conditions. It can be concluded that some evaporation of water occurs in the air-ice interface during freezing. Thus, some removal of volatile compounds may occur concurrently.

As in evaporation, the alkalinity (or acidity) of the aqueous solution is presumed to have very little effect on the freezing process. Based *Publications II and III*, the pH value of the initial wastewater was found to have no significant effect on the purification

efficiency. However, the pH of the effluent is one of the principle water quality properties to be taken into account. In the experiment with real wastewaters, pH values between the initial wastewater and ice were found to change due to the freezing process (*Publication II*, Supplementary material, Figure A.1). The pH tends to increase in landfill leachate freezing even though it is rather high initially (nearly 8). In contrast, the pH in municipal wastewater freezing tends to decrease, but not always. No clear reason for pH changes could be identified because of significant deviations in the pH results. In this study, also close to unacceptable pH levels were noticed. Hence, this issue proved to be worth further research.

4.3.3 Future prospects of freeze purification

Freeze crystallization technology has shown suitability for the treatment of a very broad spectrum of wastewaters, even dilute ones. The freezing of aqueous solutions can even enable significant amounts of water to be separated from solutions containing dissolved compounds in high concentrations, which is hardly possible with many other separation techniques. Hence, as the water content can be considerably reduced by freezing, the energy consumption of water transfer and further concentration treatment, such as evaporation, will be lower.

The parameters that influence the freeze crystallization process feature some obscure phenomena. Since it has been shown that slow freezing (i.e. a low ice growth rate) due to a small temperature gradient contributes to a higher purification efficiency, the production of ice mass over time is also low. If higher ice production is desired, the purification efficiency will be reduced due to the higher temperature gradient needed in addition to the higher energy consumption. These aspects can challenge the design and optimization of the process, in both natural and suspension freezing.

The key issue in natural freezing is whether the ice mass production over time is at a reasonable level related to the ground surface area required for the construction of basins. In future studies on the practical application of a suspension freeze crystallizer, the energy balance and consumption will be one of the main interests, as the possibility for the exploitation of natural cooling energy in Arctic regions is a strong motivator in terms of the energy efficiency and enormous cold energy source.

The fate of the concentrate formed due to the freezing process is both a challenge and an area of interest for future studies considering the further development of the treatment process. The freeze concentration method (or the production of concentrate) makes freezing a potential method for material recovery from wastewaters in the future. For instance, if it is possible to reach the saturation concentration of some compounds in the solution by freeze concentration, then the compound could be separated by evaporative crystallization more efficiently. Moreover, precipitation could be one of the potential methods in the recovery of valuable components. Clearly, possibilities for material reclamation (e.g. salts, nutrients) depend on the origin and characteristics of the wastewater, which also affect potential economic profitability.

5 Conclusions

This thesis presents the results obtained with four experimental systems of freeze crystallization in wastewater purification. The ice growth process and impurity removal efficiency of freeze purification were investigated in different experimental environments on various scales. The experiments were performed using the natural freezing method (i.e. ice growth in layers) and the suspension freeze crystallization method.

Natural freezing was demonstrated using model solutions and urban origin wastewater on two different laboratory scales and in various freezing conditions. The natural freezing process was rather complicated and challenging to control, as the system is easily exposed to various external parameters. Both natural freezing experiments confirmed the hypothesis that a higher purification efficiency can be achieved with lower ice growth rates. The study of model solutions (*Publication I*) showed that different chemical characteristics of impurities (EtOH, NaCl) in the solutions affect the structure and mechanical properties of the ice. Accordingly, distinct impurities seem to have a different effect on ice crystal growth mechanisms and the forming of impurity inclusions during the freezing, affecting the separation efficiency as well. Separation efficiencies from 47% to 86% were achieved for the model solutions at freezing temperatures from -15 °C to -5 °C. The average ice mass growth rates were between ~820 and ~450 g/(h·m^2), depending on the freezing temperature.

The effect of concentration on the ice growth rate was found to be minor in comparison with freezing conditions (the temperature or velocity of air flow) in freezing experiments with different concentrations of wastewaters (*Publication II*). In contrast, the freezing point depression (FPD) was found to indicate the concentration of wastewater (*Publication II*); the more concentrated the wastewater was, particularly with inorganics, the larger the freezing point depression was. This can be expected to influence the energy consumption of the freeze purification application, as the FPD will determine the minimum freezing temperature and thus also the required heat transfer.

The winter simulator experiments (*Publication II*) showed that the temperature has the most direct effect on the ice growth rate, but the air flow velocity was found to increase the growth significantly. Nonetheless, the ice growth rate was noticed to affect the separation efficiency in different ways in different wastewaters. In more concentrated wastewater, such as landfill leachate, the separation efficiency was observed to decrease more strongly as the ice growth rate increased. Very high separation efficiencies, up to 95% of COD, were achieved in the freeze purification of municipal wastewaters with very low ice growth rates. Similarly, separation efficiencies higher than 90% were obtained in the freeze purification of more concentrated landfill leachate. The average ice mass growth rates in experiments were roughly between 200 g/(h·m^2) (undercooling temperature 1 K and air flow velocity 0.5 m/s) and 1200 g/(h·m^2) (undercooling temperature 2 K and air flow velocity 3.0 m/s). The effect of freezing conditions on the ice mass growth rate and productivity can thus be considered very significant.

The empirical tests were conducted under real weather conditions in the environments of wastewater basins in a peat production area and at a mine site, and in a lake (*Publication III*). Contrary to even rather pessimistic expectations, these natural freezing tests showed relatively high separation efficiencies. This conclusion could be drawn based on comprehensive water quality analysis indicators used for all ice and water samples. The separation efficiencies varied between 65 and 90%. The highest, 90% efficiency was found in a highly concentrated wastewater system in an open pit basin of the mining site. Likewise, an efficiency of 88% was found within the freshwater lake, which can be considered very dilute in the concentration of impurities. In addition, a clear relationship between the ice purity and the ice strength was found: the more impure the ice was, the weaker it was, and the ice layer could thus be broken using less force.

The study of the suspension freeze crystallization included the development and design of a pilot-scale crystallizer and suspension freezing tests with landfill leachate. The separation process was proven successful, particularly considering that the up-scaling of the crystallization process is challenging in general. The main outcomes were the formation of relatively large ice crystals (500 µm) in water suspension, and high separation efficiencies of various impurities, >95-97%, which were determined by extensive analyses. The determination of a suitable undercooling temperature and the control of ice nucleation was found difficult, and thus, the freezing process proved to be rather complicated. Therefore, this information provides a good basis for the further development and research of suspension freeze crystallization in wastewater purification.

In summary, the studies presented in this thesis have increased the understanding and knowledge of freeze crystallization in wastewater purification. The freeze purification method is well suited for the treatment of various types of wastewaters from different sources. Accordingly, high removal efficiencies of impurities can be achieved in the treatment of wastewaters containing various concentrations of both organic and inorganic matter as well as suspended and dissolved impurities. This research provides valuable information about the effect of freezing conditions on the ice mass growth rate for ice productivity evaluation and the optimization of freeze purification processes.

The potential of freeze crystallization in wastewater purification is acknowledged due to its many benefits, such as high separation efficiencies and environmental sustainability. Future research could begin to focus more on application development in terms of material reclamation and reuse. In this regard, it would be important to investigate how efficiently specific fractions, such as micropollutants and plastics, can be separated from wastewater by freeze crystallization. In the same context, the energy efficiency achievable by the exploitation of natural cooling energy in Arctic regions would be important to evaluate thoroughly, particularly in the further development of the suspension freeze crystallizer.

References

Asthana, R. and Tewari, S.N. (1993). The engulfment of foreign particles by a freezing interface. *Journal of Materials Science*, 28, pp. 5414-5425.

Azouni, M.A., Kalita, W. and Yemmou, M. (1990). On the particle behaviour in front of advancing liquid-ice interface. *Journal of Crystal Growth*, 99, pp. 201-205.

Belén, F., Sánchez, J., Hernández, E., Auleda, J.M. and Raventós, M. (2012). One option for the management of wastewater from tofu production: Freeze concentration in a falling-film system. *Journal of Food Engineering*, 110(3), pp. 364-373.

Biggar, K.W., Donahue, R., Sego, D., Johnson, M. and Birch, S. (2005). Spray freezing decontamination of tailings water at the Colomac Mine. *Cold Regions Science and Technology*, 42(2), pp. 106-119.

Bogdan, A., Molina, M.J., Tenhu, H., Bertel, E., Bogdan, N. and Loerting, T. (2014). Visualization of freezing process in situ upon cooling and warming of aqueous solutions. *Scientific Reports*, 4 (7414).

Bogdan A. and Molina, J. (2017). Physical chemistry of the freezing process of atmospheric aqueous drops. *The Journal of Physical Chemistry A*, 121(16), pp. 3109-3116.

Brini, E., Fennell, C.J., Fernandez-Serra, M., Hribar-Lee, B., Lukšič, M. and Dill, K.A. (2017). How water's properties are encoded in its molecular structure and energies. *Chemical Reviews*, 117, pp. 12385−12414.

Brumberg, A., Hammonds, K., Baker, I., Backus, E.H.G., Bisson, P.J., Bonn, M., Daghlian, C.P., Mezger, M. and Shultz, M.J. (2017). Single-crystal I_h ice surfaces unveil connection between macroscopic and molecular structure. *PNAS*, 114 (21), pp. 5349-5354.

Butler, E., Hung, Y-T., Ahmad, M.S.A., Yeh, R. Y-L., Liu, R. L-H. and Fu, Y-P. (2017). Oxidation pond for municipal wastewater treatment. *Applied Water Science*, 7, pp. 31–51.

Butler, M. (2002). Freeze concentration of solutes at the ice/solution interface studied by optical interferometry. *Crystal Growth & Design*, 2 (6), pp. 541-548.

Chang, J., Zuo, J., Lu, K-J. and Chung, T-S. (2016). Freeze desalination of seawater using LNG cold energy. *Water Research*, 102, pp. 282-293.

Chen, P., Chen, X.D. and Free, K.W. (1996) Measurement and data interpretation of the freezing point depression of milks. *Journal of Food Engineering*, 30, pp. 239-253.

Chen, X.D. and Chen, P. (1996). Freezing of aqueous solution in a simple apparatus designed for measuring freezing point. *Food Research International*, 29 (8), pp. 723-729.

Chivavava, J., Rodriguez Pascual., M. and Lewis A.E. (2014). Effect of operating conditions on ice characteristics in continuous eutectic freeze crystallization. *Chemical Engineering & Technology*, 37(8), pp. 1314-1320.

Erlbeck, L. Rädle, M., Nessel, R., Illner, F., Müller, W., Rudolph, K., Kunz, T. and Methner, F.-J. (2017). Investigation of the depletion of ions through freeze desalination. *Desalination,* 407, pp. 93–102.

Erlbeck, L., Wössner D., Schlachter, K., Kunz T., Methner, F.-J. and Rädle, M. (2019). Investigation of a novel scraped surface crystallizer with included ice-pressing section as new purification technology. *Separation and Purification Technology*, 228, 115748.

Feng, W., Yin, Y., De Lourdes Mendoza, M., Wang, L., Chen, P., Liu, Y., Cai, L. and Zhang, L. (2018). Oil recovery from waste cutting fluid via the combination of suspension crystallization and freeze-thaw processes. *Journal of Cleaner Production*, 172, pp. 481-487.

Gallo, P., Amann-Winkel, K., Angell, C.A., Anisimov, M.A., Caupin, F., Chakravarty, C., Lascaris, E., Loerting, T., Panagiotopoulos, A.Z., Russo, R., Sellberg, J.A., Stanley, H.E., Tanaka, H., Vega, C., Xu, L. and Pettersson L.G.M. (2016). Water: A tale of two liquids. *Chemical Reviews*, 116, pp. 7463−7500.

Gao, W., Habib, M. and Smith, D.W. (2009). Removal of organic contaminants and toxicity from industrial effluents using freezing process. *Desalination*, 245, pp. 108-119.

Gao, W. and Shao, Y. (2009). Freeze concentration for removal of pharmaceutically active compounds in water. *Desalination,* 249, pp. 398-402.

Gao, W., Smith, D.W. and Sego, D.C. (1999). Ice nucleation in industrial wastewater. *Cold Regions Science and Technology*, 29, pp. 121-133.

Gao, W., Smith, D.W. and Sego, D.C. (2004). Treatment of pulp mill and oil sands industrial wastewaters by the partial spray freezing process. *Water Research,* 38, pp. 579-584.

GEA (2020). *Freeze Concentrators.* [Retrieved 31.1.2020], url: https://www.gea.com/en/productgroups/evaporators_crystallizers/freeze_concentrators/index.jsp

Hammonds, K. and Baker, I. (2016). The effects of Ca^{++} on the strength of polycrystalline ice. *Journal of Glaciology*, 62, pp. 954-962.

Hammonds, K. and Baker, I. (2018). The effects of H_2SO_4 on the mechanical behavior and microstructural evolution of polycrystalline ice. *Journal of Geophysical Research: Earth Surface*, 123, pp. 535-556.

Hasan, M., Filimonov, R., John, M., Sorvari, J. and Louhi-Kultanen, M. (2018). Influence and CFD analysis of cooling air velocity on the purification of aqueous nickel sulfate solutions by freezing. *AIChE Journal*, 64, pp. 200–208.

Hasan, M. and Louhi-Kultanen, M. (2015). Ice growth kinetics modeling of air-cooled layer crystallization from sodium sulfate solutions. *Chemical Engineering Science*, 133, pp. 44–53.

Hasan, M. and Louhi-Kultanen, M. (2016). Water purification of aqueous nickel sulfate solutions by air cooled natural freezing. *Chemical Engineering Journal*, 294, pp. 176-184.

Hasan, M., Partanen, J.I., Vahteristo, K.P. and Louhi-Kultanen, M. (2014). Determination of the Pitzer interaction parameters at 273.15 K from the freezing-point data available for NaCl and KCl solutions. *Industrial and Engineering Chemistry Research*, 53, pp. 5608-5616.

Hasan, M., Rotich, N., John, M. and Louhi-Kultanen, M. (2017). Salt recovery from wastewater by air-cooled eutectic freeze crystallization. *Chemical Engineering Journal*, 326, pp. 192-200.

Haynes, W. M. (Ed.) (2017). *CRC Handbook of Chemistry and Physics*. 97th Edition (Internet Version 2017), CRC Press/Taylor & Francis, Boca Raton, FL.

Ho, L.T., Alvarado, A., Larriva, J., Pompeu, C. and Goethals, P. (2019). An integrated mechanistic modeling of a facultative pond: Parameter estimation and uncertainty analysis. *Water Research*, 151, pp. 170-182.

Iliescu, D. and Baker, I. (2007). The structure and mechanical properties of river and lake ice. *Cold Regions Science and Technology*, 48(3), pp. 202-217.

Kapembwa, M., Rodriguez Pascual, M. and Lewis, A. (2014). Heat and mass transfer effects on ice growth mechanisms in pure water and aqueous solutions. *Crystal Growth & Design*, 14, pp. 389-395.

Koop, T., Luo, B., Tsias, A. and Peter, T. (2000). Water activity as the determinant for homogeneous ice nucleation in aqueous solutions. *Nature*, 406, pp. 611–614.

Körber, Ch., Rau, G., Cosman, M.D. and Cravalho E.G. (1985). Interaction of particles and a moving ice-liquid interface. *Journal of Crystal Growth*, 72, pp. 649-662.

Launiainen J. and Cheng B. (1998). Modelling of ice thermodynamics in natural water bodies. *Cold Regions Science and Technology*, 27, pp. 153-178.

Lemmer, S., Klomp, R., Ruemekorf, R. and Scholz, R. (2001). Preconcentration of wastewater through the Niro freeze concentration process. *Chemical Engineering Technology*, 24(5), pp. 485-488.

Leppäranta, M. (2015). *Freezing of lakes and the evolution of their ice cover*. Springer Berlin Heidelberg.

Light, B., Maykut, G.A. and Grenfell, T.C. (2003). Effects of temperature on the microstructure of first-year arctic sea ice. *Journal of Geophysical Research: Oceans*, 108 (C2): 3051.

Lorain, O., Thiebaud, P., Badorc E. and Aurelle, Y. (2001). Potential of freezing in wastewater treatment: Soluble pollutant applications. *Water Research*, 35(2), pp. 541-547.

Lovering, K.A., Bertram, A.K. and Chou, K.C. (2017). Transient phase of ice observed by sum frequency generation at the water/mineral interface during freezing. *Journal of Physical Chemistry Letters*, 8, pp. 871-875.

Matsumoto, M., Saito, S. and Ohmine, I. (2002). Molecular dynamics simulation of the ice nucleation and growth process leading to water freezing. *Nature*, 416, pp. 409-413.

Moore, E. and Molinero, V. (2011). Structural transformation in supercooled water controls the crystallization rate of ice. *Nature*, 479, pp. 506-509.

Mullin, J. W. (2001). *Crystallization*. 4th ed., Oxford: Butterworth-Heinemann.

Parker, L. and Martel J. (2002). Long-term survival of enteric microorganisms in frozen wastewater. US Army Corps of Engineers. Cold Regions Research and Engineering Laboratory. Technical report 02-16.

Petrenko, V.F. (1993). Electrical properties of ice. US Army Corps of Engineers. Cold Regions Research and Engineering Laboratory. Special Report 93-20.

Petrenko V.F. and Whitworth R.W. (2002). *Physics of Ice*. Oxford University Press Inc., New York. ISBN 0-19-851894-3.

Prasse, G., Stalter, D., Schulte-Oehlmann, U., Oehlmann, J. and Ternes, T.A. (2015). Spoilt for choice: A critical review on the chemical and biological assessment of current wastewater treatment technologies. *Water Research*, 87, pp. 237-270.

Randall, D.G., Nathoo, J., and Lewis A.E. (2011). A case study for treating a reverse osmosis brine using Eutectic Freeze Crystallization - approaching a zero waste process, *Desalination*, 266 (1-3), pp. 256-262.

Randall, D.G., Nathoo, J., Genceli-Güner, F.E., Kramer, H.J.M., Witkamp, G.J. and Lewis A.E. (2012). Determination of the metastable ice zone for a sodium sulphate system. *Chemical Engineering Science*, 77, pp. 184-188.

Randall, D.G., Zinn, C. and Lewis A. E. (2014). Treatment of textile wastewaters using Eutectic Freeze Crystallization. *Water Science & Technology*, 70(4), pp. 736-741.

Rahman, M.S., Guizani, N., Al-Khaseibi, M., Al-Hinai, S.A., Al-Maskri, S.S. and Al-Hamhami, K., (2002). Analysis of cooling curve to determine the end point of freezing. *Food Hydrocolloids*, 16, pp. 653-659.

Rodriguez-Narvaez, O.M., Peralta-Hernandez, J.M., Goonetilleke, A. and Bandala, E.R. (2017). Treatment technologies for emerging contaminants in water: A review. *Chemical Engineering Journal*, 323, pp. 361–380.

Rodriguez Pascual, M., Genceli, F.E., Trambitas, D.O., Evers, H., Van Spronsen, J. and Witkamp, G.J. (2010). A novel scraped cooled wall crystallizer: Recovery of sodium carbonate and ice from an industrial aqueous solution by eutectic freeze crystallization. *Chemical Engineering Research and Design*, 88(9), pp. 1252-1258.

Rumble, J.R., ed. (Internet Version 2019). *CRC Handbook of Chemistry and Physics*. 100th ed., CRC Press/Taylor & Francis, Boca Raton, FL.

Ryzhkin, I.A. and Petrenko, V.F. (1997). Physical mechanisms responsible for ice adhesion. *Journal of Physical Chemistry B*, 101, pp. 6267-6270.

Shibkov, A.A., Zheltov, M.A., Korolev A.A., Kazakov, A.A. and Leonov, A.A. (2005). Crossover from diffusion-limited to kinetics-limited growth of ice crystals. *Journal of Crystal Growth*, 285, pp. 215-227.

Shirai, Y., Sugimoto, T., Hashimoto, M., Nakanishi, K., Matsuno, R. (1987). Mechanism of Ice Growth in a Batch Crystallizer with an External Cooler for Freeze Concentration. *Agricultural and Biological Chemistry*, 51(9), pp. 2359-2366.

Shirai, Y., Wakisaka, M., Miyawaki, O. and Sakashita, S. (1998). Conditions of producing an ice layer with high purity for freeze wastewater treatment. *Journal of Food Engineering*, 38(3), pp. 297-308.

Shirai, Y., Wakisaka, M., Miyawaki, O. and Sakashita, S. (1999). Effect of seed ice on formation of tube ice with high purity for a freeze wastewater treatment system with a bubble-flow circulator. *Water Research*, 33(5), pp. 1325-1329.

Shultz, M.J., Bisson P. J. and Brumberg, A. (2014). Best face forward: crystal-face competition at the ice–water interface. *The journal of Physical Chemistry B*, 116, pp. 7972-7980.

van Spronsen, J., Rodriguez Pascual, M., Genceli, F.E., Trambitas, D.O., Evers, H. and Witkamp G. J. (2010). Eutectic freeze crystallization from the ternary Na_2CO_3–$NaHCO_3$–H_2O system: A novel scraped wall crystallizer for the recovery of soda from an industrial aqueous stream. *Chemical Engineering Research and Design*, 88(9), pp. 1259-1263.

Sulzer (2020). *Produce best-in-class concentrates with freeze concentration*. [Retrieved 31 January 2020], url: https://www.sulzer.com/en/shared/products/freeze-concentration

Tchobanoglous, G., Burton, F.L. and Stensel, D.H. (2003). *Wastewater engineering: Treatment and reuse*. 4th ed. McGraw-Hill, New York.

Timco, G. and Weeks, W. (2010). A review of the engineering properties of sea ice. *Cold Regions Science and Technology*, 60(2), pp. 107-129.

Vali, G., DeMott, P.J., Möhler, O. and Whale, T.F. (2015). Technical Note: A proposal for ice nucleation terminology. *Atmospheric Chemistry and Physics*, 15, pp. 10263-10270.

Wakisaka, M., Shirai, Y. and Sakashita, S. (2001). Ice crystallization in a pilot-scale freeze wastewater treatment system. *Chemical Engineering and Processing: Process Intensification*, 40(3), pp. 201-208.

Whale, T.F., Holden M.A., Wilson, T.W., O'Sullivan, D. and Murray, B.J. (2018). The enhancement and suppression of immersion mode heterogeneous ice-nucleation by solutes. *Chemical Science*, 9, pp. 4142-4151.

Widehem, P. and Cochet, N. (2003). *Pseudomonas syringae* as an ice nucleator - application to freeze concentration. *Process Biochemistry*, 39, pp. 405-410.

Williams, P.M., Ahmad M., Connolly, B.S. and Oatley-Radcliffe, D.L. (2015). Technology for freeze concentration in the desalination industry. *Desalination* 356, pp. 314-327.

WWAP (World Water Assessment Programme) (2017). 2017 UN World Water Development Report: Wastewater, the Untapped Resource [Retrieved 4 October 2019], url: https://reliefweb.int/report/world/2017-un-world-water-development-report-wastewater-untapped-resource

Yin, Y., Yang, Y., de Lourdes Mendoza, M., Zhai, S., Feng W.L., Wang, Y., Gu, M., Cai, L. and Zhang, L. (2017). Progressive freezing and suspension crystallization methods

for tetrahydrofuran recovery from Grignard reagent wastewater. *Journal of Cleaner Production,* 144, pp. 180-186.

Zhang, Y., Li, C., Zhang, X., Shi, X. and Li, W. (2011). The research on purification mechanism of natural cool energy and its application in wastewater treatment. *Energy Procedia*, 5, pp. 2554-2561.

Publication I

John, M., Suominen, M., Kurvinen, E., Hasan, M., Sormunen, O.-V., Kujala, P., Mikkola, A., and Louhi-Kultanen, M.
Separation efficiency and ice strength properties in simulated natural freezing of aqueous solutions

Reprinted with permission from
Cold Regions Science and Technology
Vol. 158, pp. 18-29, 2019

Cold Regions Science and Technology 158 (2019) 18–29

Contents lists available at ScienceDirect

Cold Regions Science and Technology

journal homepage: www.elsevier.com/locate/coldregions

Separation efficiency and ice strength properties in simulated natural freezing of aqueous solutions

Miia John[a,*], Mikko Suominen[b], Emil Kurvinen[c], Mehdi Hasan[a], Otto-Ville Sormunen[b], Pentti Kujala[b], Aki Mikkola[c], Marjatta Louhi-Kultanen[a,d]

[a] Separation and Purification Technology, LUT School of Engineering Science, Lappeenranta University of Technology, P.O. Box 20, FI-53850 Lappeenranta, Finland
[b] Department of Mechanical Engineering, School of Engineering, Aalto University, P.O. Box 15300, FI-00076 Aalto, Finland
[c] Department of Mechanical Engineering, LUT School of Energy Systems, Lappeenranta University of Technology, P.O. Box 20, FI-53850, Lappeenranta, Finland
[d] Department of Chemical and Metallurgical Engineering, School of Chemical Engineering, Aalto University, P.O. Box 16100, FI-00076 Aalto, Finland

ARTICLE INFO

Keywords:
Flexural strength
Ice purity
Natural freezing
Natural frequency

ABSTRACT

In geographical regions with sub-zero temperatures, natural freezing can potentially be used as an energy-efficient purification technique for industrial wastewaters. The utilization of this technique requires knowledge of the effect of impurities on the strength of the ice to enable the effective harvesting of produced ice. Previous studies of the mechanical properties of model-scale ice have tended to focus on the initial solution, and little consideration has been given to the amount of impurities trapped inside the ice. The aim of this research is to evaluate the separation efficiency during the natural freezing process by quantifying the impurities trapped inside the ice formed from known concentrations of aqueous solutions and to investigate the effect of impurities on the bulk mechanical properties of the ice.

In this study, twenty similar size ice beams were prepared in freezing boxes in a temperature-controlled cold room from five different aqueous solutions – tap water, and ethanol and sodium chloride aqueous solutions of two different molalities, i.e. 0.1 mol/kg and 0.3 mol/kg. The bending strength and natural frequencies of the ice samples were measured in the freezing conditions, and the concentrations of impurities in melted ice samples were determined. The research shows that with the ethanol and sodium chloride solutions, the concentration of impurities inside the ice clearly decreased in comparison to the initial solution. The structure of the ice from the different solutions differed significantly; as the tap water formed columnar ice, ethanol ice grew through large platelets, while the structure of the sodium chloride ice was a mixture of the two forms. The tap water yielded the highest strength ice and the ice formed from the ethanol aqueous solutions the weakest ice. The measurements indicated that the concentration of impurity in the ice reduces the mechanical strength and the magnitude of the effect varies with the chemical characteristic of impurity.

1. Natural freeze crystallization and mechanical properties of ice

The insufficiency of accessible water and worsening of water quality due to industrial discharges have made it necessary to find alternative and energy efficient water purification methods. The conventional processes to treat wastewaters are adsorption, chemical precipitation, electrolytic treatment, flotation, ion exchange, and membrane filtration, which all have unique properties and suitable water types. Natural freezing is an alternative method to achieve purification. When freezing is implemented in a wastewater basin under natural weather conditions, the cooling energy of arctic sub-zero temperature regions can be utilized to energy efficient wastewater treatment. A pure ice layer is forming over the wastewater basin similar way as in lakes, rivers and seas. A conceptual approach for wastewater purification by natural freezing is presented in Fig. 1.

During the freezing of a solution, heat of crystallization is released into the surroundings. The ice crystal lattice usually rejects solute molecules/ions because of their excessive size, preventing the formation of a solid solution with water (Petrich and Eicken 2010). Thus, solutes redistribute during ice crystallization. The extent of the redistribution is attributed to the capability of the solute to diffuse away from the ice-solution interface (Butler 2002). Succeeding these points of view, the temperature and concentration gradients are created adjacent to the growing ice front (Butler 2002; Hasan and Louhi-Kultanen 2015).

* Corresponding author.
E-mail address: miia.john@lut.fi (M. John).

https://doi.org/10.1016/j.coldregions.2018.11.006
Received 16 February 2018; Received in revised form 29 June 2018; Accepted 7 November 2018
Available online 08 November 2018

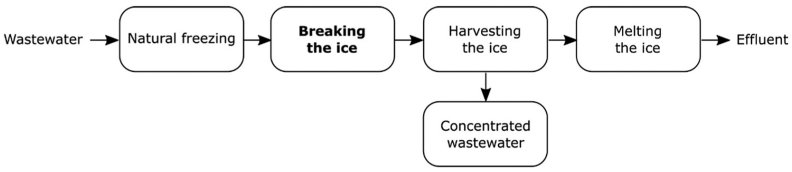

Fig. 1. Conceptual approach for wastewater purification by natural freezing.

Sea ice is a paradigm of natural freezing. The main source of impurity in sea-ice is the formation of brine pockets within the ice matrix (García et al. 2014). Analogously, the impurity of ice forming from any type of solution could be interpreted by the entrapment of the freeze concentrated solution in the ice crystal lattice. The efficiency of natural freezing is influenced by solution concentration and different growth conditions, such as the ambient temperature, freezing time and freezing rate. The effect of these factors on ice purity is epitomized by ice formation from sodium sulphate solutions. Experimental results show that a lower growth rate and solution concentration are in favour of higher ice purity (Butler 2002).

The mechanical properties of ice have been the interest of research in glaciology and geosciences for decades (Schulson and Duval 2009) and many different methods have been utilized in various studies. The dynamic modulus of elasticity of freshwater and saline ice has been studied by Snyder et al. (2016) with ultrasonic measurement. The effect of porosity on the dynamic modulus of elasticity found to be aligned with earlier researches (Snyder et al. 2015; Schulson and Duval 2009). Yasui et al. (2017) used a three-point bending test for determining the fracture toughness of ice. The Acoustic Emission (AE) was utilized to detect failure in a cyclic test of ice (Hammond et al. 2018). The effects of various mixtures of compounds on formed ice have also been an interest of studies. Recent research has been focused on studying the effect of freshwater ice and silica mixture on the mechanical properties of ice (Yasui et al. 2017) and sulfuric acid doped ice under tension and compression (Hammonds and Baker, 2018). The effects of $Ca++$ doped ice to the ice strength (Hammonds and Baker 2016) and the mechanical properties of saline ice (Snyder et al. 2016) have been studied as well.

The strength of sea ice and parameters affecting the strength have been the object of study for decades. In terms of impurities, the salinity (through brine volume) has been observed to have a clear effect on the mechanical properties of ice, see e.g. Timco and O'Brien (1994) for the flexural strength and Timco and Weeks (2010) for modulus of elasticity. Timco and O'Brien (1994) have combined several databases and shown that the flexural strength can be determined based on the square root of the brine volume, which can be determined based on temperature and salinity. Values over 1.5 MPa have been measured for the flexural strength of first-year sea ice, but values typically range from 1 MPa and decrease with the brine volume, being of the order of 100 to 150 kPa for warm sea ice (Timco and Weeks 2010). The estimates for the flexural strength of old ice, i.e. second year and multiyear sea ice, would be of the order of 0.8 to 1.1 MPa in the winter and 0.4 to 0.6 MPa in the summer (Timco and Weeks 2010). In the Baltic Sea, the four-point bending tests have shown the flexural strength to be 0.58 MPa on average and from 0.42 MPa to 0.55 MPa when determined form cantilever beam tests (Enkvist 1972; Määttänen 1976; Kujala et al. 1990).

In addition, the studies have shown that the brine volume has a clear effect on the elastic and static modulus. The elastic modulus here refers to Young's modulus (E) determined with dynamic measurements and a static modulus to Young's modulus determined from static tests. The dynamic measurements are commonly determined by measuring the rate of wave propagation in ice or by exciting the natural resonant frequencies of different vibration modes (Weeks and Hibler 2014). The experimental results have shown that the values of the elastic modulus vary between 1.7 and 5.7 GPa when determined from flexural waves, and from 1.7 to 9.1 GPa when determined from body-wave velocities (Weeks and Assur 1968). Anderson (1958) has shown that there is a clear decreasing trend in the elastic modulus as a function of brine volume. The static modulus for sea ice has been commonly determined from the bending tests (see e.g. Dykins 1971). Similar to dynamic tests, the static tests have shown that the static modulus decreases as a function of brine volume (see e.g. Vaudrey 1977). The static modulus measurements have shown a great scatter and the values have been, on average, between 1 and 5 GPa (Timco and Weeks 2010). For more detailed discussions on the effect of brine volume and other environmental factors on the elastic and static modulus of sea ice, see (Borland 1988; Hirayama 1983; Lau et al. 2007; Lehmus 1988; Nortala-Hoikkanen 1990; Riska et al. 1994; Weeks and Hibler 2014).

Besides salt (sodium chloride), the development of model scale ice has raised interest towards the effect of other chemicals on the strength of ice. The general conclusion is that adding these dopants to the water weakens the formed ice in terms of flexural strength (e.g. Borland 1988), and the elastic modulus (Hirayama 1983). As the flexural strength has been considered the most important mechanical property of ice for ship model scale testing, the development has focused on scaling the flexural strength correctly and then confirming that the ratios between other parameters are in the same range as with sea ice. Due to the typical size of the ships with respect to the size of the model scaled ships, the typical scale ratio for the model is 10 to 40, and thus, the required flexural strength is from 15 kPa to 60 kPa in model scale (Lau et al. 2007). Therefore, the minimum for the ratio between the static modulus and the flexural strength is 2000, and it can reach a value of 8000 (see e.g. Riska et al. 1994; Timco 1980).

Timco (1981) conducted the most extensive flexural strength tests with different chemicals. The chemicals included acetates, amides, various inorganic salts as well as sucrose with fixed mass fractions (Timco 1981). Timco (1981) compared the influence of various mass fractions of the selected chemicals on the flexural strength of ice. The higher mass fractions led to lower flexural strength of ice (Timco 1981). Furthermore, different model scale basins have ended up using different chemicals, which include urea, a mixture of ethylene glycol, aliphatic detergent and sugar (EG/AD/S), alcohol and sodium chloride (see e.g. Borland 1988; Hirayama 1983; Lau et al. 2007; Riska et al. 1994; Lehmus 1988; Nortala-Hoikkanen 1990), for studies with different types of model scale ice. The measurements have shown that with these chemicals combined with different ice production methods (seeding or spraying) the flexural strength can be scaled to 15–60 kPa with different solutions (Lau et al. 2007). However, the measurements have shown that the ratio between the elastic modulus and the flexural strength of the urea doped model ice is $< \mathbf{2000}$ (Hirayama 1983; Narita et al. 1988). The range for EG/AD/S doped ice is 1000–3000 (Timco 1986) and for the correct density (CD)-EG/AD/S 2000–3250 (Lau et al. 2007). The fine-grained ethanol ice, however, covers the ratio range of 1750–5000 (Riska et al. 1994).

However, in the development of the model scale ice, the interest is commonly in the initial solution and freezing process. Thus, the studies generally account for the mass concentration of the chemical in the initial solution and neglect how much of the chemical is trapped inside the ice, i.e. the amount of chemical actually affecting the properties of

the ice. These simplifications are usually for practical reasons (it is easier to observe and control the mass concentration of the initial solution and then check the obtained mechanical properties). Furthermore, due to the weakening effect of chemicals, the model scale ice is difficult to move from in-situ without damaging it. Thus, the static modulus is commonly determined from the plate deflection and the flexural strength is determined from a cantilever beam test, as recommended by ITTC guidelines (ITTC guidelines 2014). In addition, the dynamic measurements are conducted with a scanning laser Doppler vibrometer (SLDV) to measure the natural frequencies (Polytec 2017).

The natural frequencies of the ice indicate the internal structure dynamic behaviour for a known geometry, i.e. an ice beam. They can be considered a measure determining the mechanical dynamic property of the ice. (Rao 2007). The formed ice beams consisted of many interconnected different shaped, sized and oriented ice crystals. In this study, the complete ice beam dynamics response was measured. The ice in solid form was then assumed to behave like a solid particle, where the natural frequencies of a solid particle are fundamentally related to the square root of mass divided by stiffness (Carvill 1994). Knowing the natural frequencies of an ice sample allows calculating the equivalent modulus of elasticity, i.e. the overall stiffness, which is important to know when modelling the sample that has the same dynamical behaviour as the actual formed ice. Calculating the modulus of elasticity requires, in addition, knowledge of the ice sample's physical dimensions, density and area moment of inertia. For a beam shaped ice piece, the modulus of elasticity can be analytically calculated. The assumption is that the impurities captured in the ice have an impact on the stiffness of the ice and thus the impurities could be detected from the natural frequencies. The ice can be excited at natural frequencies, which causes energy to collect in the ice and the ice to yield and break into smaller parts.

In the application of wastewater purification by freezing, measuring and determining the mechanical properties of ice are important. This information can be used to estimate the ice strength and to evaluate the needed force for breaking and collecting the ice in a purification process application. Analysing the ice strength by the four point bending test has been found to be accurate and commonly used method (Kujala et al. 1990). Compared with the three point bending test, the shear force does not change rapidly in the location where the failure is assumed to occur, i.e. in the middle of the loaded beam, as can be seen from beam theories, see e.g. (Parnes 2001). The advantage of using simple beam tests over the cantilever beam tests is that root stresses do not disturb the measurements by lowering the measured flexural strength values as noted by Timco and O'Brien (1994). The information about the ice mechanical rigidity can be gained through measuring the natural frequencies. Natural frequencies can be measured without breaking the ice sample e.g. by exciting the ice externally, recording the velocity response and post-processing it. Natural frequencies can be detected with non-contact and non-destructive method, which is beneficial for detecting the ice mechanical rigidity.

Hence, the aim of this research is to determine the amount of ethanol and sodium chloride trapped inside the laboratory-produced ice and their effect on the mechanical properties of the ice: the flexural strength, static and dynamic elastic modules. These parameters are required when designing a wastewater purification apparatus and testing the performance of ice breaking vessels.

2. Freezing test procedure

To our best understanding, the chemical quantity in the solution determined by the molality (moles of chemical per kg of water) is a better measure for the comparison of chemical impacts than using the mass percent (wt-%) based quantity due to the different molar masses of the studied chemicals. The molar mass of sodium chloride NaCl, 58.443 g/mol, is much higher than the molar mass of ethanol C_2H_5OH, 46.068 g/mol (Haynes 2017). Due to this fact, in the present work we fixed the solute quantities based on molality (mol chemical/kg tap water). In this study, five different solutions were prepared: tap water (basic liquid), two organic aqueous solutions and two inorganic aqueous solutions, both with two different molal concentrations, 0.1 mol/kg and 0.3 mol/kg. The initial solution was mixed in a 100 kg batch. The solutions were prepared in room temperature and an agitator was used to achieve sufficient mixing during dissolution. The initial aqueous ethanol solutions were prepared by dissolving ethanol (ETAX B16 with 92.4% ethanol content supplied by Altia Industrial) in tap water. The initial aqueous sodium chloride solutions were prepared by dissolving 99.9% pure sodium chloride (supplied by VWR Chemicals) in tap water. The tap water was high-quality drinking water with a temperature of 13–15 °C at that time. The quality of water is guaranteed by the water supplier and contains very low concentrations of impurities due to requirements. Samples of 500 ml from every five initial solutions were obtained after preparation. The solutions were carried in lidded containers to a cool storage where they awaited further test preparation.

After the solutions were prepared, each batch was divided into four freezing boxes made of insulated material, Finnfoam (housing insulation material, polystyrene), to prevent freezing on the sides and bottom, i.e. the cold was affecting the surface layer while the foam walls insulated the sides and bottom, thus replicating natural freezing. Therefore, the heat flux migrated mainly from the solution through the ice layer to cooling air. In total, twenty similar freezing boxes were used in the freezing experiments. The boxes consisted of outer and inner boxes. The utilization of two boxes allowed removing of the ice sample with low effort, as the ice could be taken out easily by lifting the inner box with the sample. The inner dimensions of the inner boxes were 60 cm in length and 15 cm in width. The depth of the inner box was lower than the depth of the outer box, as the aim was to freeze half of the solution in maximum. Thus, the separation efficiency of natural freezing could be kept at moderate level when < 50% of solution is frozen (Hasan and Louhi-Kultanen 2016).

The interior of the outer freezing box was lined with plastic to make the box waterproof. The open section between the inner and outer boxes was insulated by placing a piece of joint insulation foam, commonly used in buildings, between the boxes. Thus, it prevented the boxes from freezing together. An elastic rope was placed into the box to mount the frozen samples for the natural frequency measurements. Prior to pouring the solutions, each box was weighed with a Sartorius LC 34000P balance (capacity 34 kg and readability 0.5 g). Each sample contained 24 kg of the initial solution and was weighed in room temperature.

After all of the boxes were prepared, weighed and filled with solutions, the boxes were taken into the cold room, where the targeted temperature was −5 °C. The samples were placed in the room in a four by five matrix form where each column formed a line of similar initial samples. The first row of solutions was closest to the door and the fourth row closest to the back wall. Fig. 2a shows the arrangement and naming of the samples. The naming is in sequential order. The first letter “P” refers to the tap water, “E” to the ethanol solution and “S” to the sodium chloride solution. The preceding numbers 1, 2, 3 and 4 represent the row number. The third item refers to the molality: “a” to 0.1 mol/kg and “b” to 0.3 mol/kg. The fourth letter refers to the ice section: “t” to the top (upper) section of the ice, “c” the centre section and “b” the bottom section. In the results, the naming labels, e.g. “E1at” refers to ethanol solution, row 1, molality of 0.1 mol/kg and top section. Fig. 2b shows the freezing arrangement in the cold room.

A temperature sensor was placed in each box in the first row to monitor the temperature in the liquid during freezing, and in addition, the ambient temperature was measured from the middle of the first row. A total of six PT100 thermometers were connected to two PicoLog PT-104 data loggers, which were connected via USBs to a laptop.

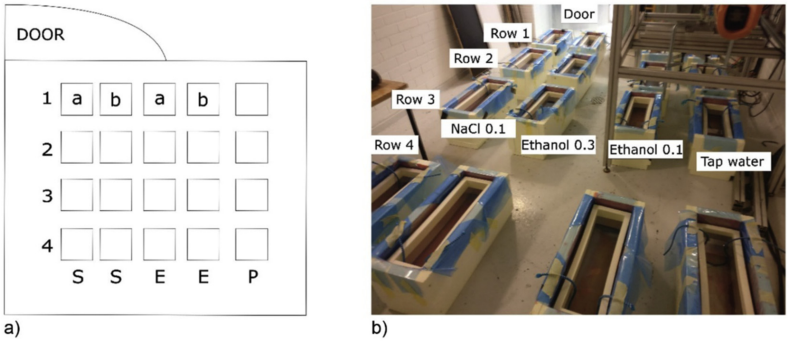

Fig. 2. Freezing arrangement. a) Layout of freezing boxes. b) Picture taken in the cold room (NaCl 0.3 has not been carried in yet).

2.1. Natural frequency

The natural frequencies were measured in the cold room to avoid the melting of the ice samples. The measurement was conducted with an optical scanning laser Doppler vibrometer (SLDV). The SLDV is a non-contact and non-destructive method of measuring surface velocities and consequently natural frequencies. The optical signal allows measuring through transparent media, e.g. glass or water. It is based on the Doppler effect and measures the surface velocity of excited ice. (Polytec 2017). In practice, the laser signal is focused on a predefined plane, which is the front of the measured sample. An example of using SLDV for measuring through a glass window into a water tank to measure an ultrasonic transducer far-field characteristics can be seen from Cooling et al. (2010). The ice was excited with a piezo exciter (PI P-844.10) and the frequency response was recorded at given locations. To be able to record the reflective laser signal, a 10 mm wide retro-reflective tape (A-RET-T010) was attached by freezing with a small amount of 0 °C tap water vertically on the upper surface of the ice. The possible detrimental effect of the retroreflective tape on the dynamic motion of the measurements can be neglected as the thickness of the tape (0.1 mm) is very small in comparison with the ice thickness (minimum ~30 mm). In addition, the small amount of water to bond the tape on the ice is so thin that the effect on dynamics is negligible.

The ice was hung with elastic rope, which was placed in the solution prior to freezing. There is a large difference in the stiffness of the ice and the elastic rope with which it is hung. This enables capturing only the ice internal dynamical behavior. The ice samples were also supported from the bottom to limit the rigid body motion. Fig. 3a depicts the hardware located outside the cold room: a Polytec PSV-500 scanning head and an OFV-505 reference laser pointed directly at the glass window. Fig. 3b depicts the ice hanging setup inside the cold room. The measurement procedure has three initial steps. The first is to set a measurement plane, that is in this case the top surface of the ice beam. Secondly, the visible laser is focused on the top of the plane. Thirdly, the 3D orientation is defined by the origo, Y-direction and XY-plane. The scanning hardware operation temperature is limited to the range of +5 to +40 °C; thus, the measurement was conducted through the transparent glasses. The piezo exciter's operating temperature is limited to −20 to +80 °C, and it could thus be used in the cold room to excite the ice sample. The exciter is made from steel and was stored in the cold room to avoid melting the ice sample when in contact with it. Fig. 3c depicts the front surface of the ice sample. The ice pieces that were strong enough to hang from the flexural rope were measured. The natural frequencies were measured from the upper surface of the ice and the excitation was given from the bottom layer.

The modulus of elasticity (via dynamic measurement) E_d is calculated based on beam theory

$$E_d = \frac{(f_n \bullet 2\pi)^2 \bullet A \bullet \rho \bullet L_B^4}{k^4 \bullet I}, \quad (1)$$

where f_n is the natural frequency, A is the cross sectional area, ρ is the ice density, L_B is the ice beam length, k is a factor dependent on the support. For free-free supported body, i.e. freely floating body, as is in this case, the factor for the first flexural natural frequency is 4.730, and I is the area moment of inertia. (Rao 2007).

2.2. Flexural strength

The flexural strength of ice was measured with a four-point bending test in the cold room. Fig. 4 presents the test setup. The test sample was placed on top of the rounded wooden supports. The two load sensors were mounted with an aluminium profile onto the electrically driven piston. The load sensors were HBM S2M 500 N. Rounded wooden parts were attached under the sensors, which were in contact with the ice beam in the loading. The rounded wood pieces allow rotational movement in the ice under loading. In each test, the displacement was measured at the mid span of the ice beam with HBM WA 10 mm displacement sensors. The forces and displacement were recorded with a frequency of 1.2 kHz.

After the loading, the distance of the breaking point was measured from the left-hand side support. In addition, the thickness and the width of the ice beam at the breaking point were measured. The ice beam is assumed to behave as an Euler-Bernoulli beam. At first, the moment equation along the beam is determined from the free-body diagram. It is assumed that the first failure in a bending situation occurs on the surface in tension, as the axial stress (in the longitudinal direction) maximum occurs on the surface of the beam. Knowing the relation (Parnes 2001):

$$\sigma_x = \frac{My}{I} \quad (2)$$

where σ_x is the axial stress, M is the moment affecting the cross-section, y is the distance from the neutral axis, and I is the second moment of inertia. Inserting the moment equation in this equation we obtain the following form for the flexural strength (σ_f):

$$\sigma_f = 3 \bullet \frac{(L-x) \bullet x \bullet \rho \bullet g}{h} + 6\frac{(L-x) \bullet a \bullet F_B + a \bullet x \bullet F_A}{L \bullet b \bullet h^2}, \quad (3)$$

where L is the distance between the supports, x is the distance of the crack from the left-hand side support, g is the gravitational acceleration, h is the thickness of ice, a is the distance of a sensor from the same side support, F_A is the load measured with the right load sensor, F_B is the

Fig. 3. Setup for measuring natural frequencies of the ice samples: a) Polytec vibrometer unit outside of the cold room b) ice sample hanging with flexible ropes and stabilized in the bottom with additional flexible ropes. c) Retroreflective tape frozen to the front surface of the ice.

load measured with the left load sensor, b is the width of the sample.

2.3. Static modulus of elasticity

The displacement was measured simultaneously with the force. This enables the determination of the static modulus of elasticity (E_s), i.e. the effective Young's modulus. In this case, the ice beam is assumed to behave as an Euler-Bernoulli beam. After the moment equation along the beam is determined, the displacement equation, w, for the beam can be derived from the following relation (Parnes 2001):

$$EI\frac{d^2w}{dx^2} = -M(x). \tag{4}$$

After the displacement equation is determined and the displacement is measured from a known location, the static modulus (E_s) of elasticity can be determined from the following equation:

$$E_s = \frac{(34 \cdot a \cdot L^2 - 64 \cdot a^3) \cdot F_B + 16 \cdot a \cdot L^2 \cdot F_A}{384 \cdot I \cdot w_{centre}}, \tag{5}$$

where the second moment of inertia (I) was determined by measuring the width and the height of the tested beam from the location the failure occurred and w_{centre} is the width at the failure location. This assumes the beam is solid with negligible porosity and uniform thickness and the width of the beam over the length.

Unfortunately, some of the ice beams were broken when taken out from the freezing boxes. 4 of 30 beams (or halves) broke before the measurements. The fourth row of ice was mainly too weak for the bending strength test. Row 2 ice was measured as full beams. Rows 1 and 3 ice beams were cut in half for the bending test and static modulus of elasticity. Due to the test set-up, it was not possible to mount the displacement sensor on the rig for samples broken when taken out from the freezing boxes, as the span between the supports was small.

2.4. Chemical analyses

The formed ice layer and concentrated residual solution under the ice layer were separated after the freezing test period by lifting up the ice layer from the freezing box. The total mass of the ice layer was

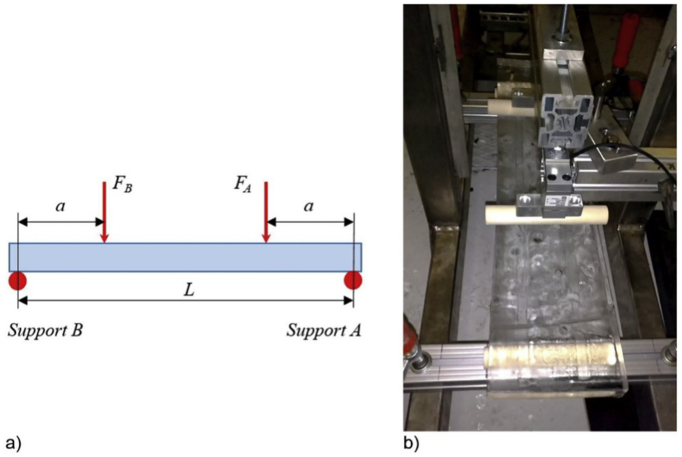

Fig. 4. Four-point bending test setup. a) The principle picture from the test. b) The device measuring the P4 ice sample.

weighed and the ice was moved to mechanical testing. A 500 ml sample was taken (after agitating the liquid) from the concentrated solution remaining in the box. After the mechanical tests of ice (the frequency measurement and flexural strength test), the ice samples for chemical analysis were collected within various horizontal layers sliced in sections of 1 to 4 cm thicknesses using a band saw. The ice pieces were rinsed with purified water, produced by Elga PureLab water system (resistivity 18.2 MΩ·cm, TOC < 5 ppb) to avoid external contamination during the ice handling. Composite ice samples from a layer were collected into a plastic bag for crushing with a hammer. The crushed ice was packed tightly in 250–500 ml polyethylene bottles for freeze storing, transporting and further chemical analysis. The total amount of samples was 70: 5 initial solution samples, 20 concentrated solution samples, 10 whole ice layer section cut samples and 35 ice layer samples from different horizontal layers. Furthermore, vertical and horizontal ice layer samples were cut and collected from the ice samples in rows two and three to visually observe the crystal structure by placing the samples between two polarizing films and directing light through the arrangement.

All freeze stored samples were melted at room temperature. The samples containing tap water and ethanol were analyzed with a total organic carbon (TOC) analyser (Shimadzu TOC-L + ASI-L Autosampler, detection limit 4 µg/l) to determine the concentration of total organic carbon. Ethanol concentrations were further calculated based on TOC concentrations. Molar mass of ethanol C_2H_5OH is 46.068 g/mol, of which 52.50% is carbon (Haynes 2017). Electrical conductivities of samples containing tap water and sodium chloride were measured by a Consort C3040 Multi-parameter analyser with conductivity electrode SK20T (range 1.0 µS/cm to 100 mS/cm, cell constant 1.0 1/cm). Sodium chloride concentrations were determined by linear fitting based on conductivity values reported in literature (Haynes 2017). The densities of all samples (melted ice, initial solution and concentrated solution) were determined by an Anton Paar DMA4500 density meter (repeatability with density $1{\cdot}10^{-5}$ g/cm^3 and temperature 0.01 °C). NaCl and ethanol concentrations were determined by linear fitting based on density values reported in literature (Haynes 2017).

3. Results

3.1. Temperature profile

The temperatures were recorded from the first row samples with an interval of one minute until the samples in the second last row (row 2) were taken out from the freezing boxes. Fig. 5 depicts the logged temperature profile, and the vertical lines indicate the times of ice removal from the boxes. At first, the cooling rates varied considerably due to the diverse temperatures of the liquids when the cooling and freezing started. After 45 h of freezing, temperatures of liquids attained final constant temperatures. Tap water, the 0.1 mol/kg NaCl solution and the 0.3 mol/kg NaCl solution stayed at temperatures −0.03 °C, −0.33 °C and − 1.07 °C, respectively, and were close to known freezing point depression (FPD) temperatures ~0 °C, −0.34 °C and − 1.02 °C reported in literature (Haynes 2017). The ethanol 0.1 mol/kg solution appeared slightly undercooled with a temperature of −0.28 °C when the FPD temperature is −0.17 °C (Haynes 2017). The 0.3 mol/kg ethanol solution was rather warm with a temperature of −0.42 °C when compared to the FPD temperature of −0.54 °C (Haynes 2017). Unexpectedly, this concentrated ethanol solution also started to cool down after 70 h of freezing, when the temperature of the freezing room was decreased and the solution reached an undercooled temperature of −1.7 °C. The temperature probe used for the 0.3 mol/kg sodium chloride solution shows a colder temperature after 70 h, as it was accidentally pulled out from the solution and exposed to the cold room temperature. The aim was to seed the solutions prior to ice forming. However, after ten hours, it was noted that frazil natural ice formed on the surface of tap water and 0.1 mol/kg ethanol solutions as well as rows three and four of 0.3 mol/kg ethanol solutions. Thus, these samples were not seeded, whereas all the sodium chloride solutions and ethanol solutions E1b and E2b were.

The samples in row four were taken out after 53 h of freezing at −5 °C. However, the samples were rather thin (P4 35 mm, E4a 12 mm and E4b 9 mm, S4a 22 mm and S4b 19 mm). The S4a and P4 samples were the only ones rigid enough to be hung from the flexural rope for the elastic modulus measurements. Then, the ice growth continued in other rows at lower temperatures for longer freezing times to be able to produce thicker ice layers for mechanical testing purposes. The temperature was first lowered to −15 °C for 13 h, and after that raised to −10 °C. As a result, the samples in row three were taken out after 75 h of freezing, of which 60 h was at −5 °C, 13 h at −15 °C and 2 h at −10 °C. The thicknesses of the ice samples were 59 to 72 mm and the samples were strong enough for the mechanical property tests. To stop the ice growth in the two remaining sample rows, the temperature was increased to −5 °C. The samples in rows two and one were frozen an additional 4.5 and 6 h, respectively, at −5 °C before removal from the freezing boxes.

3.2. Properties of ice

The ice samples could be distinguished from the outlook from the surface of the ice; see row a) in Fig. 6. From the left, the first column is

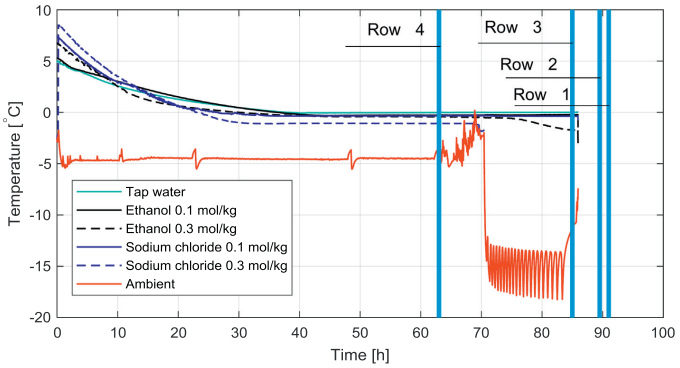

Fig. 5. Freezing temperatures and actions conducted during the measurement. Vertical lines represent the removal of each row of ice.

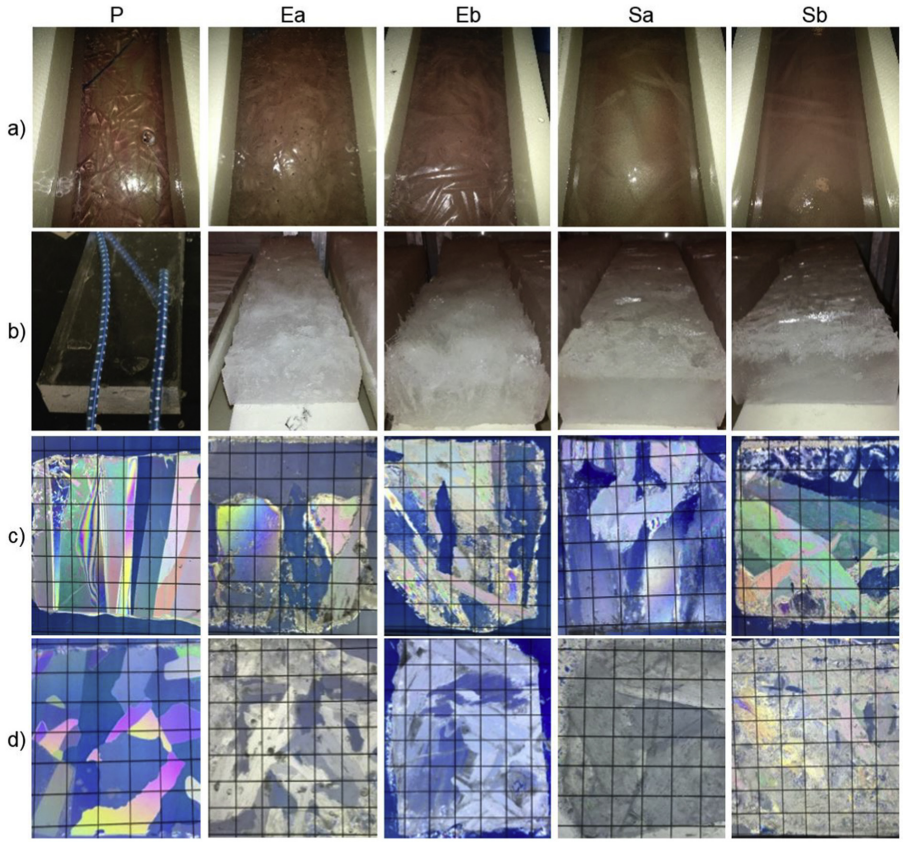

Fig. 6. Pictures of the ice samples (from row three). The columns from left to right are P, Ea, Eb, Sa, and Sb; a) the samples in the freezing boxes, b) the samples upside down after recovery, c) vertical thin sections from row two, and d) horizontal thin sections from row three. The scale bar is 1 cm × 1 cm.

tap water (P) ice, which was clear and did not contain any bubbles. The second (Ea) and third (Eb) columns are the ethanol solutions that had some bubbles and were not fully transparent. The fourth (Sa) and fifth columns (Sb) are the sodium chloride solution and appear cloudy. After the samples were taken out from the freezing boxes, they were placed bottom up on an even surface to protect the fragile bottom ice crystals; see row b) in Fig. 6. After the mechanical properties of the ice were measured, vertical and horizontal thin sections were prepared from the samples; see rows c) and d) in Fig. 6.

The ice from tap water (P) had the most homogeneous ice crystal structure. The ice samples were clearly transparent and the top and bottom surfaces were smooth. The ice structure was columnar, with all of the crystals oriented almost vertically; see the vertical thin section in Fig. 6c) and d). However, the crystal (or grain) size in the horizontal direction varied from 10 to 40 mm and was irregular. The irregular structure is considered to result from the unseeded origin of the ice growth, as earlier studies have shown that ice with a relatively homogeneous grain size can be obtained by seeding with ice crystals (Gow et al. 1988).

The ice grown from ethanol solutions (Ea and Eb) had the most irregular structure. The ice first grew an approximately 9 mm solid layer. After this layer, dendritic crystal platelets started to grow. The diameters of the platelets were up to 100 mm, the thickness was up to 5 mm, and the orientation appeared to be random. There were distinguished regions between the platelets, and many platelets were not connected. Fig. 7 shows the E4b sample after being taken out from the freezing box at this stage of the growth.

When the freezing continued, bridges between the platelets started to form, leading to a more solid ice structure. However, the bottom of the ice remained irregular and thin sections showed that the gaps had not fully closed; see Fig. 6c) and d). Thus, the ice was porous, and in some cases, the platelets growing together might have entrapped ethanol solution inside the ice.

The ice from the sodium chloride solution (Sa and Sb) had a structure between the tap water and ice frozen in the ethanol solution. The ice was cloudy and almost opaque. The top surface was smooth but the bottom surface rough. The ice grew in platelets, but thinner and smaller in diameter than in the ice obtained from the ethanol solution. The platelets were oriented locally in the same direction, see Fig. 6c) and d). The ice was also less porous than the ice obtained from the ethanol solution, as the platelets seemed to grow almost at the same rate. Thus, the ice formed in the sodium chloride solution was more

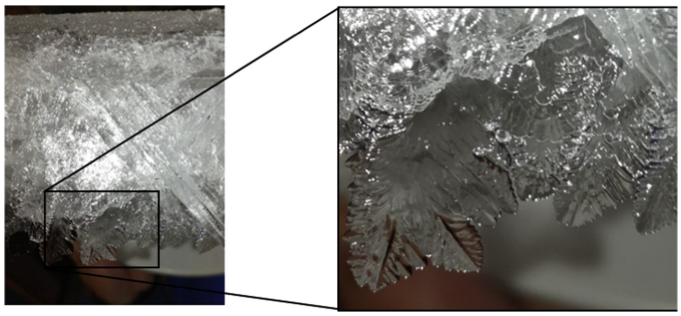

Fig. 7. Close-up of E4b ice structure from the side. On the top, approximately 9 mm of solid ice structure and then large dendritic platelets oriented towards the liquid.

solid than the ice obtained from the ethanol solution.

Prior to the mechanical and chemical measurements, the physical properties were measured. The average length of the ice samples was 567 mm and the width 143 mm. Table 1 presents the thickness, mass and growth rate of the samples. The chemical and mechanical properties were determined after physical measurements with the procedures described in Section 2. Table 1 and Table 2 present the results of the chemical and mechanical property measurements for each sample, respectively. The average ice layer growth rate ($\cdot 10^{-7}$ m/s) was calculated by the measured average ice layer thickness formed during freezing time. The average ice mass growth rate (g/h,m^2) was calculated by the mass of ice layer formed during freezing time per freezing area.

Average ice mass growth rates (g/h, m^2) of measured ice samples are plotted in Fig. 8 and average flexural strength values (kPa) in Fig. 9.

4. Discussion

In the following section, the average properties of each measurement are calculated from the samples of rows one, two and three, and results are compared. The samples of the fourth row were taken out first when the amount of ice was still very low and mechanical measurements could not be performed with three ice samples out of five.

4.1. Average ice properties of the tap water

Table 3 summarizes the average properties of tap water ice samples one to three. If the properties for the top and bottom layer were measured separately, the average of the layer measurement was used as a value for the sample. The tap water ice properties were measured for reference values to compare the difference in the ice structures grown in ethanol and sodium chloride solutions. As the ethanol and sodium chloride were mixed with the tap water, the effect on its properties was captured. The average mass of ice that was created was 5242 g, and the

Table 1
Physical and chemical properties of the ice.

	Sample	Ice mass	Thickness	TOC	Conductivity	Calculated molality	Ice layer growth	Ice mass growth
		g	mm	mg/l	µS/cm	mol/kg H_2O	$\cdot 10^{-7}$ m/s	g/h m^2
Tap water	P1	5702 (2787[1a)])	72 (45.6[1a)])	0.7 (3.9[2)])	15 (121.8[2)])	–	2.46	823
	P2	5224	66	0.2	2.9	–	2.30	769
	P3	4801 (2473[1a)])	61 (31[1a)])	0.7	6.7	–	2.26	749
	P4	2392	31	0.9	4.0	–	1.65	528
EtOH 0.1 m	E1a	4985	71	1174 (2349[2)])	–	0.044 (0.089[2)])	2.44	720
	E2a	5079	70	1452	–	0.053	2.44	747
	E3a	4987	66	1207	–	0.045	2.45	778
	E4a	2288	29	629.8	–	0.024	1.53	505
EtOH 0.3 m	E1b	4803	75	2293 (7401[2)])	–	0.091 (0.292[2)])	2.58	693
	E2b	5095	73	2959	–	0.119	2.56	750
	E3b	4800	72	2594	–	0.103	2.66	749
	E4b	2125	27	2230	–	0.086	1.42	469
NaCl 0.1 m	S1a	5196 (2410[3)])	66 (32.95[3)])	–	2922 (9610[2)])	0.029 (0.104[2)])	2.25	750
	S2a	5212	64	–	3010	0.030	2.24	767
	S3a	5067	63	–	2894	0.030	2.34	790
	S4a	2386	29	–	1622	0.015	1.51	526
NaCl 0.3 m	S1b	5071 (2193[1c)])	63 (29.8[1c)])	–	9285 (26200[2)])	0.101 (0.302[2)])	2.17	732
	S2b	4641	59	–	7580	0.080	2.06	683
	S3b	4592	59	–	9620	0.103	2.17	716
	S4b	1983	27	–	7710	0.082	1.40	438

[1a)] Mass and thickness of the bottom ice sample when measuring natural frequency
[1b)] Average mass from the top and bottom sections when measuring natural frequency
[1c)] Mass and thickness of the top ice sample when measuring natural frequency
[2)] TOC/conductivity/molality for the initial solution
[3)] Average mass and thickness from top and bottom sections of the natural frequency measurement

Table 2
Mechanical properties of the ice.

	Sample	Natural frequency (flexural)	Flexural strength	Dynamic Modulus of elasticity	Static Modulus of elasticity
		Hz	kPa	GPa	GPa
Tap water	P1	580.80[1a)]	971.00[1d)]	7.38	–
	P2	601.00	890.00	7.93	1.27
	P3	267.10[1a)]	1384.50[1d)]	8.00	6.08[1d)]
	P4	316.50	1072.00	9.24	4.57
EtOH 0.1 m	E1a	–	366.50[1d)]	–	–
	E2a	634.50	144.00	7.22	1.12
	E3a	620.00	275.50[1d)]	7.89	1.26[1d)]
	E4a	–	–	–	–
EtOH 0.3 m	E1b	–	128.50	–	–
	E2b	–	56.00	–	–
	E3b	–	146.67	–	–
	E4b	–	–	–	–
NaCl 0.1 m	S1a	288.05[1b)]	581.00[1d)]	6.82	3.93[1d)]
	S2a	407.60	202.00	3.95	0.58
	S3a	389.40	438.50[1d)]	3.69	7.69[1d)]
	S4a	230.80	248.00	6.83	–
NaCl 0.3 m	S1b	240.50[1c)]	622.00[1d)]	5.75	4.12[1d)]
	S2b	383.00	152.00	3.98	0.57
	S3b	474.50	303.50[1d)]	6.15	5.09[1d)]
	S4b	–	–	–	–

[1a)] Natural frequency of bottom ice part
[1b)] Average natural frequency of top and bottom sections.
[1c)] Natural frequency of the top ice part
[1d)] Average value from upper and lower part

measured density was 934 kg/m^3. The natural frequency is related to the thickness of the ice, as the width and length of the beams were identical. This gives a value for the stiffness of the ice that formed in relation to the thickness of the ice. The higher the value for Hz/mm is, the stiffer the formed ice layer is. The modulus of elasticity is calculated from the first flexural natural frequency and beam theory (Eq. 1). The static modulus of elasticity is calculated from the displacement during the flexural strength test that is based on a static test (Eq. 5). In addition, the flexural strength was measured for the created ice samples. The ice formed from the tap water has the highest natural frequency per thickness, modulus of elasticity and flexural strength; compare Table 3, Table 4and Table 5.

4.2. Average ice properties of the ethanol solutions

Table 4 shows the average properties for the ice grown from ethanol solutions. The ice formed from the 0.3 mol/kg solution was very weak, and only part of the measurements were possible to conduct. Compared to the tap water properties, the ice mass growth rate was lower but the ice layer growth rate was higher. The average natural frequency per thickness was lower, meaning that the ethanol ice was softer. The flexural strength was significantly lower compared to the tap water ice, which is also visible from the modulus of elasticity (static) that was determined from the four-point bending test. Table 4 shows that the ice that formed from the concentrated ethanol solution is clearly mechanically weaker, as expected. The average separation efficiency was 47% with a dilute 0.1 mol/kg ethanol solution and the effective distribution coefficient K was 0.53 (i.e. the ratio between impurity concentrations in the ice and in the initial solution), whereas with the concentrated 0.3 mol/kg ethanol solution the obtained K was 0.36 and separation efficiency 64%. In this case, the average separation efficiency was higher with a more concentrated initial solution.

4.3. Average ice properties of sodium chloride solutions

Table 5 shows the average properties for the ice samples formed from 0.1 and 0.3 mol/kg sodium chloride solutions. A comparison of Table 3 to Table 5 shows that the values of mechanical ice properties and ice growth rates for the sodium chloride solution are smaller than for tap water but higher than for the ethanol solution. In general, it was noticed that the ice formed from sodium chloride solutions are mechanically harder than the ice formed from ethanol solutions. The ice formed from a concentrated 0.3 mol/kg sodium chloride solution was mechanically harder (flexural strength 359 kPa) than ice formed from a dilute 0.1 mol/kg ethanol solution (262 kPa), even though the impurity concentration of sodium chloride ice was double when compared with the concentration of ethanol ice, i.e. 0.095 mol/kg vs. 0.047 mol/kg, respectively. The separation efficiency was 71% with a dilute 0.1 mol/kg sodium chloride solution (and the effective distribution coefficient, K, 0.29), whereas with a concentrated 0.3 mol/kg sodium chloride solution it was 69% (and K 0.31).

4.4. Comparison between the formed ice and to earlier studies

Table 6 depicts the discovered impurities of ice, ice growth rates and mechanical properties related to properties of tap water ice. The ethanol concentration 0.104 mol/kg in the ice (initial solution 0.3 mol/kg) reduced the flexural strength 90% when compared to the flexural strength of tap water ice. Sodium chloride concentration 0.095 mol/kg in the ice (initial solution 0.3 mol/kg) reduced the flexural strength 67%, while a half lower ethanol concentration 0.047 mol/kg in the ice (initial solution 0.1 mol/kg) generated a 76% strength reduction. Increasing the sodium chloride concentration in the ice from 0.030 mol/kg to 0.095 mol/kg did not have a very noticeable effect on the mechanical rigidity of the ice. The obtained natural frequency per thickness decreased only 9% with 0.047 mol/kg ethanol ice compared to tap water ice. Based on the research, the source of impurity is distinguishable from the differences in the natural frequencies of the ice beams, i.e. the effective stiffness of the ice is at a specific level.

The flexural strength results show that tap water ice is the strongest, as expected, and the ethanol solution ice is the weakest. This may partly

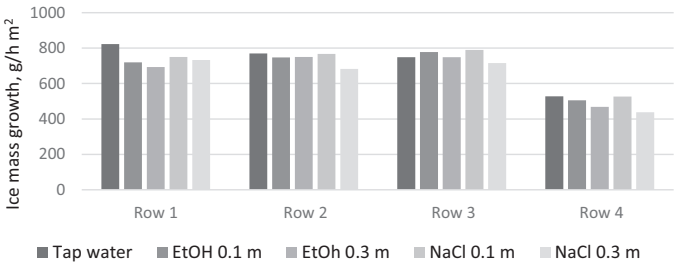

Fig. 8. Average ice mass growth rates (g/h m^2) of measured ice samples.

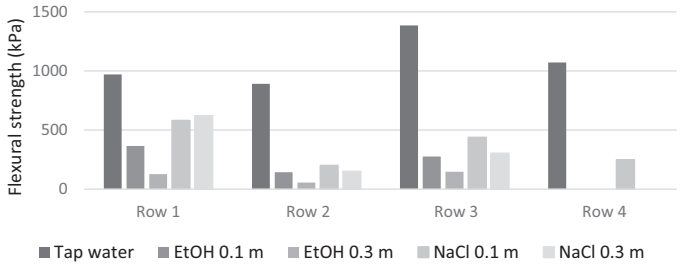

Fig. 9. Average flexural strength values (kPa) of measured ice samples.

Table 3
Averafge ice properties of the tap water samples one to three.

Property	Unit	Tap water
Mass growth rate per unit surface area	g/h m^2	780
Linear growth rate	m/s	$2.34{\cdot}10^{-7}$
Mass	g	5242
Density	kg/m^3	934
Natural frequency	Hz	483
Thickness	mm	66.33 (47.47)[1)]
Average natural frequency per mech. thickness	Hz/mm	10.17
Dynamic modulus of elasticity	GPa	7.77
Flexural strength	kPa	1082
Static modulus of elasticity	GPa	3.68

[1)] Average thickness from natural frequency measurements

Table 4
Average properties of ice obtained with ethanol solution concentrations 0.1 and 0.3 mol/kg.

Property	Unit	Ethanol 0.1 mol/kg H_2O	Ethanol 0.3 mol/kg H_2O
Mass growth rate per unit surface area	g/h m^2	748	731
Linear growth rate	m/s	$2.44{\cdot}10^{-7}$	$2.60{\cdot}10^{-7}$
Mass	g	5017	4899
Density	kg/m^3	907.6	–
Natural frequency	Hz	627	–
Thickness	mm	69 (68.05)[1)]	73.33
Average natural frequency per thickness	Hz/mm	9.21	–
Dynamic modulus of elasticity	GPa	7.56	–
Flexural strength	kPa	262	110
Static modulus of elasticity	GPa	1.2	–
Measured initial impurity molality in solution	mol/kg H_2O	0.089	0.292
Impurity molality in ice	mol/kg H_2O	0.047	0.104

[1)] Average thickness from natural frequency measurements.

result from the structure of the ice. As noted in the method description, the beams were assumed to be solid in the calculation of the second moment of inertia as it was not possible to measure the actual porosity. It should be noted that, especially, in the case of ethanol ice, the beams were to solid ice through the thickness and contained pores. Thus, the determined I is overestimating the stiffness that leads to the underestimation of the flexural strength in these cases. When compared the studied ice conformations, the structure of tap water ice was the most dense (less porous) and the orientation of the crystals columnar. Ethanol ice had large crystals oriented in different directions, and there were clear regions between the platelets. Thus, the ice was more porous, and concentrated ethanol solution might have been entrapped inside the ice when the platelets were freezing together, i.e. the ice was

Table 5
Average properties of ice obtained with sodium chloride solution concentrations 0.1 and 0.3 mol/kg.

Property	Unit	Sodium chloride 0.1 mol/kg H_2O	Sodium chloride 0.3 mol/kg H_2O
Mass growth rate per unit surface area	g/h m^2	769	710
Linear growth rate	m/s	$2.28{\cdot}10^{-7}$	$2.13{\cdot}10^{-7}$
Mass	g	5158	4768
Density	kg/m^3	961	938
Natural frequency	Hz	362	366
Thickness	mm	64.33 (53.35)[1)]	60.33 (49.13)[1)]
Average natural frequency per thickness	Hz/mm	6.78	7.45
Dynamic modulus of elasticity	GPa	4.82	5.29
Flexural strength	kPa	407	359
Static modulus of elasticity	GPa	4.07	3.26
Measured initial impurity molality of solution	mol/kg H_2O	0.104	0.302
Impurity molality in ice	mol/kg H_2O	0.030	0.095

[1)] Average thickness from natural frequency measurements

becoming more dense. The ice from sodium chloride solutions had a structure between these two – the crystals were oriented less randomly and the ice was less porous than the ethanol solution ice but not as dense and even-structured as tap water ice. Thin sections also showed that the crystals of the tap water ice were more rounded, whereas ethanol solution ice had platelet shaped crystals, and sodium chloride solution ice crystal shapes were between these two, see Fig. 6c and d.

When these conducted measurements are compared with the previous studies about naturally formed ice in lakes, rivers and seas, the results are reasonable. The tap water represents (in terms of salinity) freshwater ice and the measured values are similar to the values of freshwater ice. The strength of the sodium chloride solutions is similar to lower values of the sea ice strength. Also the static and dynamic elastic modulus values of the tap water and sodium chloride solutions are in the same range as with sea and freshwater ice. The ice grown from the ethanol solution showed higher values than those obtained with fine grained ethanol model scale ice as addressed by Riska et al. (1994). This is reasonable due to structural differences. When the fine grained ethanol ice is produced by spraying, see Von Bock Und Polach et al. (2013) the obtained grain size is 1 mm or smaller and the grains are sphere-like. The fracture process occurs along the grain boundaries and by having smaller grain sized ice it leads to weaker ice. Timco (1981)

Timco (1981) conducted an extensive test series with different aqueous solutions. He noted that the flexural strength decreases as a function of the solute mass fraction increase until a transition concentration point where the ice strength approaches a constant level. The

Table 6
Average properties of ethanol and sodium chloride ice compared to properties of tap water ice, samples from rows one to three.

Samples (rows 1 to 3)	Impurity molality mol/kg H_2O	Layer growth[1)]	Mass growth[1)]	Flexural strength[1)]	Static modulus of elasticity[1)]	Natural frequency/thickness (mech)[1)]	Dynamic modulus of elasticity[1)]
Tap water (P)	–	1.00	1.00	1.00	1.00	1.00	1.00
EtOH 0.1 m (Ea)	0.047	1.04	0.96	0.24	0.32	0.91	0.97
EtOH 0.3 m (Eb)	0.104	1.11	0.94	0.10	–	–	–
NaCl 0.1 m (Sa)	0.030	0.97	0.99	0.38	1.11	0.67	0.62
NaCl 0.3 m (Sb)	0.095	0.91	0.91	0.33	0.89	0.73	0.68

[1)]Related to tap water ice value.

results presented in this paper with sodium chloride solutions are consistent with Timco's results. In the present work, molalities were used for the more accurate comparison of the influence of organic compounds and inorganic salt on ice properties. In addition to mechanical property measurements, the thin sections and structure of obtained ice were presented in this paper, describing the structure of ice more clearly.

The results show that the average separation efficiency with a 0.3 mol/kg ethanol solution, 64%, is higher than with a 0.1 mol/kg ethanol solution, 47%, whereas separation efficiencies with both sodium chloride solutions are at the same level, close to 70%. This peculiar difference in efficiencies could not be noticed within row four ice samples with a higher freezing temperature (−5 °C) and therefore induced lower ice growth rates. The separation efficiency with the 0.3 mol/kg ethanol solution was 71% and with 0.1 mol/kg 73%, while with a 0.3 mol/kg sodium chloride solution it was 73% and with 0.1 mol/kg as high as 86%. It is already recognised that higher separation efficiencies can be achieved with lower ice growth rates and dilute solutions (Butler 2002; Hasan and Louhi-Kultanen 2015), but no clear explanation for the variation in the ice growth mechanism is known. It might be a result of the structure of the ice in the intermediate stages, i.e. during the growth process, or due to the different properties of the organic (EtOH) and inorganic solutions (NaCl). As this is beyond the scope of this paper, the explanation to this would require additional ice structure studies in relation to ice crystallization kinetics and thermodynamics.

5. Conclusions

The five different initial aqueous solutions – tap water, ethanol and sodium chloride solutions of molalities 0.1 and 0.3 mol/kg – transformed into visually distinguishable ice structures during natural air-cooled freezing. The differences were noticeable also in terms of the conducted chemical and mechanical measurements. Tap water was used as a reference liquid as well as a solvent in ethanol and sodium chloride solutions to compare the properties of the studied ice when ice formed from tap water had the highest flexural strength and natural frequency. The dopants added to the tap water changed the mechanical properties and chemical analysis results of the ice. The platelet diameter and thickness in the intermediate growth stage were the greatest and the orientation was the most random for ice formed from ethanol solutions, which affected the final structure of the ice so that the ethanol ice had the most irregular structure. Based on the research, the ice formed from the ethanol solution is more fragile than the ice formed from the tap water, as the flexural strength is much lower than in tap water ice and sodium chloride ice. Ethanol appeared to weaken the ice more effectively compared to sodium chloride.

In summary, the amount of added chemical dopants, ethanol and sodium chloride, was reduced with variation from 47% to 86% by natural freezing at cooling air temperatures −15 °C and −5 °C, respectively. This verifies the assumption that higher separation efficiencies can be obtained by lower ice growth rates at higher freezing temperatures, but different chemical characteristics still seem to affect the efficiency level as well. The present study gives a good basis for further research concerning the development of ice harvesting techniques and purification efficiency investigations of freeze separation applications with real wastewaters.

Acknowledgements

The project was funded by the Academy of Finland, project no. 285065, 286184 and 285064. We would like to thank Roman Repin, M.Sc., Ari Tuononen, D.Sc., Mikko Kotilainen, M.Sc., Martin Bergström, PhD, Li Fang, M.Sc., and Mr. Teemu Päivärinta for their contribution to the experiments. The earlier contribution of R.U. Franz von Bock und Polach, D.Sc. (Tech.), and Antti Valkeapää, D.Sc. (Tech.), during the research project is also acknowledged.

References

Anderson, D.L., 1958. Preliminary results and review of sea ice elasticity and related studies. Trans. Eng. Inst. Canada 2, 116–122.
Borland, S., 1988. The growth of EG/AD/S model ice in a small tank. In: OMAE 1988 Houston. Proceedings of the Seventh International Conference on Offshore Mechanics and Arctic Engineering. Vol. 4. Arctic Engineering and Technology, Houston, Texas, pp. 47–53 February 7–12.
Butler, M.F., 2002. Freeze concentration of solutes at the ice/solution interface studied by optical interferometry. Cryst. Growth Des. 2, 541–548.
Carvill, J., 1994. Mechanical engineer's Data Handbook. Butterworth-Heinemann.
Cooling, M., Humphrey, V., Theobald, P., Robinson, S., 2010. Underwater ultrasonic field characterisation using Laser Doppler Vibrometry of transducer motion. In: Proceedings of 20th International Congress on Acoustics.
Dykins, J.E., 1971. Ice engineering: Material properties of saline ice for a limited range of conditions. In: Tech. Rept. R720. Naval Civ. Eng. Lab, Port Hueneme, CA.
Enkvist, E., 1972. On the ice resistance encountered by ships operating in continuous mode of ice breaking. Dissertation. The Swedish Academy of Engineering Science in Finland (Report 24. Helsinki. 181 p).
García, V., Häyrynen, P., Landaburu-Aguirre, J., Pirilä, M., Keiski, R.L., Urtiaga, A., 2014. Purification techniques for the recovery of valuable compounds from acid mine drainage and cyanide tailings: application of green engineering principles. J. Chem. Technol. and Biotechnol. 89, 803–813.
Gow, J., Ueda, H., Govoni, J., Kalafut, J., 1988. Temperature and structure dependence of the flexural strength and modulus of freshwater model ice. CRREL Report 8–68.
Guidelines, I.T.T.C., 2014. Test methods for model ice properties. In: ITTC Recommended Procedures and Guidelines Section 7.5–02–04-02.
Hammond, N.P., Barr, A.C., Cooper, R.F., Caswell, T.E., Hirth, G., 2018. Experimental constraints on the fatigue of icy satellite lithospheres by tidal forces. J. Geophys. Res. Planets 123 (2), 390–404.
Hammonds, K., Baker, I., 2016. The effects of ca + + on the strength of polycrystalline ice. J. Glaciol. 62, 954–962.
Hammonds, K., Baker, I., 2018. The effects of H_2SO_4 on the mechanical behavior and microstructural evolution of polycrystalline ice. J. Geophys. Res. Earth Surf. 123, 535–556.
Hasan, M., Louhi-Kultanen, M., 2015. Ice growth kinetics modelling of air-cooled layer crystallization from sodium sulfate solutions. Chem. Eng. Sci. 133, 44–53.
Hasan, M., Louhi-Kultanen, M., 2016. Water purification of aqueous nickel sulfate solutions by air cooled natural freezing. Chem. Eng. J. 294, 176–184.
Haynes, W.M. (Ed.), 2017. CRC Handbook of Chemistry and Physics. 97th Edition (Internet Version). Vol. 2017 CRC Press/Taylor & Francis, Boca Raton, FL.
Hirayama, K.-I., 1983. Experience with urea doped ice in the CRREL test basin, Helsinki. In: Proceedings of the 7th Port and Ocean Engineering Under Arctic Conditions Conference. Technical Research Center of Finland in Helsinki, April 5–9, pp. 788–801. http://www.spri.cam.ac.uk/library/catalogue/records/95170/.
Kujala, P., Riska, K., Varsta, P., Koskivaara, R., Nyman, T., 1990. Results from in-situ four point bending stress tests with Baltic Sea ice. Proceedings of IAHR Ice Symposium 1, 261–278 Espoo.
Lau, M., Wang, J., Lee, C., 2007. Review of ice modeling methodology. In: Proceedings of

Port and Ocean Engineering under Arctic Conditions (POAC). Dalian, China, June 27-30.
Lehmus, E., 1988. The properties of EG/AD-model ice in VTT ice basin. In: Proceedings of Polartech '88. International Conference on Technology for Polar Areas, the Norwegian Institute of Technology. Trondheim, Norway, 15–17 June 1988. Vol. 2, pp. 661–668.
Määttänen, M., 1976. On the flexural strength of brackish water ice by in-situ tests. Mar. Sci. Commun. 2, 125–138.
Narita, S., Inoue, M., Kishi, S., Yamauchi, Y., 1988. The model ice of the NKK ice model basin. In: Proc. of the IAHR Ice Symposium. Sapporo, Japan.
Nortala-Hoikkanen, A., 1990. FGX model ice at the Masa-Yards arctic research centre. In: Proceedings of the 10th IAHR International Symposium on Ice. Espoo, Finland, August 20–23. Vol. 3. Helsinki University of Technology, pp. 405–408.
Parnes, R., 2001. Solid Mechanics in Engineering, 1st edition. Wiley 728 pp.
Petrich, C., Eicken, H., 2010. Growth, structure and properties of sea ice. In: Thomas, D.N., Dieckmann, G.S. (Eds.), Sea Ice, 2nd Edition. pp. 23–77.
Polytec, 2017. Polytec Scanning Vibrometer PSV-500 Datasheet. Polytec Inc.
Rao, S.S., 2007. Vibration of Continuous Systems, 1st edition. John Wiley & Sons, Hoboken, New Jersey.
Riska, K., Jalonen, R., Veitch, B., Nortala-Hoikkanen, A., Wilkman, G., 1994. Assessment of ice model testing techniques. In: Proceedings of Ships and Marine Structures in Cold Regions (ICETECH). Calgary, Canada, March 1994.
Schulson, E.M., Duval, P., 2009. Creep and Fracture of Ice. Cambridge University Press Cambridge.
Snyder, S.A., Schulson, E.M., Renshaw, C.E., 2015. The role of damage and re-crystallization in the elastic properties of columnar ice. J. Glaciol. 61, 461–480.
Snyder, S.A., Schulson, E.M., Renshaw, C.E., 2016. Effects of prestrain on the ductile-to-brittle transition of ice. Acta Mater. 108, 110–127.
Timco, G., 1980. The mechanical properties of saline-doped and carbamide (urea)-doped model ice. Cold Reg. Sci. and Technol. 3, 45–56.
Timco, G., 1981. Flexural strength of ice grown from chemically impure melts. Cold Reg. Sci. and Technol. 4, 81–92.
Timco, G., 1986. EG/AD/S: a new type of model ice for refrigerated towing tanks. Cold Reg. Sci. and Technol. 12, 175–195.
Timco, G.W., O'Brien, S., 1994. Flexural strength equation for sea ice. CRST 22 (3), 285–298.
Timco, G., Weeks, W., 2010. A review of the engineering properties of sea ice. Cold Reg. Sci. and Technol. 60, 107–129.
Vaudrey, K.D., 1977. Ice engineering: Study of related properties of floating sea-ice sheets and summary of elastic and viscoelastic analysis. In: US Navy Civil Engineering Lab Rept no TR-860. Hueneme, CA, Port.
Von Bock Und Polach, R., Ehlers, S., Kujala, P., 2013. Model-scale ice – Part A: Experiments. Cold Reg. Sci. and Technol. 94, 74–81.
Weeks, W.F., Assur, A., 1968. The mechanical properties of sea ice. In: Proc. Conf. on Ice Pressures Against Structures Tech Memo no 92, Quebec, Laval University, Assoc. Comm. on Geotech. Res., Nat. Res. Council of Canada: 25–78. (CRREL Monograph II-C3.).
Weeks, W.F., Hibler, W.D., 2014. On Sea Ice. University of Alaska Press.
Yasui, M., Schulson, E.M., Renshaw, C.E., 2017. Experimental studies on mechanical properties and ductile-to-brittle transition of ice-silica mixtures: Young's modulus, compressive strength and fracture toughness. J. Geophys. Res. Solid Earth 133, 6014–6030.

Publication II

John, M., Häkkinen, A., and Louhi-Kultanen, M.
Purification efficiency of natural freeze crystallization for urban wastewaters

Reprinted with permission from
Cold Regions Science and Technology
Vol. 170, 102953, 2020

Cold Regions Science and Technology 170 (2020) 102953

Contents lists available at ScienceDirect

Cold Regions Science and Technology

journal homepage: www.elsevier.com/locate/coldregions

Purification efficiency of natural freeze crystallization for urban wastewaters

Miia John[a,*], Antti Häkkinen[a], Marjatta Louhi-Kultanen[b]

[a] Department of Separation and Purification Technology, LUT School of Engineering Science, LUT University, P.O. Box 20, FI-53850 Lappeenranta, Finland
[b] Department of Chemical and Metallurgical Engineering, School of Chemical Engineering, Aalto University, P.O. Box 16100, FI-00076 Aalto, Finland

ARTICLE INFO

Keywords:
Freezing point depression
Ice purity
Impurity removal
Natural freezing
Wastewater treatment

ABSTRACT

Human population growth and urbanization are aggravating water quality problems in many regions, and wastewater volumes and quantities of pollutants are increasing due to greater industrial and urban activity. Thus, it is necessary to find efficient, sustainable and simple methods to separate miscellaneous impurities from wastewaters. One potential separation methods is freeze crystallization, because of its non-selective nature. However, previous research investigating freeze separation using real wastewaters has been rather marginal.

This study examines natural freeze crystallization in purification of urban origin wastewaters, that is, municipal wastewater and landfill leachate of various organic and inorganic matter concentration. The effect of different freezing conditions on ice growth and separation efficiency in terms of ice impurity relative to initial solution impurity was investigated with a laboratory scale winter simulator. The results showed air flow velocity to have an almost as significant an influence on ice mass growth as air temperature. Although separation efficiencies decreased linearly with increased ice growth rates, no clear correlation was found between the impurity concentration of the wastewater and the ice mass growth rate. This finding notwithstanding, the separation efficiency of freeze crystallization of concentrated wastewater (landfill leachate) was noted to decrease more clearly with increased ice growth rate. Purification efficiencies of 95% to nearly 100%, determined by indicators such as chemical oxygen demand (COD), were achieved in treatment of municipal wastewater when using low ice growth rates. These findings indicate that the approach can meet future legislative requirements for treatment plants and that further research of the utilization of freezing techniques for wastewater purification is warranted.

1. Introduction

Increased environmental awareness among urban populations means that there is now little need to restate arguments articulating the importance of water saving and water protection activities. To date, conventional wastewater treatment plants are designed to remove organic matter and nutrients from wastewaters for environmental protection and to minimize pathogenic microorganism populations in effluent for sanitary reasons. However, concerns have recently been raised over the adequacy of the wastewater treatment methods currently used and the quality and characteristics of the effluent discharged (Prasse et al., 2015).

Constantly improving living standards among urban populations together with wastewater treatment plants with very large population equivalent have resulted in increased quantities of so-called emerging contaminants in discharged effluents. Enrichment of effluents with micropollutants like pharmaceuticals, antibiotics, synthetic sweeteners and personal care products used in everyday life affect adversely the aquatic environment, flora and fauna, and, ultimately, human health (Rodriguez-Narvaez et al., 2017). Improved knowledge and a changed socioeconomic context thus mean that new or complementary methods are needed for advanced wastewater treatment to ensure adequate removal of organic and inorganic matter, nutrients and micropollutants. In addition to being effective, the capital, operating and maintenance costs of such innovative wastewater treatment technologies must remain economically acceptable.

Freeze crystallization is one potential alternative wastewater purification method, as ice possesses natural high intolerance towards impurities (Bogdan and Molina, 2017). When impure water freezes, the water molecules tend to crystallize, i.e. arrange into as pure ice as possible, while impurities are disposed to the remaining liquid water. High separation efficiency of impurities is therefore achievable,

* Corresponding author.
E-mail address: miia.john@lut.fi (M. John).

https://doi.org/10.1016/j.coldregions.2019.102953
Received 12 July 2019; Received in revised form 7 November 2019; Accepted 18 November 2019
Available online 21 November 2019
0165-232X/

provided impurities are not entrapped as inclusions inside the bulk ice. Freeze crystallization is recognized as an energy-efficient and simple water treatment process that needs no chemicals, and it can be assumed that operating costs will be modest and total environmental impact relatively minor (Yin et al., 2017). In the freeze separation process, nutrients in the wastewater are concentrated in the residual liquid in their initial form, for the most part, because no significant biological or chemical reactions occur. As a result, efficient and sustainable recovery of nutrients is possible.

Ice and the freezing process have been studied for decades in many different fields of engineering science and there are many applications where freezing is used to separate water from liquid mixtures and solutions. For instance, freeze concentration has been used in the food industry to produce high quality fruit juice and coffee extracts. Similarly, freeze separation has been used as a desalination process in fresh water production, although mainly on a laboratory scale (Chang et al., 2016; Williams et al., 2015). Eutectic freeze crystallization (EFC), a special form of melt crystallization, can be considered a fairly sophisticated application for water and salt separation because at the eutectic point, ice and salt can be crystallized simultaneously from the electrolyte solution. In EFC studies, attention has been directed to recovery of the salt formed as well as the water treatment itself (Hasan et al., 2017). In recent years, freeze crystallization research has principally focused on the development of experimental or pilot-scale equipment and devices for separation of a specific compound, e.g. sodium carbonate or sodium sulphate from specific industrial wastewater streams or brine (Williams et al., 2015; Randall and Nathoo, 2015). For example, Randall et al. (2014) used wastewater from a textile plant in investigation of a cascading EFC procedure in a jacketed crystallizer. In their study, 98% ice purity and 30% yield of sodium sulphate were achieved. Ice produced by suspension freeze crystallization from brines has also been shown to be very pure. For instance, van der Ham et al. (2004) obtained impurity concentrations in ice below 100 ppm of copper in an EFC-based cooled disk column crystallizer with an initial copper sulphate solution concentration of 0.145 $kg_{salt}/kg_{solution}$. Utilization of more efficient washing of ice enabled levels of 5 ppm or less to be achieved.

Freeze purification (or separation) studies have been undertaken mostly using model or synthetic wastewater and few studies have used real wastewaters. Work reporting the purification efficiency of total organic or inorganic matter when using urban origin wastewaters, which are complex multi-component aqueous solutions, is even more limited. In the area of industrial wastewaters, Gao et al. (1999) studied ice nucleation by spray droplets with a pulp mill effluent, piggery wastewater and oil sands tailings pond water. They continued their spray freezing studies in field conditions with the same industrial waters and achieved ≥60% impurity reduction efficiencies for chemical oxygen demand (COD), electrical conductivity and color. Different efficiencies were found for organic and inorganic matter (Gao et al., 2004). A few years later, the same research group compared laboratory-scale spray and unidirectional downward freezing techniques with oil refinery and pulp mill effluents. Layer freezing with mixing of the liquid resulted in the greatest organic contaminants reduction, 90–96% reduction (based on COD and total organic carbon (TOC) analysis). Without mixing, the efficiency was much lower; it was at the same level as spray freezing (Gao et al., 2009).

The separation efficiency of freeze concentration with a rotating evaporator for soluble pollution in urban wastewater, food factory effluents and cutting oil wastewater was studied by Lorain et al. (2001). The study attained close to 100% separation efficiency for TOC (i.e. organic matter). Similar very high purity of the ice layer (measured by COD) was found also by Shirai et al. (1998) in layer freezing studies with food industry (dairy and rice cracker) wastewaters. The spray freezing research carried out in field conditions by Bigger et al. (2005) with mining tailings lake water achieved 87–99% removal of mostly inorganic matter when measured with electric conductivity. Their work also analyzed removal of some ions, elements and toxins such as arsenic and cyanide. It should be noted, however, that mining waters can also contain significant amounts of organic matter in addition to heavy metals, as detected in our previous study of natural freezing in mine wastewater basins (John et al., 2018).

Some freezing studies have investigated compounds that are now classified as micropollutants. Gao and Shao (2009) studied two commonly used pharmaceuticals, namely the anti-inflammatory drug ibuprofen and the antibiotic sulfamethoxazole. Their work used model solutions and analyzed TOC as a gross parameter. They found that pharmaceuticals content reduced by 84-92% in single-stage freeze concentration and about 99% in a two-stage ice layer freezing process. Yin et al. (2017) studied a Grignard reagent wastewater from a pharmaceutical intermediates company that contained the organic solvent tetrahydrofuran. COD removal of > 90% was found when using layer freezing and suspension crystallization. Feng et al. (2018) proposed a freezing concept for use with oil recovery from waste cutting fluids. 90% COD removal efficiency was obtained with suspension crystallization.

Previous freezing studies with real wastewaters have implemented freezing techniques at temperatures varying from −2 °C in the laboratory to −33 °C in field conditions. The studies give only little information about the ice production rate at specific conditions, and appraisal of the total potential efficacy of the freeze separation process is hence difficult, even though the separation efficiency for some impurities was shown to be high and sometimes close to 100%.

This study investigates ice layer growth and purification efficiency of natural air-cooled freezing of urban wastewaters originating from a municipal wastewater treatment plant and solid waste landfill. The effect of freezing conditions (i.e. air flow velocity and temperature) on ice mass growth and separation efficiency was examined under controlled conditions using winter simulation apparatus. The freezing point depression temperatures of the studied wastewaters were experimentally determined to initialize the thermodynamic actions and to ensure the comparability of the freezing temperatures of the different wastewaters.

2. Materials and methods

2.1. Wastewaters

In this study, real wastewaters from a municipal wastewater treatment plant and leachate from a solid waste landfill were used as the feed water for the freezing experiments. Both sites, the Toikansuo wastewater treatment plant and the Kukkuroinmäki landfill, are situated in the city of Lappeenranta in southeastern Finland. The municipal wastewater contains mainly domestic wastewater, with some industrial wastewater, from a residential population of 60,000 and average daily wastewater volume is 16,000 m^3. The wastewater for the tests was collected from the open water stream after primary clarification and before the water flows to the biological (activated sludge) reactor tank. The wastewater is chemically pretreated in a primary sedimentation basin with calcium hydroxide $Ca(OH)_2$ and ferric sulphate $Fe_2(SO_4)_3$ (feeds ~150 g per m^3 wastewater) for pH adjustment and suspended solids reduction, respectively. Fully processed effluent from the same plant was also collected to be able to test very dilute wastewater. The landfill is situated next to the regional solid waste management center serving municipalities in the area. The landfill leachate water was collected from the inspection and pumping well that captures infiltration water from the normal (non-hazardous) solid waste fill. Total daily leachate volume of the landfill varies from 80 to 120 m^3.

Urban wastewater is a very complex mixture of compounds and pollutants that have accumulated in water. The quality and composition of the wastewater also varies periodically due to fluctuating flow rates caused by domestic water use and precipitation. Infiltration water of landfills is formed by precipitation and melting snow and contains

Table 1
Composition of tested wastewaters.

Wastewater	COD	Color	Turbidity	Conductivity	pH	Total solids
	(mg L^{-1})	(PtCo)	(FTU)	(μS cm^{-1})		(mg L^{-1})
Municipal effluent	21–29	47–66	9–12	575–602	6.16–6.45	–
Municipal pretreated	127–465	360–816	67–151	719–786	7.56–9.12	470–630
Landfill leachate	447–638	450–975	85–184	1850–5005	7.70–8.42	1300–3200

residues from the waste material as well as solid filling material. Both sites, the wastewater treatment plant and the landfill, have a statutory obligation to monitor water quality frequently. Average analyzed compositions of the studied wastewaters are presented in Table 1. Although the landfill leachate contains almost twice the amount of organic matter found in the municipal pretreated wastewater, the biological activity of the municipal pretreated wastewater can be expected to be higher due to its larger microbial population. The measured conductivity of the leachate is high, indicating a high concentration of ionic inorganic matter. The landfill leachate most likely contains small particles like microplastics and fibers, as bigger pieces were visible in the raw water samples.

2.2. Experimental setup

The natural freezing of wastewater was done in a wind tunnel-like laboratory-scale apparatus custom-made of a thermally insulated chest freezer. The arrangement enables simulation of natural freezing conditions because the temperature and velocity of cooling air can be carefully controlled. Fig. 1 shows the experimental setup for natural freeze purification of wastewaters. Winter simulator apparatus with a similar set-up was used in our previous freezing experiments with electrolyte solutions (Hasan et al., 2018).

Wastewater samples of 500 mL volume in plastic crystallizer vessels (volume of ~710 mL, edge dimensions ~40 mm · 87 mm · 58 mm) were allowed to freeze so that an ice layer formed on the upper surface of the wastewater. The water surface level was about 15 mm below the upper edge of the vessel and, thus, the freezing area was ~0.013412 m^2. Heat losses through the other sides of the vessels were avoided by thermal insulation when the vessels were installed inside the floor level of the wind tunnel. The designed undercooling temperature degree (ΔT) was obtained by circulating aqueous ethylene glycol coolant in heat exchangers. Air temperature in the wind tunnel was controlled with a Lauda Proline RP 850 thermostat connected to a PT100 sensor measuring air temperature. Cool air flow in the tunnel was produced with a blower. The air production of the blower was adjusted with a frequency converter based on verified operating air flow velocity (v_{air}) measured with a Kimo VT100 (or VT210) anemometer (accuracies ± 0.1 ms^{-1} and ± 0.3 °C, respectively). The temperatures of the wastewater samples in the vessels were measured with PT100 platinum resistance thermometers. Temperature data was collected by Pico PT-104 Data Logger (resolution 0.001 °C, accuracy ± 0.015 °C) and PicoLog software.

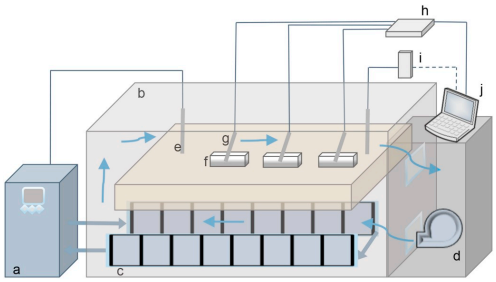

Fig. 1. Experimental setup for natural freeze purification of wastewaters: a) thermostat, b) chest freezer, c) heat exchangers, d) blower, e) temperature sensor, f) crystallizer vessels, g) PT 100 thermometers, h) data logger, i) anemometer and probe, j) computer.

2.3. Freezing point depression test

The freezing point depression (FPD) temperatures (T_f) of different types of real wastewaters were determined to enable comparison of the undercooling temperature degree (ΔT) in the freezing experiments. The FPD test was executed with a simple cooling curve method in which measured temperature responses during cooling were plotted as a function of time. A 200 mL wastewater sample was poured into a jacketed class reactor equipped with a magnetic stirrer. The circulation of ethylene glycol coolant in the jacket was controlled by a Lauda Proline RP 850 thermostatic unit. The temperatures of the water were measured with a PT100 sensor connected to the thermostat and the temperature data was logged to a file by a computer and Lauda Wintherm Plus software. The reference junction (calibration) of the thermostatic unit and probe was obtained with a pure ice and water mixture and verified using a mercury thermometer with a certificate of calibration.

2.4. Experimental procedures and methods

500 mL samples of well-stirred wastewater were prepared for the freeze separation tests. Two or three replicates were prepared and frozen at the same time. Although the wastewater contained some visible solids, no pre-filtering or settling were used in order to simulate the process realistically. Before the freezing test, the water samples were allowed to cool to near to freezing temperature in a freezer room at −18 °C to avoid too high undercooling degree and to generate initial seed ice crystals for the freezing test. The precooling time needed varied between 30 and 50 min depending on the wastewater type.

Before and immediately after the freezing test, the masses of the samples in the vessels were measured (balance Precisa BJ2200C, capacity 2200 g, readability 0.01 g) to determine the total mass loss, i.e. evaporated water, during the test. After the test period, the vessels were removed from the winter simulator and the remaining concentrated liquid (residual) and the formed ice layer were separated. The mass of the ice was measured as well as the volume of the concentrated liquid. The average thickness (mm) of the ice layer was determined by multipoint measuring with a caliper. The ice piece was lightly rinsed with pure water cooled to near to 0 °C to avoid adherence of external contaminants on the ice surface during manual sample handling. All ice and residual concentrated liquid were collected and stored in a freezer at −18 °C for further analyses.

The ice layer growth rate is known to decrease during the freezing process as the heat insulating effect of the ice layer increases with increasing layer thickness (Hasan et al., 2017). For this reason, the freezing time was set at a constant 24 h to be able to study how two controllable variable parameters, i.e. air temperature and air flow velocity, affect ice growth rate and separation efficiency. The basic parameters used were undercooling temperature degrees ΔT 0.5, 1.0,

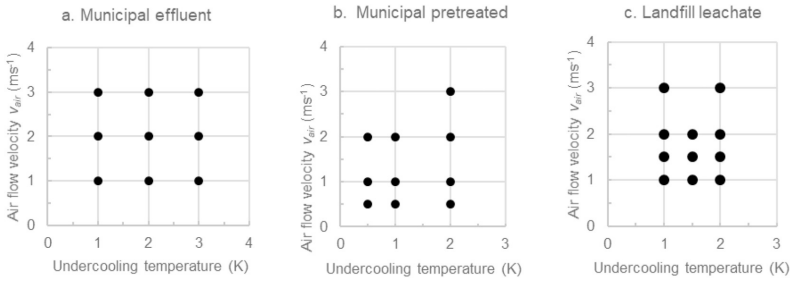

Fig. 2. Design of experiments for different wastewaters with the used combinations of undercooling temperature and air flow velocity with freezing test time of 24 h.

1.5, 2.0 and/or 3.0 °C (or K), and air flow velocities v_{air} 0.5, 1.0, 1.5, 2.0 and/or 3.0 ms^{-1}. Thus, at least nine different freezing conditions were assessed with each type of wastewater, see the experimental design in Fig. 2.

Similar freezing tests were carried out with ultrapure water produced with an Elga PureLab water purification system (TOC < 5 ppb, resistivity 18.2 MΩ cm) as blank samples for comparison. Additionally, some tests were performed with different times: 5, 48 and 72 h, and temperatures: ΔT 5 °C and 10 °C, to be able to survey the limitations of the experimental set-up used, for example, regarding the effect of the obtained freezing ratio on the separation efficiency. The assumption was that the separation efficiency will decrease if the freezing ratio is over 50% (i.e. half of the water is frozen) due to enrichment of the solution (Hasan and Louhi-Kultanen, 2016). The obtained freezing ratio (%) was determined and confirmed by calculation of the percentage of the ice mass formed from the initial water mass.

The average linear ice layer growth rate (ms^{-1}) was determined by dividing the average ice layer thickness by the total freezing time. This calculation method enables comparison with previous studies. The average ice mass growth rate, g h^{-1} m^{-2}, was calculated by dividing the measured totally formed ice mass by the freezing time and surface area. The evaporation (or sublimation) rate, g h^{-1} m^{-2}, can be determined in the same manner as the ice mass growth rate by dividing the measured total mass loss by the freezing time and the surface area of the vessel.

Differences in the polycrystalline ice structures formed were observed macroscopically by polarized light and microscopically (Olympus BH2-UMA) for visualization of the impurity inclusion, veins and pockets in the ice. In these studies, however, the focus is on determination of purification efficiency, and ice characteristics are not studied in detail. Thus, the primary use of ice samples with limited volume was for chemical analyses.

2.5. Chemical analyses and methods

The analysis methods used were chosen to indicate the general quality of the water and to indicate the feasibility of freezing as an unselective purification method. When analyzing real wastewaters, the indirect measurements used in the present work, i.e. electrical conductivity and chemical oxygen demand (COD), give overall information about inorganic and organic matter content, respectively. Ice and wastewater samples were analyzed using similar methods as used in previous freezing studies to enable comparison of the achieved purification efficiency with prevailing practices.

Before analysis, the melted ice samples and stored wastewater samples were kept at room temperature to attain ambient temperature. A spectrophotometer HACH DR/2000 was used to determine the apparent color (PtCo, 455 nm) and turbidity (± 2.0 FTU, 450 nm). The chemical oxygen demand (COD, mg L^{-1}) was analyzed by spectrophotometer and a dichromate oxidation method corresponding to APHA 5220 D (Greenberg et al., 1995) with a Spectroquant COD reaction cell test measuring ranges 0–150 mg L^{-1} (± 2.7 mg L^{-1}, 420 nm) and 0–1500 mg L^{-1} (± 14 mg L^{-1}, 620 nm). A Consort C3040 multi-parameter analyzer was used to measure pH and electrical conductivity (probe with temperature compensation, cell constant 1.0 cm^{-1}, range 0.001–100 mS cm^{-1}). Dry matter content as total solids (TS, mg L^{-1}) was determined by an evaporation-weighing method corresponding to APHA 2540 B (Greenberg et al., 1995) for initial wastewater samples. Almost all ice samples had to be excluded because of limited liquid volumes. As the quality of raw wastewater changes even during short cool storing, the initial wastewater used was analyzed for every experiment. Purification efficiency *E(%)* was calculated with Eq. 1:

$$E(\%) = 100 \bullet \left(\frac{C_{ww} - C_{ice}}{C_{ww}} \right), \quad (1)$$

where C_{ww} is the concentration or other measured value in the initial wastewater and C_{ice} the concentration or other measured value in the ice.

3. Results and discussion

3.1. Freezing point depression

The determined freezing point depression (FPD) temperatures and obtained supercooling temperatures of the studied wastewaters are presented in Table 2. It is important to define these temperatures as temperature difference is the driving force for the ice crystallization process. Freezing temperature and the degree of supercooling used affect the ice nucleation and ice crystal growth. The FPD temperatures of the municipal wastewaters, effluent and pretreated wastewater were quite similar. The FDP temperature was slightly lower with pretreated wastewater and the supercooling degree quite moderate, 2 to 3 °C. As expected, landfill leachate showed approximately four times lower FPD temperatures than municipal wastewaters, −0.220 °C at their lowest, because landfill leachate contains more ionic matter. An example of a cooling curve recorded in an FPD test for landfill leachate is presented in Fig. 3. It was of importance to determine the FPD temperature, as

Table 2
Determined freezing point depression temperatures and supercooling temperatures of the studied wastewaters.

	Municipal effluent	Municipal pretreated	Landfill leachate
FPD temperature (°C)	−0.035…-0.048	−0.040…-0.060	−0.185…-0.220
Supercooling temperature (°C)	n/a	−1.860…-3.010	−2.880…-3.350

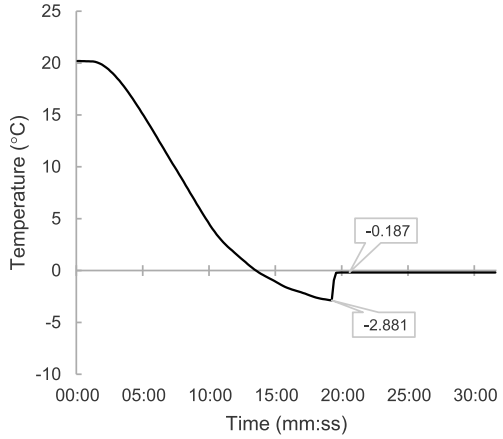

Fig. 3. Cooling curve from a freezing point depression test of landfill leachate at a cooling rate of 1.5 °C min^{-1}. The freezing point and subcooling temperatures are marked within the curve.

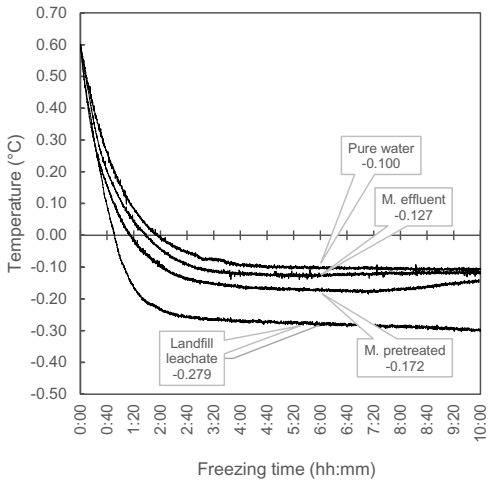

Fig. 4. Temperature profiles of purified water, effluent wastewater, pretreated wastewater and landfill leachate in the crystallization vessel in the wind tunnel during 10 h' freezing, conditions of ΔT 2 K and v_{air} 2 ms^{-1}. Temperatures (°C) within 6 h freezing marked in the curves.

FPD of wastewaters is rarely studied. The FPD seemed to indicate the total impurity of wastewater rather sensitively, especially inorganic matter.

With the studied wastewaters, the freezing point depression was not very significant compared to common dilute salt solutions. More important was the variation in FPD temperatures with the same type of wastewater. The FPD temperature of the wastewaters varies because of the differing composition of the sampled raw wastewater batches. The FPD temperature was also found to change during storage of the wastewater, presumably due to decomposition of impurities in the water. Although the FPD temperature differences between the different wastewaters seemed insignificant, it should be noted that even small temperature difference (0.1 or 0.2 °C) in used freezing temperature may have a significant effect on the heat transfer and hence on total energy consumption of the utilized freezing process.

3.2. Freezing process

The ice layers formed in a quite similar manner in the different wastewaters in the winter simulator. Usually, the crystal growth began from ice crystal seeds that had formed during the precooling in a freezer. Ice crystal growth continued, forming needle-, dendrite- and/or platelet-like ice on the surface of the water, until the surface was totally covered with a very thin ice layer. The initial dendritic tree-like growth on the liquid surface is presumably due to simultaneous evaporation of water and freezing, and the needle-like ice forms due to seeding and quick cooling (Mullin, 2001). Thin ice formations were sometimes difficult to observe visually (and by a camera) because of their transparency, see Fig. 5a and d. After surface ice growth, the ice layer continued growing towards the liquid water.

The measured temperatures of the water under the ice were seen to plateau near the determined freezing temperatures or at lower temperatures with minor supercooling, as can be seen in the freezing temperature profiles of the different waters under the same cooling conditions (ΔT 2 K and v_{air} 2 ms^{-1}) in Fig. 4. With lower air temperatures (< -3 °C) and higher air velocities (> 3 ms^{-1}) the temperature of the water began to decrease with freezing time due to more intense forced convection. It was noticed, however, that the surface started to freeze before attaining equilibrium freezing temperature, and sometimes even at 0 °C, as the temperature probe measured the average bulk temperature of the water but not the temperature at the ice-water interface. Controlled precooling of the water samples proved to be difficult and the temperature of the replica samples varied at the beginning of the freezing test despite similar preparation for the same time. As a consequence, the starting temperature of the freezing tests varied from 0.75 to 2.25 °C.

Freezing time of approximately two hours was required to form an ice layer fully covering the upper liquid surface. With lower temperatures, development of the ice layer happened a little faster. An exception here was that in some cases, mostly with low air velocity of 0.5 ms^{-1} or undercooling temperature of 0.5 K, no uniform ice layer was formed. In other cases, only two thirds or half of the upper surface was frozen after 24 h freezing time and the temperature of the water in the vessel remained higher than the freezing temperature and sometimes even above 0 °C. Many of the ice pieces were wedge-shaped with a quite planar upper surface and the thinner end edge facing towards the air flow: ice under the air inlet was thinner than the ice layer under the air outlet. This exceptional shape was most likely due to the experimental setup, i.e. local turbulent air flow conditions. Therefore, ice growth rates were primarily assessed by measured ice mass and ice layer thickness was calculated as the average thickness of multiple measurement points. Some suspended solids settled on the bottom of the vessel during freezing of more concentrated wastewater, as can be seen in the municipal pretreated wastewater in Fig. 5b.

3.3. Formed ice

All the ice layer samples seemed to have relatively high mechanical strength compared, for example, with the fairly soft ice formed from salt solutions in previous studies. Thicker ice pieces could not be broken without tools. Some small bubbles or thin veins inside the ice were noticed (see Fig. 5c) but no regular patterns. The upper surface of the ice was mostly planar (with some mild humps and bumps) and clear, and no accumulated solid matter could be seen. The bottom of the ice was also mostly planar, although in some cases the bottom had spiky (small needles) ice formed by higher growth rates. However, no regular patterns, e.g. dendritic platelets, were observed.

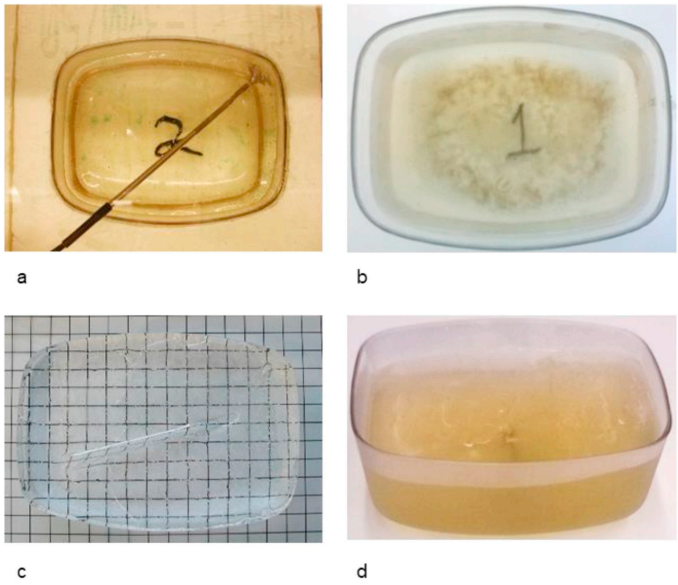

Fig. 5. a) Ice and municipal effluent in the crystallizer vessel with the temperature probe: b) some suspended solids of municipal pretreated wastewater settled on the bottom of the vessel during freezing – notice the pattern; c) an ice piece formed from municipal effluent, measure grid 1 cm × 1 cm; and d) ice and landfill leachate in the crystallizer vessel.

The visual color of the ice varied from very transparent ice for municipal effluent to shades of a yellow brownish color for landfill leachate ice. The values of apparent color and turbidity measured in the melt ice did not always match visual observations; ice with high measured values could look misleadingly clear and transparent. Generally, no explanatory correlation could be found between the visual characteristics of the ice and the purification efficiency. In most cases, the purified wastewater water (melt ice) smelled like dilute wastewater, i.e., it was not odorless, even though it looked like clear ice. Microscopic observation revealed clear differences in ice characteristics (Fig. 6). Whereas fairly clean ice showed as blank spaces with clear ice crystal boundaries (Fig. 6a), the municipal effluent ice clearly contained impurity inclusions (Fig. 6b). In addition, landfill leachate ice incorporated small solid grains (Fig. 6c). It was difficult to observe the ice crystal boundaries of impure polycrystalline ice and identify any impurities (fibers, micro-organisms, microplastics etc.) due to overlaps in the structure.

3.4. Ice growth rate

Some correlation was found between the wastewater freezing results and the freezing conditions in the winter simulator. An almost linear function for ice mass growth rate (g h^{-1} m^{-2}) as a function of air flow velocity (ms^{-1}) with different undercooling temperatures (K) was obtained based on simple linear regression model fitting results, see Fig. 7. Linear fitting with all experiments gave R^2 (the coefficient of determination) varying from 0.856 to 0.998. As expected, freezing conditions, i.e. air flow velocity and temperature, directly affected the ice growth rate, as can be seen in Fig. 7a, b and c, for different wastewaters, whereas the effect of wastewater quality can be considered to be more moderate or minor. When all the mass growth rates of the different wastewaters and air velocities with undercooling temperatures 1 K and 2 K were fitted in the same linear model (Fig. 7d) the R^2 values were still at a good level: 0.898 with ΔT 1 K and 0.783 with ΔT 2 K. The lines are very parallel with almost equal slopes (236 and 237).

Deviations and lower R^2 values are more likely due to the

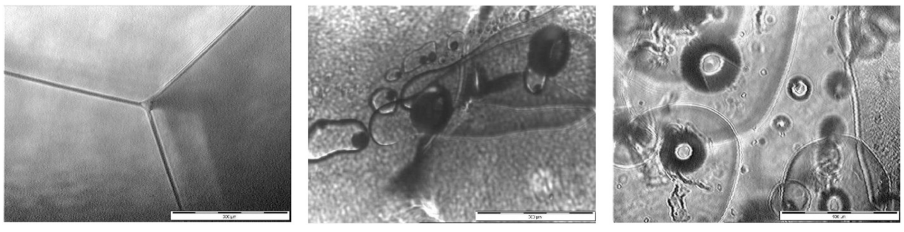

Fig. 6. Microscopic characteristics of ice formed with different waters and under different freezing conditions (undercooling degree temperature and air flow velocity): a) pure water (1 K, 3 ms^{-1}) b) municipal effluent ice (1 K, 1 ms^{-1}) and c) landfill leachate ice (1 K, 2 ms^{-1}), bar scale 500 μm, magnification 5×.

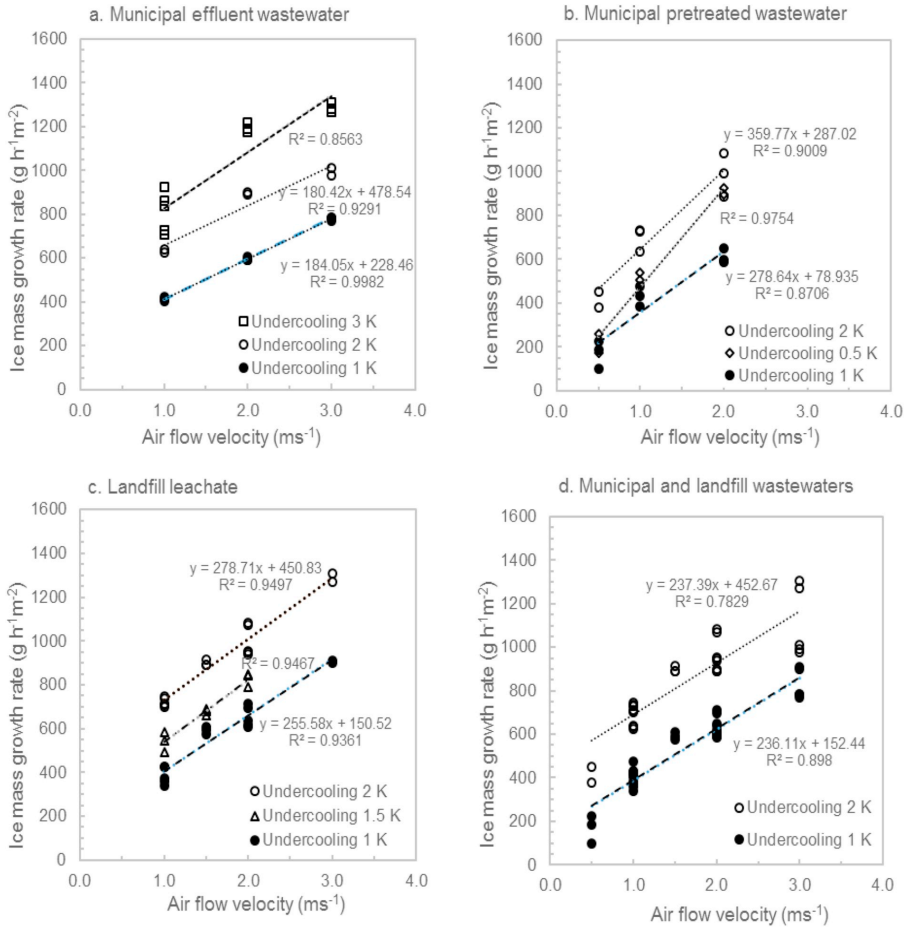

Fig. 7. Ice mass growth rates as a function of air flow velocity with different undercooling degree temperatures: a) effluent, b) pretreated wastewater, c) landfill leachate and d) the combined results of all municipal and landfill wastewaters with undercooling temperatures 1 and 2 K. Linear fittings, N = 6–28.

experimental setup and measurement conditions, that is, vibration of the chest freezer, humidity differences or minor human errors etc., than the wastewater composition. As was previously noticed for ice pieces formed with low undercooling temperature of 0.5 K, the air-cooled freezing process is very easily influenced by factors that are difficult to measure. This issue can be seen in Fig. 7b, where the line for 0.5 K undercooling indicates higher ice mass growth rates than 1 K undercooling. A part of the water surface was open to air and the increased air flow intensified the ice growth, both as regards mass and ice layer thickness (ms^{-1}).

Based on the results of these freezing experiments and the simple model used for the freezing conditions, it can be seen that the undercooling temperature defines the base level of the ice growth rate on the intersection of the y-axis and the air velocity gives the coefficient or impact factor for the intensity of the growth rate by the slope of the linear line (Fig. 7d). For example, with conditions ΔT = 1 K and v_{air} = 1 ms^{-1}, the average mass growth rate (i.e. the ice mass production) was 389 g h^{-1} m^{-2}. When air velocity was increased from 1 ms^{-1} to 2 ms^{-1}, the ice mass growth rate increased by 236 g h^{-1} m^{-2} to 625 g h^{-1} m^{-2}. With undercooling temperature of 2 K, the growth rate behaved in the same way. The same linearity can be found with ice layer growth rates (ms^{-1}). Verification of the presumption of linearity with lower freezing temperatures vs. growth rates as a function of air flow velocity could not be examined due to limitations in the experimental setup used.

Comparison of the ice growth rate results of the present work and previous studies reported in literature is problematic because most research has been carried out in very different conditions, i.e. with much colder temperatures and lower air flow velocities. However, the ice layer growth rates obtained in our previous study with electrolyte solutions (nickel sulphate) correspond somewhat with the growth rates in freezing of wastewater found in this work. For similar conditions

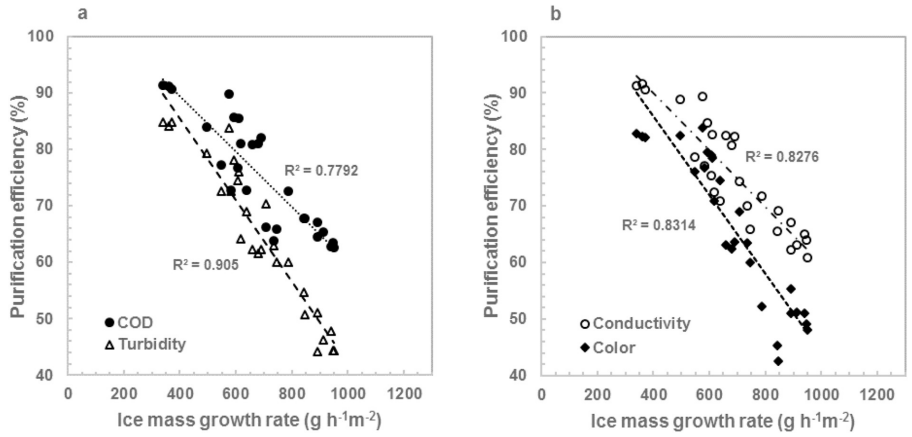

Fig. 8. Purification efficiencies of a) COD and turbidity and b) conductivity and color with different ice mass growth rates in freezing tests of landfill leachate. Linear fittings, $N = 27$.

($\Delta T = 1$ K, $v_{air} = 2$ ms^{-1}, 24 h), the salt solutions had an average ice layer growth rate of ~2.5 ·10^{-7} ms^{-1} (Hasan et al., 2018) and in this study the average rate was 2.05 ·10^{-7} ms^{-1}.

3.5. Purification efficiency

As previously described in section 3.4., the ice growth rate results from factors determining the freezing conditions, i.e. air temperature and velocity, and similar growth rate can be obtained with various combinations of these parameters. Therefore, when considering the purification efficiency of different wastewaters, it is more meaningful to compare the ice growth rate than the freezing conditions directly.

The calculated results showed that the greater the ice growth rate, the lower the purification efficiency. The effect is clearly seen in more concentrated wastewaters with inorganics, like landfill leachate, see Fig. 8. With a lower ice mass growth rate of 400 g h^{-1} m^{-2}, the average purification efficiency was near to 90%. The efficiency decreased to 60–70% when the ice mass growth rate increased to 800 g h^{-1} m^{-2}. With the effluent, no obvious correlation between ice growth and purification could be found, partly due to limitations in the analysis methods when used for very dilute wastewaters. However, the average purification efficiency was mainly in the range 75–90% for all water quality indicators and the effect of higher ice mass growth rate on purification can thus be considered to be less significant with dilute effluent.

With pretreated wastewater, the effect of ice mass growth rate was not as evident as with landfill leachate since the decrease in purification efficiency related to an increase in ice mass growth is much lower and R^2 values are somewhat lower, see the trend lines in Fig. 9. For instance, lower ice mass growth rates of 200 and 400 g h^{-1} m^{-2} showed average purification efficiencies of around 90% and a higher growth rate of 800 g h^{-1} m^{-2} resulted in efficiencies slightly under 80%. Unexpectedly, very fast freezing of municipal pretreated wastewater over 5 h' freezing time, $\Delta T = 10$ K, $v_{air} = 0.5$ ms^{-1} and growth rate of ~800 g h^{-1} m^{-2} also resulted in 90% COD reduction. The difference between the test result with the same undercooling degree and a higher air flow velocity of 1 ms^{-1} and growth rate of ~1800 g h^{-1} m^{-2} is noteworthy, as it resulted in 76% COD reduction. The more extreme freezing conditions should be investigated further, as ice mass production over time might be a significant factor in utilization of natural freezing processes.

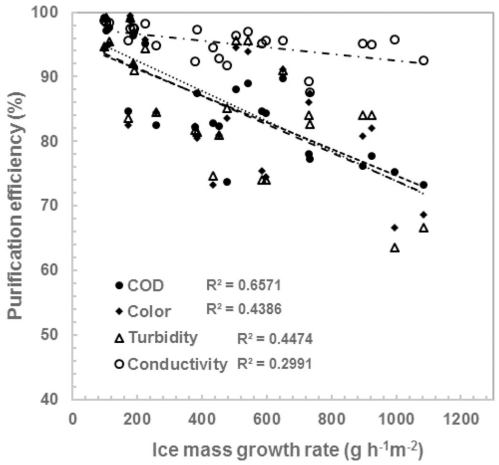

Fig. 9. Purification efficiencies of COD, color, turbidity and conductivity with different ice mass growth rates in freezing tests of municipal pretreated wastewater. Linear fittings, $N = 25$. Trend lines of COD, color and turbidity are almost parallel.

When municipal pretreated wastewater was frozen under conditions of $\Delta T = 1$ K and $v_{air} = 0.5$ ms^{-1}, the highest purification efficiencies, > 95%, were obtained for all water quality indicators with very low ice growth rates. Longer freezing time of 72 or 48 h did not show any effect on purification efficiency, i.e. the efficiency was at the same level as in 24 h freezing. These conditions were not tested with landfill leachate, since using a velocity of 0.5 ms^{-1} (or a 0.5 K undercooling degree) was earlier seen to cause unexpected deformations in the ice pieces. Very low ice growth rates should be tested with an improved experimental set-up. However, based on these results, it can be concluded that very high purification efficiencies can be achieved with very slow freezing.

The tendency of wastewaters of different concentrations to form

more impure ice with an increasing ice growth rate can be seen in Figs. 7, 8 and 9. When comparing municipal pretreated wastewater with more concentrated landfill leachate, it is noticed that the effect of higher ice mass growth rate on purification efficiency is much stronger with landfill leachate, i.e. the direction of the trend line is decreasing and the incline is steeper (Fig. 8). The same trend was seen also in previous studies for freezing salt solutions of different concentrations when plotting the purification efficiency in terms of the effective distribution coefficient as a function of the ice layer growth rate (Hasan and Louhi-Kultanen, 2015; Hasan and Louhi-Kultanen, 2016; Hasan et al., 2018). Based on this observation, it can be deduced that the type of wastewater (i.e. impurity concentration) can affect the ice crystallization process and the impurity rejection efficiency.

Despite the very different wastewaters and freezing conditions, the purification efficiencies obtained in the present work are rather similar to previous natural freeze crystallization studies reported in literature. In the present study, COD concentrations in the initial wastewaters were 21–638 mg L^{-1} for freezing temperatures of ~ − 0.5 to −3.2 °C with a freezing ratio < 50%. Yin et al. (2017) studied highly concentrated effluent (20000–30,000 mg L^{-1} COD) containing organic pharmaceutical intermediates. Their study obtained a COD removal efficiency of 70–90% with an ice formation ratio of 20% at temperatures of −4 to −12 °C. Gao et al. (2009) reported 90–96% COD and TOC reduction in freezing of petroleum refiner effluent with initial COD concentration of 767 mg L^{-1}(freezing ratio 70% at −10 and − 25 °C). Soluble pollutants of urban wastewaters were studied by Lorain et al. (2001) using a non-air-cooled freezing setup. Near 90% efficiency was attained (freezing ratio 64%, −7 °C) for freeze crystallization of the wastewater after primary settling. In our previous study (John et al., 2018), comparable separation efficiencies of 65–90% were attained for naturally frozen ice in wastewater basins of a mining site.

When the results obtained in this study are compared with current regulations for municipal wastewater treatment plants, the best purification efficiencies achieved can be considered to be at a good level. For instance, the environmental permit of the Toikansuo wastewater treatment plant, which is the source of the wastewater samples, limits the COD concentration (average of quarterly sampled results) of the effluent to 70 mg L^{-1}, i.e. the minimal acceptable purification efficiency of the plant is 80%. In this study, this requirement was met in freeze crystallization of municipal pretreated wastewater at lower ice growth rates, where COD concentration varied from < 3 to 41 mg L^{-1}. It is known that regulations are going to become more stringent in the near future and many wastewater treatment plants are already exceeding minimal requirements. Indeed, the old Toikansuo treatment plant has attained COD concentration in effluent of 30–40 mg L^{-1}, giving a purification efficiency of 95%.

3.6. Further remarks

The effect of the acidity or alkalinity of aqueous solutions is rarely studied in freeze crystallization as pH is assumed to have very minor or negligible effect on the freezing process, although Gao et al. (1999) suggested that pH has an effect on freezing temperature and nucleus concentrations of wastewaters. However, pH is a relevant factor when evaluating the quality of the effluent to be discharged into the environment.

In the freezing experiments in this work, it was noticed that the pH values of the melted ice or concentrated residual may be significantly different from the pH of the initial wastewater (Supplementary material, Fig. A.1). The pH value of the ice can be either higher or lower than that of the initial wastewater depending on the source of the wastewater. Generally, an increase of 0.5–1.0 pH (e.g. increase from pH 7.7 to 8.7) was noticed with landfill leachate freezing. Then the highest pH values of ice were still allowable. The largest decrease, from pH 8.8 to 6.5, was detected with pretreated municipal wastewater, although the pH of the ice remained at a rather neutral level as the initial pH of the

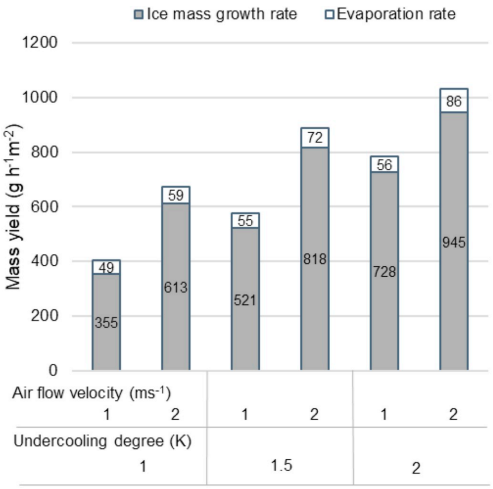

Fig. 10. Average evaporation rates (determined by mass loss measurements) and ice mass growth rates in landfill leachate freezing at undercooling temperatures 1, 1.5 and 2 K and air flow velocities 1 and 2 ms^{-1}.

wastewater was quite high. The most remarkable decrease in pH was found with effluent. The lowest final pH value of effluent melt ice was 4.2 pH (for effluent with a quite low initial pH of < 6.5 pH).

Low alkalinity of the effluent because of earlier bio-chemical water treatment could explain the decrease in pH. However, if chemicals are not added to the water in the freeze crystallization, the changes in hydrogen-ion concentration must occur internally. As the pH value changes during the freezing processes were rather chaotic, it is speculated that the changes in pH might be related to decomposition of organic matter in the wastewater resulting in carbon dioxide release to the water. Based on the present study, no direct relationship between pH and purification efficiency could be found. Changes in pH and the factors causing such changes during the freezing process should be studied more comprehensively, because effluent whose pH deviates significantly from the recommended pH of 6.5–8.5 (Tchobanoglous et al., 2003) can not be discharged or recycled without neutralization.

The undercooling temperature and air flow velocity affected the rate of evaporation (or sublimation), g h^{-1} m^{-2}. The effect on evaporation of temperature alone was minor, but combined with air flow velocity, lower temperature increased the evaporation, as shown for instance in Fig. 10 with landfill leachate freezing tests. The determined amount of water evaporation/sublimation mass during the freezing tests varied from 7 to 15% of the formed ice mass. Hence, evaporation proved to be a significant factor in mass balance of the freeze purification process design and greater attention should be paid to evaporation in future natural freezing experiments.

Based on this study, natural freeze crystallization of wastewaters was found to be a rather complex process. Many parameters affect the system, which made precise control of process conditions challenging and led to unpredictability in the purification efficiency attained. The required effluent quality can be achieved by one-time natural freezing if the wastewater is frozen very slowly. However, low ice growth rates generally require a low temperature gradient, i.e. rather high freezing temperatures, and consequently, a very large freezing surface as well as long freezing time are needed to maintain sufficient ice mass production. Thus, considerable challenges could be faced in optimization of process design, i.e. when resolving the optimal freezing ratio and recycling of concentrated wastewater in the process. Consequently,

multiple sequenced freezing processes are likely to be more efficient than simple one-time freezing. The results of ice mass production and purification efficiencies gained in this study are of importance in future studies when realistically evaluating the possible utilization of freeze separation techniques in wastewater purification. Freeze purification could be seen more as an alternative method to be used in conjunction with conventional treatment in purification of a very specific wastewater fraction or when reduction of the volume of wastewater is needed. Due to the (theoretically) non-selective nature of ice crystallization as regards the rejection of impurities, further research is still required on separation of specific fractions like microplastics and fibers.

4. Conclusions

In the present study, the ice growth rates and purification efficiencies of urban wastewaters subject to various freezing conditions (different temperature and air flow velocity) were determined. The research approach used enabled simple evaluation of the purity and mass production rate of ice in freeze purification of wastewaters. The ice growth rate was found to be clearly temperature-dependent, but air flow velocity also had a significant direct effect on ice growth. Temperature change of +1 °C caused the ice mass growth rate to increase by 300 g h^{-1} m^{-2}. 1 ms^{-1} increase in air flow velocity (at the same temperature) caused the ice mass growth rate to increase by 230 g h^{-1} m^{-2}. The influence of wastewater concentration on ice growth was found to be minor compared to the effect of temperature and air flow.

The hypothesis of the inverse effect of increased ice growth rate on water purification was shown to be valid also with wastewaters (as studied previously with salt solutions): higher purification efficiencies were obtained with lower ice growth rates. The highest purification efficiencies > 95% (COD concentrations in ice < 10 mg L^{-1}) were obtained with pretreated municipal wastewater and ice mass growth rate of < 200 g h^{-1} m^{-2} (at ~ − 1 °C and 0.5 ms^{-1}). With landfill leachate the highest COD separation efficiency 90% (~50 mg L^{-1}) was obtained with an ice mass growth rate of < 400 g h^{-1} m^{-2} (at ~ − 1 °C and 1 ms^{-1}) but the efficiency began to decrease as the growth rate increased. Nevertheless, natural freezing can be considered as a potential treatment method for wastewaters containing significant amounts of organic and inorganic matter. This outcome together with the findings for ice growth provide a good basis for further studies in the area of the freeze purification application design.

Acknowledgements

The research was funded by the Academy of Finland, project no. 285064. The authors wish to thank Riitta Moisio at Lappeenrannan Lämpövoima Oy and Heidi Oksman-Takalo at Etelä-Karjalan Jätehuolto Oy for their co-operation and assistance. The contribution of Mr. Maxime Demuyter and Mr. Lucas Goarvot during the experimental work is also acknowledged.

Declaration Competing of Interest

The authors declare that they have no known competing financial interests or personal relationships that could have appeared to influence the work reported in this paper.

Appendix A. Supplementary data

Supplementary data to this article can be found online at https://doi.org/10.1016/j.coldregions.2019.102953.

References

Bigger, K.W., Donahue, R., Sego, D.J., M Birch, S., 2005. Spray freezing decontamination of tailings water at the Colomac Mine. Cold Reg. Sci. Technol. 42, 106–119. https://doi.org/10.1016/j.coldregions.2004.12.005.

Bogdan, A., Molina, J., 2017. Physical chemistry of the freezing process of atmospheric aqueous drops. J. Phys. Chem. A 121 (16), 3109–3116. https://doi.org/10.1021/acs.jpca.7b02571.

Chang, J., Zuo, J.L., K-J, C.T.-S., 2016. Freeze desalination of seawater using LNG cold energy. Water Res. 102, 282–293. https://doi.org/10.1016/j.watres.2016.06.046.

Feng, W., Yin, Y., de Lourdes Mendoza, M., Wang, L., Chen, P., Liu, Y., Cai, L., Zhang, L., 2018. Oil recovery from waste cutting fluid via the combination of suspension crystallization and freeze-thaw processes. J. Clean. Prod. 172, 481–487. https://doi.org/10.1016/j.jclepro.2017.09.281.

Gao, W., Shao, Y., 2009. Freeze concentration for removal of pharmaceutically active compounds in water. Desalination 249, 398–402. https://doi.org/10.1016/j.desal.2008.12.065.

Gao, W., Smith, D.W., Sego, D.C., 1999. Ice nucleation in industrial wastewater. Cold Reg. Sci. Technol. 29, 121–133. https://doi.org/10.1016/S0165-232X(99)00019-1.

Gao, W., Smith, D.W., Sego, D.C., 2004. Treatment of pulp mill and oil sands industrial wastewaters by the partial spray freezing process. Water Res. 38, 579–584. https://doi.org/10.1016/j.watres.2003.10.053.

Gao, W., Habib, M., Smith, D.W., 2009. Removal of organic contaminants and toxicity from industrial effluents using freezing process. Desalination 245, 108–119. https://doi.org/10.1016/j.desal.2008.06.013.

Greenberg, A.E., Franson, M.A.H., Eaton, A.D., Clesceri, L.S., 1995. Standard Methods for the Examination of Water and Wastewater, 19th ed. American Public Health Association, Washington (DC).

van der Ham, F., Seckler, M.M., Witkamp, G.J., 2004. Eutectic freeze crystallization in a new apparatus: the cooled disk column crystallizer. Chem. Eng. Process. Process Intensif. 43 (2), 161–167. https://doi.org/10.1016/S0255-2701(03)00018-7.

Hasan, M., Louhi-Kultanen, M., 2015. Ice growth kinetics modeling of air-cooled layer crystallization from sodium sulfate solutions. Chem. Eng. Sci. 133, 44–53. https://doi.org/10.1016/j.ces.2015.01.050.

Hasan, M., Louhi-Kultanen, M., 2016. Water purification of aqueous nickel sulfate solutions by air cooled natural freezing. Chem. Eng. J. 294, 176–184. https://doi.org/10.1016/j.cej.2016.02.114.

Hasan, M., Rotich, N., John, M., Louhi-Kultanen, M., 2017. Salt recovery from wastewater by air-cooled eutectic freeze crystallization. Chem. Eng. J. 326, 192–200. https://doi.org/10.1016/j.cej.2017.05.136.

Hasan, M., Filimonov, R., John, M., Sorvari, J., Louhi-Kultanen, M., 2018. Influence and CFD analysis of cooling air velocity on the purification of aqueous nickel sulfate solutions by freezing. AICHE J. 64, 200–208. https://doi.org/10.1002/aic.15885.

John, M., Suominen, M., Sormunen, O.-V., Hasan, M., Kurvinen, E., Kujala, P., Mikkola, A., Louhi-Kultanen, M., 2018. Purity and mechanical strength of naturally frozen ice in wastewater basins. Water Res. 145, 418–428. https://doi.org/10.1016/j.watres.2018.08.063.

Lorain, O., Thiebaud, P., Badorc, E., Aurelle, Y., 2001. Potential of freezing in wastewater treatment: Soluble pollutant applications. Water Res. 35 (2), 541–547. https://doi.org/10.1016/S0043-1354(00)00287-6.

Mullin, J.W., 2001. Crystallization, 4th ed. Butterworth-Heinemann, Oxford.

Prasse, G., Stalter, D., Schulte-Oehlmann, U., Oehlmann, J., Ternes, T.A., 2015. Spoilt for choice: a critical review on the chemical and biological assessment of current wastewater treatment technologies. Water Res. 87, 237–270. https://doi.org/10.1016/j.watres.2015.09.023.

Randall, D.G., Nathoo, J., 2015. A succinct review of the treatment of reverse Osmosis brines using freeze Crystallization. J. Water Proc. Eng. 8, 186–194. https://doi.org/10.1016/j.jwpe.2015.10.005.

Randall, D.G., Zinn, C., Lewis, A.E., 2014. Treatment of textile wastewaters using Eutectic freeze Crystallization. Water Sci. & Techn. 70 (4), 736–741. https://doi.org/10.2166/wst.2014.289.

Rodriguez-Narvaez, O.M., Peralta-Hernandez, J.M., Goonetilleke, A., Bandala, E.R., 2017. Treatment technologies for emerging contaminants in water: a review. Chem. Eng. J. 323, 361–380. https://doi.org/10.1016/j.cej.2017.04.106.

Shirai, Y., Wakisaka, M., Miyawaki, O., Sakashita, S., 1998. Conditions of producing an ice layer with high purity for freeze wastewater treatment. J. Food Eng. 38 (3), 297–308. https://doi.org/10.1016/S0260-8774(98)00115-0.

Tchobanoglous, G., Burton, F.L., Stensel, D.H., 2003. Wastewater Engineering: Treatment and Reuse. 4. McGraw-Hill, New York.

Williams, P.M., Ahmad, M., Connolly, B.S., Oatley-Radcliffe, D.L., 2015. Technology for freeze concentration in the desalination industry. Desalination 356, 314–327. https://doi.org/10.1016/j.desal.2014.10.023.

Yin, Y., Yang, Y., de Lourdes Mendoza, M., Zhai, S., Feng, W.L., Wang, Y., Gu, M., Cai, L., Zhang, L., 2017. Progressive freezing and suspension crystallization methods for tetrahydrofuran recovery from Grignard reagent wastewater. J. Clean. Prod. 144, 180–186. https://doi.org/10.1016/j.jclepro.2017.01.012.

Publication III

John, M., Suominen, M., Sormunen, O.-V., Hasan, M., Kurvinen, E., Kujala, P., Mikkola, A., and Louhi-Kultanen, M.

Purity and mechanical strength of naturally frozen ice in wastewater basins

Reprinted with permission from
Water Research
Vol. 142, pp. 418-428, 2018

Water Research 145 (2018) 418–428

Contents lists available at ScienceDirect

Water Research

journal homepage: www.elsevier.com/locate/watres

Purity and mechanical strength of naturally frozen ice in wastewater basins

Miia John [a, *], Mikko Suominen [b], Otto-Ville Sormunen [b], Mehdi Hasan [a], Emil Kurvinen [c], Pentti Kujala [b], Aki Mikkola [c], Marjatta Louhi-Kultanen [d]

[a] Department of Separation and Purification Technology, LUT School of Engineering Science, Lappeenranta University of Technology, P.O. Box 20, FI-53850 Lappeenranta, Finland
[b] Department of Mechanical Engineering, School of Engineering, Aalto University, P.O. Box 15300, FI-00076 Aalto, Finland
[c] Department of Mechanical Engineering, LUT School of Energy Systems, Lappeenranta University of Technology, P.O. Box 20, FI-53850 Lappeenranta, Finland
[d] Department of Chemical and Metallurgical Engineering, School of Chemical Engineering, Aalto University, P.O. Box 16100, FI-00076 Aalto, Finland

ARTICLE INFO

Article history:
Received 30 May 2018
Received in revised form
23 August 2018
Accepted 28 August 2018
Available online 29 August 2018

Keywords:
Compressive strength
Flexural strength
Ice impurity
Natural freezing
Wastewater treatment

ABSTRACT

A fairly clean ice cover can form over a contaminated water pond when the air-cooled surface of water freezes and impurities are efficiently expelled to the remaining water underneath. Natural freeze crystallization has recently been studied as a potential wastewater purification method with aqueous solutions on a laboratory scale. The effect of impurity inclusions on ice strength has been researched in model ice basins over the past few decades. It is of interest to discover how efficiently natural freeze separation works under real weather conditions before freezing can be utilized for wastewater treatment application. Herein, understanding the mechanical strength properties of naturally frozen wastewater (ice) is important when planning ice breaking and harvesting devices.

This research implemented in-situ measurements of the flexural and compressive strength of ice in natural ice-covered environments of a freshwater lake, two peatlands and three mining site basins, and compares the determined strength with analyzed impurities of the ice. The results showed that despite varying ice growth conditions and initial water constituents, it was possible to deduce an evident yet simple relationship between mean ice strength and ice impurities: the more impure the ice is, the lower the value of strength is Based on this exploration, it was concluded that separation efficiencies, i.e. the impurity removal ratio between basin water and ice, from 65% up to 90% can be achieved by natural freezing.

1. Introduction

The major industries in raw material production and final product manufacturing produce large quantities of wastewaters, which also more often contain toxic heavy metals and other inorganic constituents in low concentrations. For instance, millions of cubic meters of water can be consumed annually in a mine during the extraction and processing of minerals. This is likely to pollute fresh water sources in the mine environment through acid mine drainage, leaks and the disposal of tailings (Akcil and Koldas, 2006; García et al., 2014). Thus, the large quantities of industrial wastewaters have generated a need to develop energy efficient wastewater treatment methods.

A naturally cold climate could be utilized as a sustainable cooling energy source to purify wastewaters in basins by means of freezing. Several studies have proved that the purification of aqueous solutions and wastewater by natural freezing is a simple, efficient and cost-effective method (Lorain et al., 2001; Hasan and Louhi-Kultanen, 2015; Shirai et al., 1998), which makes natural freezing a potential purification technique to treat huge volumes of wastewaters. The conventional industrial wastewater purification methods based on biological and physico-chemical treatment, such as adsorption, chemical precipitation, electrolytic treatment, flotation, ion exchange and membrane filtration, have some limitations (Fu and Wang, 2011; Kurniawan et al., 2006). In contrast, in wastewater freezing these can be turned to advantages:

* Corresponding author.
E-mail address: miia.john@lut.fi (M. John).

https://doi.org/10.1016/j.watres.2018.08.063
0043-1354/

- Devoid of adding chemicals (Lorain et al., 2001),
- No waste product generation as in chemical precipitation and adsorption (Babel and Kurniawan, 2003),
- No high operational costs caused e.g. by fouling and cleaning of membrane filters or high energy consumption in electrodialysis (Kurniawan et al., 2006),
- High separation efficiency and non-selectivity in impurities are achievable, as ice is naturally highly intolerant to impurities (Bogdan et al., 2014; Lorain et al., 2001).

Sustainable wastewater management includes efficient water purification and provides the possibility for the recovery of valuable materials as well. Particularly with certain industrial wastewaters, natural freezing provides these both, as ice and salt can be crystallized simultaneously in eutectic condition (Hasan et al., 2017). Ice and salt can be separated due to gravity, when salt settles down and ice floats (Randall et al., 2011). If the purity of the ice layer is high, it could be recycled as process water or utilized further as a cold storing material for cold heat storage (Shirai et al., 1999).

Fig. 1 presents a conceptual design of wastewater freezing in a basin with downstream processing of the naturally frozen ice layer. At first, the surface of the wastewater is frozen naturally in the basin. This ice layer is broken into pieces, which could be collected and separated from the concentrated wastewater in the subsequent steps. For ice breaking device design and the optimization of the ice harvesting process, it is of great importance to have knowledge of the mechanical properties of the ice layer, such as bending and compressive strength, the influence of freezing conditions (consequently the purity of the ice) and wastewater composition. The ice strength, together with the ice thickness, determines the design requirements of the ice breaking device, i.e. the strength defines the force needed to break the ice. This research assays the variability on ice strength in the studied wastewaters and gives an overview of further device planning.

Natural ice consists of ice crystals whose orientation, shape and size determine the structural characteristics of the ice as well as impurity inclusions due to the formation of aqueous solution pockets and veins and gas bubble voids in the ice cover. Ice properties such as temperature and structure are considered to affect the physical and mechanical properties of the ice (Light et al., 2003; Timco and Weeks, 2010). Bogdan and Molina (2010, 2017) investigated the impacts of a freeze-concentrated solution on complex phase transformations (such as ice crystallization) during the cooling and warming of bulk solution droplets in emulsions in a highly controlled manner in a temperature range between 133 K and 278 K. They evidenced that the processes yielded mixed-phase particles formed of an ice core with a freeze-concentrated solution coating. The effects of impurities on sea ice in the form of brine (salt) have been studied to a great extent in the past. The studies have shown that increasing the brine content in ice weakens the ice significantly; see Timco and Weeks (2010) for a review study.

The effects of chemicals on the mechanical properties of ice have been studied to some extent already decades ago. These studies have focused on scaling down the mechanical properties of the ice to a suitable strength for model testing in ice basins by weakening the ice (Borland, 1988). Hirayama (1983a) showed a clear decreasing trend in the ice flexural strength and elastic modulus with increased urea concentration; the top layer of the urea doped is thicker than what is observed in sea ice (Hirayama, 1983b). Timco (1981) tested various salts, alcohols, acetates, amides and sugar and came to similar conclusions regarding the reduction in flexural strength with increasing impurities. Timco (1981) reported that the lower the molecular weight of the doped substance is, the lower the concentration required to reduce ice strength is. The same applies for the saturation point, i.e. the point whereafter the ice strength does not decrease (Timco, 1981). Some interaction between various chemicals that intensify the weakening of the ice has also been postulated between aliphatic detergent and ethylene glycol (Lehmus, 1988).

However, studies focusing on purification by freezing have not clearly addressed the effect of impurities on the mechanical properties of ice. Studies focusing on the effect of doped substances on the mechanical properties have considered the concentration of the initial solution, but the purification has not been studied precisely. Furthermore, studies on purification by freezing have been conducted in laboratory conditions where the environment and the initial impurities have been controlled. In contrast, real wastewater is a complicated mixture of various impurities, as it contains constituents that the water accumulates through different processes. When the wastewater is exposed to the open environment conditions, the freezing process is hardly controlled. To use natural freezing for wastewater purification in practice and to be able to break and harvest the purified ice, a few issues need to be clarified: 1) how efficiently the natural freezing purifies the wastewater in the open environment; 2) what the mechanical properties of the ice are; 3) how impurities affect the mechanical properties of ice and 4) how the purity and strength of ice could be assessed.

In this study, the flexural and compressive strength tests for ice were carried out and ice and water samples were collected for chemical impurity analyses from several locations in different types of natural water and wastewater environments. As a result, the effects of impurities on the mechanical properties of ice were

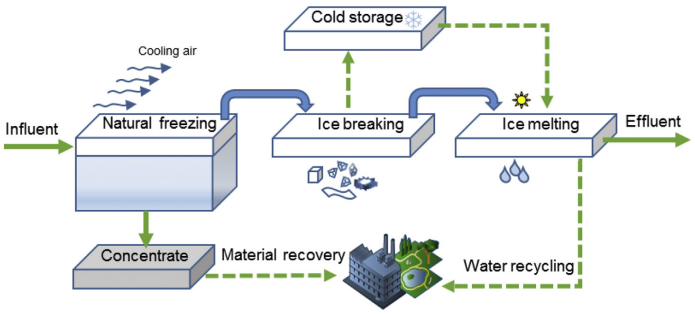

Fig. 1. Principled process of water purification by natural freezing.

analyzed and the parameters that could indicate the impurity level and the strength of ice were identified. The study outlined separation efficiencies of freezing in the studied ice-water basin systems and evaluated how well legislative requirements can be met.

2. Materials and methods

2.1. Measurement sites

The measurements were performed in six different locations in Finland, northern Europe, in winter conditions in March 2017. Fig. 2 presents the geographic locations of the measurement sites. The site characteristics observed during the measurement survey are further presented below.

On the first exploration day, 1 March 2017, Maavesi was chosen as the experiment and sampling site, referred to here as *Lake*. Maavesi is a small 17.9 km^2 lake area isolated from the larger freshwater Lake Saimaa in Southeast Finland. This naturally eutrophic lake is located next to the peat extraction area Suursuo and close to forestry and agricultural areas with draining ditches. Water in the lake is very shallow with a 1.9 m mean depth and low water flow circulation (Sääksjärvi et al., 2016). The ice samples are taken ca. 80 m from the shoreline.

The second (8 March 2017) and third (9 March 2017) sites were situated on peatlands called Suursuo (*Peat I*) and Konnunsuo (*Peat II*) in Southeast Finland. Peat has been extracted from both of these peat bogs for decades. Leachate water from peat production fields flows in a controlled manner along ditches and is channeled to multiunit sedimentation ponds. The water contains suspended solids and nutrients and is treated with the overland flow method and chemical purification before it is released into the environment. The amount of flowing water and water levels in the system are changing due to precipitation and meltwater. During winter, less water flows under ice covered channels and basins. Rain water and trickling leachate from the soil embankment may flow to the ice surface and cause colorful ice layering. (Kuokkanen, 2017). Real water depths were difficult to determine due to mushy sludge sediment layers on the pond bottoms. Ice blocks studied in this research were cut from the center of the ice cover of the sedimentation ponds, areas of ~1700 m^2 (*Peat I*) and ~500 m^2 (*Peat II*).

The fourth, fifth and sixth ice samplings and in-situ experiments were performed in a mining territory in Sotkamo in Northern Finland in 28–30 March 2017. The mining company produces nickel, zinc, cobalt and copper by open pit mining and bioleaching. Water cycles within the wide surface area and water purification processes are distributed to several purification units due to water being used in production and the requirement of controlling rain and meltwaters. The main purification methods are lime milk neutralization for all wastewaters and reverse osmosis for production water. The annually collected or treated total water amount is about 6–10 million m^3. In every studied pond, water flow fluctuated under the ice cover due to varied pumping and piping actions during the ice layer generation. The temperature of the pumped water may also vary. (Terrafame Ltd., 2018). Accordingly, the total influence of circulating water is difficult to assess.

Experiment site no. 4 called *Pond* was a dammed flood pond (area ~160 000 m^2), which has been deployed to secondary settling and water storage use. Most of the incoming waters can be

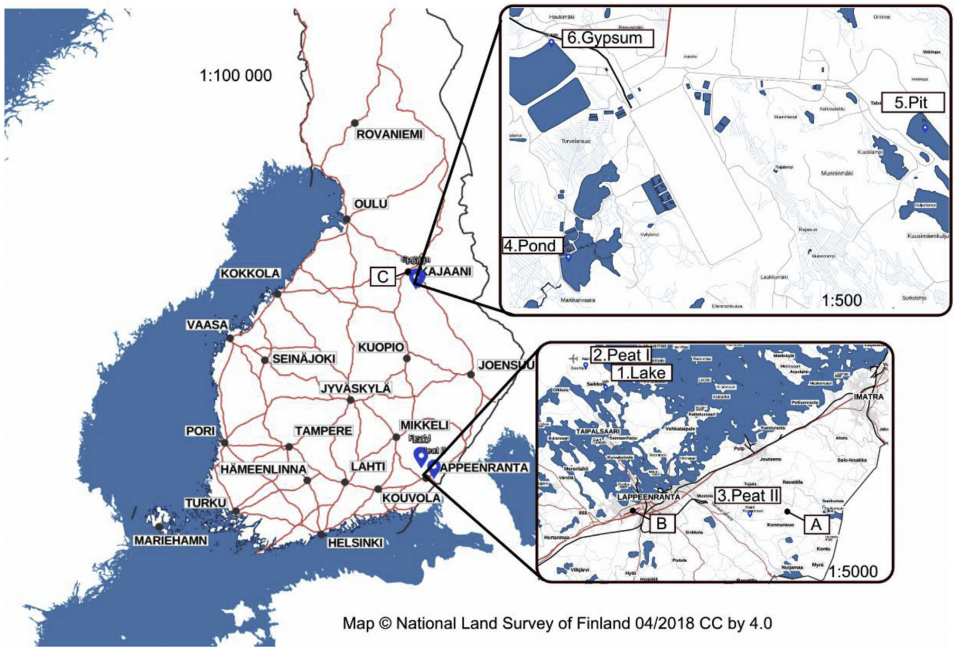

Fig. 2. Locations of the measurement sites in Finland: 1. Lake, 2. Peat I, 3. Peat II, mining site, 4. Pond, 5. Pit, 6. Gypsum. Points A, B and C show the locations of the national recording weather stations near the measurement sites.

considered as a type of natural leachate or drain water from the surroundings. Intensive pumping was causing a curving unfrozen stream through the pond surface, so presumably water flow and circulation is high in the mid-section of the pond. Experiment site no. 5 *Pit* situated in an open mining pit from which around half (area ~180 000 m^2) was dammed for water storage. The other half was in ore mining process use at the moment. Experiment site no. 6 Gypsum was located in a gypsum pond (area ~200 000 m^2), which is used for the sedimentation and settling of chemically treated water in lime purification. Ice samples were cut from the ice surface over the end part of the multiunit water pond flow system, so water was assumed to be quite pure already.

The water ponds or basins in this study are open to air and enfold naturally or are built up in soil walls and the ground. Only the base of the gypsum pond is isolated with a special membrane. Weather conditions (air temperature, humidity, wind and precipitation) as well as water level, the temperature and the flow fluctuation in the water system during the ice cover formation affect the natural freezing process. These conditions have effects on the ice layer growth rate, the characteristics of forming ice and the separation efficiency of impurities (Leppäranta, 2015; Light et al., 2003; Shirai et al., 1998). As the test sites consist of settling basins in real processes designed for different uses, changes in conditions were not possible to determine locally near the ice sheets or under the ice.

2.2. Ice strength measurements

The flexural and compressive strength tests were conducted in-situ next to the ice sampling location. The ice samples for strength tests were extracted by sawing a 120 cm × 20 cm block with a chain saw and then pulled off the ice cover, as Fig. 3a shows. The mobile bending test device can handle a maximum height of 20 cm beams. In the measurement locations, the ice thickness exceeded 40 cm and was sliced into two or three horizontal beams; see Fig. 3b. Each ice beam was then tested individually. For the compression test (see Fig. 3c), a 10 cm × 10 cm x 10 cm cube was cut with a band saw. The temperature of the ice beam during the test was measured by drilling a small hole for the temperature probe.

The flexural strength test was performed in a similar manner as in previous work (Suominen et al., 2013) with a three-point bending device, where the ice beam was seated on two supports. The loading was executed with a piston which was coupled with a recording force sensor. The geometry of each beam and the span were measured after the test. The flexural strength was taken as the tensile axial stress on the bottom surface of the beam. Here, it is assumed that the failure starts on the surface as the axial stress over the cross-section of the beam is the highest on the beam surface. Assuming the beam behaves as an Euler-Bernoulli beam, the flexural strength σ_{Flex} (Pa) was calculated from Equation (1) (Suominen et al., 2013).

$$\sigma_{Flex} = \frac{3\,x}{W\,H^2}\,[F + (L - x)g\,\rho\,W\,H] \quad (1)$$

In Equation (1), L (m) is the length of the span, x (m) is the distance from the support to the location where the ice failed, W (m) is the width of the beam, g (m/s^2) is the gravity, H (m) is the height of the beam, F (N) is the force and ρ (kg/m^3) is the density. The density was determined after the test by cutting a sample of the beam and measuring the dimensions and weight of the cube. It should be noted that the beam theory applied assumes a homogeneous and isotropic material, which ice is not. However, the flexural strength is taken as an index value to estimate the force needed to break the ice by bending.

The uniaxial compressive strength test was produced with a hydraulic piston coupled with a force recording load sensor as in the previous study of Suominen et al. (2013). After the dimensions and the mass of the ice cube were determined, the cube was placed between two metal plates and pressed until it broke. The loading was applied from the vertical direction of the original ice layer, i.e. it was parallel in the growth direction of the ice layer thickness. The compressive strength σ_{Comp} (Pa) was calculated from Equation (2) (Suominen et al., 2013).

$$\sigma_{Comp} = \frac{F + m_p g}{W\,D} \quad (2)$$

In Equation (2), D (m) is the depth of the beam and m_p is the mass of the plate (here 1.852 kg) which was placed on top of the sample; see Fig. 3c.

2.3. Impurity analysis

The guidance on sampling of the European Standard EN ISO 5667 Water quality was followed, where applicable, to be able to obtain representative samples under quite different fieldwork conditions around the sampling locations. A sampling point at a ca. 10 m distance from the hole sawn with a motor saw was chosen to avoid contamination from the motor saw (oil, exhaust fumes and metals). The ice sampling started by removing the loose snow and slush with a shovel. Four holes were drilled in a square form with an auger, and a cubic ice block was extracted with an ice saw and

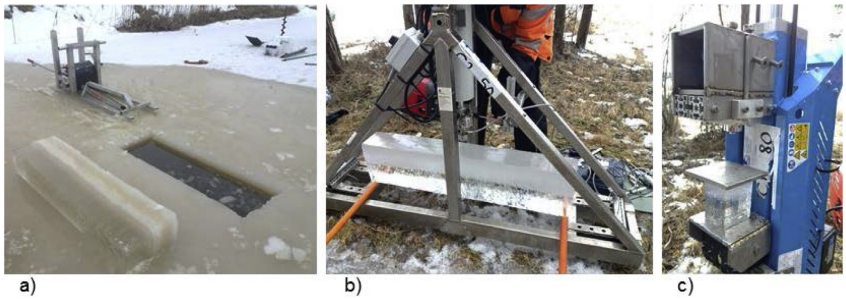

Fig. 3. Setup for in-situ measurements: (a) ice sample extraction before cutting the sample into horizontal slices (*Peat II* ice), (b) the flexural strength test (lake ice) and (c) the compressive strength test (lake ice).

pulled off. The ice block was sliced in sections and composite samples were collected from the whole ice layer and different horizontal layers. Snow ice was not collected within the ice layer samples to avoid air mediated contamination (dust from production areas).

Water samples were collected from the free water under the ice cover through the sampling hole. The temperature and pH of the water were measured. For the water samples, a manually closable pipe sampler with an arm was used to collect 10 × 1 dl subsamples about 0.5 m under the ice. Only from *Peat I*, a water sample was collected from the flowing effluent, as there it was possible to do so in winter. All water and ice samples were collected into polyethylene bottles and closed tightly to be kept cool in a cooler box during transportation to the laboratory. The samples were stored in a freezer room at −18 °C temperature and melted at room temperature for analyses in the laboratory.

In this case, the studied water quality parameters were defined and chosen based on previous data collected in past years and decades at sites for obligatory pollutant monitoring by authorities and companies. This data provided general characteristics of the waters and also showed that the pollutants in the water remain rather constant over long periods. The electrical conductivity (probe with cell constant 1.0 cm^{-1}, range 0.001–100 mS/cm) and pH were measured with a Consort C3040 Multi-parameter analyzer. The apparent color (PtCo) and turbidity (FTU) were measured with a colorimetric method using a Hach DR/2000 spectrophotometer (455 nm, 450 nm). The chemical oxygen demand (COD, mg/L) was determined by a dichromate oxidation method with a spectrophotometer (420 nm, 620 nm) using COD reaction cell tests. Anions – sulphate, nitrite, nitrate and chloride – were analyzed with IC Ion Chromatography, Thermo Scientific Dionex ICS-1100. For IC analysis, samples were prepared with a 0.45 μm syringe filter and Dionex OnGuard II H cartridge filter for metal removal. Chosen elements (Ag, As, Ca, Cd, Co, Cr, Fe, Hg, K, Mg, Mn, Mo, Na, Ni, Pb, Se, Tl, U, V, Zn) were analyzed with inductively coupled plasma mass spectrometry, Agilent 7700 ICP-MS. For ICP-MS analysis, samples were prepared with a 0.45 μm syringe filter and diluted with a mixture of 1% HNO_3 and 0.5% HCL.

3. Results and discussion

3.1. Ice characteristics

Fig. 4 presents the visual characteristics of the ice from the different sites. All ice at the sites seemed to grow in layers. The lake ice also exhibits bubbles appearing as layers of pearls; see Fig. 4a. These can be assumed to be gas bubbles that floated up from the bottom of the lake sediment and were trapped inside the ice. The bubble size increases towards the ice bottom. In the peatland, the ice samples have layers with brown coloring, which may indicate that water rich in humus flows onto the existing ice cover. The *Peat I* ice also exhibits liquid inclusions and the *Peat II* ice showed a very clear column like bottom ice layer; see Fig. 4b and c. The mine site ice – in particular the *Pond* ice (see Fig. 4d) – showed clear colorings almost all the way through. The ice was so weak that sampling for flexural tests was often very difficult as the beams would collapse under their own weight or when lifting. Ice from *Pit* (Fig. 4e) and *Gypsum* (Fig. 4f) also showed distinct layering, where several layers can be considered separate instead of a solid beam. This ice layering with loose grain like ice caused the ice to shatter easily in small ice hails with a diameter of a few millimeters, even when squeezed in the hand.

Table 1 depicts the ice thickness and water temperature under the ice as well as the water depth under the ice and air temperature at the sampling location. Ice layers at the mining site are somewhat thicker than in the lake and peatland due to more freezing degree days and a lower average air temperature. Nevertheless, at the mining site, the difference in thicknesses is 10 cm between pond ice (thickness 0.50 m) and gypsum ice (0.60 m), although the weather conditions during winter are similar. Also lake ice and Peat I ice have a 3 cm difference in thickness, although the distance between these locations is only a few kilometers. It is noticeable that based on the measurement, the water temperature right under the ice cover seemed to be below 0 °C in all wastewater ponds as the waters are undercooled and the freezing point is depressed. As Table 1 shows, the temperatures of the ice were close to 0 °C with in the lake and peatlands and slightly below 0 °C at the mine site, where the weather was also colder during tests. The temperature difference in the ice is so small that the effect on strength measurement results can be considered negligible when compared with other factors, i.e. the direct effect of impurities and structure can be supposed to be more significant here.

3.2. Ice strength results

Figs. 5 and 6 show the calculated results from Equations (1) and (2) for the flexural and compressive strength tests. The measured and calculated results are presented in supplementary material (Supplementary material, Table A.4 and Table A.5). In some tests (particularly in compressive strength; see Fig. 6), differences in strength values between the individual layers were observed. The statistical significance of possible differences in strength between different ice layer measurements from individual sites was tested using ANOVA (Supplementary material, Table A.2). The mean values of flexural and compressive strengths were calculated for different ice layers, and the mean value for the whole ice layer of the site was determined. The strength test devices were selected on the basis of the loading rates causing brittle failure in both flexural and compressive strength tests. The flexural strength measuring device has a nominal loading rate of 11 mm/s and a nominal loading capacity of 4 kN. The compressive strength measuring device has a nominal loading rate of 24.2 mm/s and a nominal loading capacity of 69 kN. However, despite the applied loading rate, some samples failed, clearly in a ductile manner. To keep the results more comparable, these measured ductile results were excluded from the calculations.

Fig. 7 presents the overall mean values of the flexural and compressive strengths of ice samples for all test sites. The lake ice exhibits a much higher flexural strength mean value (1469 kPa) than the peat ice (638 and 518 kPa), whereas the mine site ice has the lowest values (239–373 kPa). The results of the freshwater lake ice are at the same level as presented by Timco (1981), 1200–1400 kPa, and Timco and O'Brien (1994), 1760 kPa. For the sea ice, the values vary from 1000 kPa to as low as 100–150 kPa depending on the salinity and temperature (Timco and Weeks, 2010). Ice is an anisotropic material; thus, variation in the structure causes differences in results when the ice is exposed to different loadings, as in flexural and compression strength tests. This variation can be seen in the results of compressive strength in this study as well as in literature. Timco and Weeks (2010) give a variation on values between 500 and 5000 kPa for sea ice.

3.3. Water and ice impurities

The definition for pollution is interrelated with the environment of the water system, and for that reason, some comparisons are made here only from the viewpoint of the freezing process in general. Some constituents in the studied samples could not be determined at all, as they were below the detection limit. However, the differences in water composition and quality between the sites

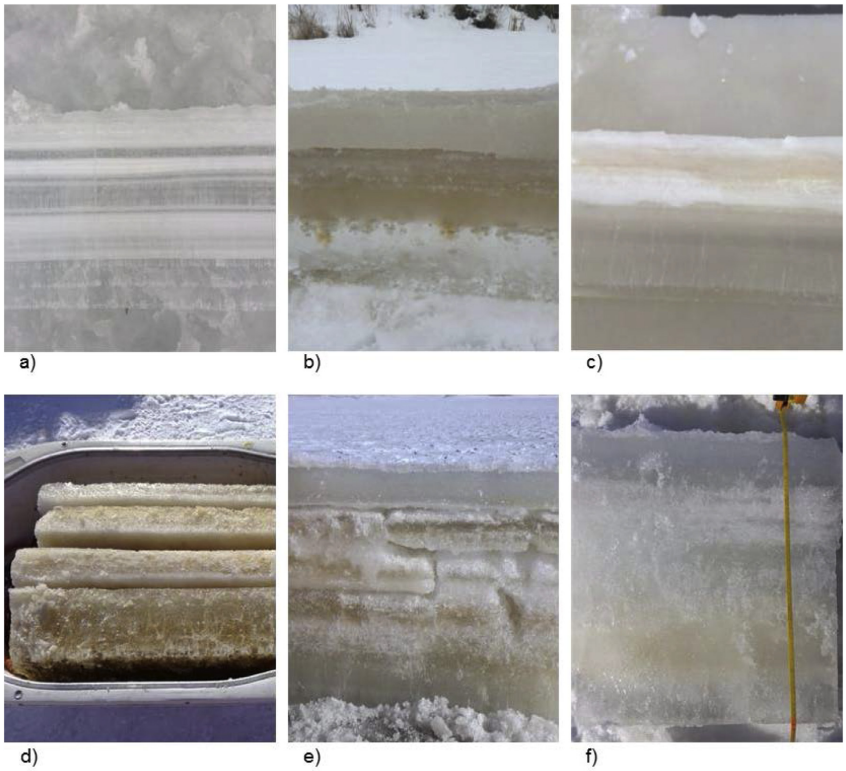

Fig. 4. Ice cross-sections from sites: a) Lake, b) Peat I, c) Peat II and from mine sites d) Pond, e) Pit and f) Gypsum.

Table 1
Observations during on-site measurements at different sites: ice cover thickness, temperature of ice, water depth, temperature of water under the ice, and air temperature during the test day. In addition, freezing degree days (FDD)/total days of monitored winter period and average temperatures recorded by weather stations (locations in Fig. 2) during the winter so far are shown (Data © Finnish Meteorological Institute 04/2018 CC by 4.0.).

Site name	Ice thickness (m)	Ice temp. (°C)	Water depth (m)	Water temp. (°C)	Air temp. (°C)	FDD	Average temp. (°C)
Lake	0.45	0.0	1	0.0	2.5	100/128	−3.68
Peat I	0.42	0.0	2	−0.3	0.0	100/128	−3.68
Peat II	0.41	0.0	2	−0.3	0.0	96/128	−3.74
Pond	0.50	−0.4	6	−0.7	−2.0	124/151	−5.34
Pit	0.55	−0.6	15	−0.7	−7.0 … -2.0	124/151	−5.34
Gypsum	0.60	−0.6	3	−0.5	−12.5 … -2.0	124/151	−5.34

can be seen clearly in the results presented in Table 2. The lake water quality is almost at the same level as the peatland water quality when measured with the chosen indicators. Obviously, the waters of the mine site contain a great number of pollutants, but COD levels as high as 400 mg/L in *Pond* and *Pit* waters were not expected. Tchobanoglous et al. (2003) give similar concentrations for untreated domestic wastewater. *Pond* water can be considered as the richest with impurities of these three mine sites, although color and turbidity are at a very high level in *Pit*. The same trend can also be seen with ice samples; see Table 3 for the average results of ice layers of different sites. The results of analyzed constituents are presented in supplementary material (Supplementary material, Table A.6).

In this dataset, a strong correlation was found between many contaminant variables. On the one hand, this limits statistical multivariate analysis due to collinearity problems, but on the other, knowing one impurity allows predicting other impurity values. (Supplementary material, Table A.1).

The ice purity levels of the collected samples were relatively high in terms of effluent regulations, when the analyzed impurities

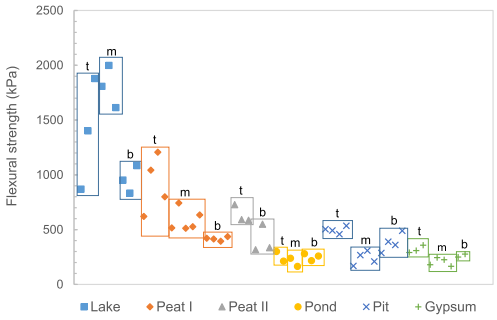

Fig. 5. Flexural strengths of all test site ice samples, ice layers: t - top, m - middle and b - bottom.

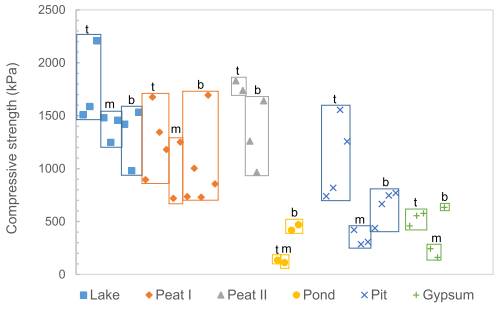

Fig. 6. Compressive strengths of all test site ice samples, ice layers: t - top, m - middle and b - bottom.

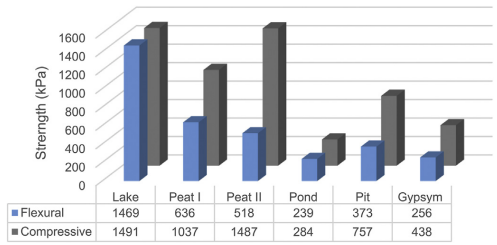

	Lake	Peat I	Peat II	Pond	Pit	Gypsym
Flexural	1469	636	518	239	373	256
Compressive	1491	1037	1487	284	757	438

Fig. 7. Average ice flexural and compressive strength results, all sites.

in the ice were compared with concentration levels regulated by the mining company's environmental permits (Terrafame Ltd., 2018). For example, the maximum concentration limit for the main emission sulphate is 4000 mg/L (for a single sample) in the discharge water pipe, whereas about 2000 mg/L has been reached. In the future, the recommended target will be as low as 1000 mg/L. The sulphate concentrations in every ice of three mine basins were below that: in Pit ice the sulphate concentration was the lowest, i.e. 316 mg/L, and in Gypsum ice the highest, 727 mg/L; see Table 3. It was also positive that the ice of peatlands is cleaner than that of lake water, as their effluents are usually led to natural water systems, such as lakes and rivers.

3.4. Effective distribution coefficient

The effective distribution coefficient K describes the relative impurity constituent in the ice when compared with impurity in basin water. This gives the separation efficiency of the freezing process with this particular constituent as well. The effective distribution coefficient K is determined as $K = C_i/C_w$, where C_i is the concentration (or other measured value indicating water quality) of the constituent in ice and C_w is concentration (or value) of the constituent in basin water.

Figs. 8 and 9 show the calculated effective distribution coefficient K values of relevant constituents for all sites. An approximated average K value of all constituents gives an overview of the total separation efficiency for a process of a certain site. As the COD and turbidity results for *Gypsum* water and ice are very low, the values were excluded from the calculation. The average effective distribution coefficient is the highest, $K = 0.10$, for the *Pit* site, meaning a 90% separation efficiency, while the *Gypsum* site had the lowest one, 65% ($K = 0.35$). The impurity separation process is highly efficient in every pond despite very different water composition concentrations.

There is very little variation in the K values of various constituents at the *Pit* site, whereas other sites have considerably more variation. For example, the K values of two significant constituents, calcium and magnesium, are 0.25 and 0.09, respectively, for the *Pond* site. It is important to be aware of the reasons behind this variation. Most likely, the changes in conditions (initial water flow and quality) are causing impurity inclusions during ice layer growth. As expected, the best separation and the smallest variation in coefficients can be found in the open pit pond where the steadiest state conditions were observed.

3.5. Combined ice strength and impurity analysis

The ice strength as a function of the analyzed impurities was evaluated by fitting various models (linear, polynomial and exponential) to the data, both for the averaged flexural and compressive strengths. This was done at three levels: the individual sample, the layer means and the test site means.

As Figs. 5 and 6 indicate, some of the ice samples show

Table 2
Analysis results of water samples, relevant parameters shown.

	Conductivity (µS/cm)	pH	COD (mg/L)	Color (PtCo)	Turbidity (FTU)	SO_4 (mg/L)	Ca (mg/L)	Fe (mg/L)	K (mg/L)	Mg (mg/L)	Mn (mg/L)	Na (mg/L)
Lake	82.4	6.65	27	73	14	19	7.83	0.07	1.85	2.49	0.07	4.97
Peat I	78.1	6.46	27	125	22	10	6.94	0.11	2.03	2.72	0.14	3.82
Peat II	85.8	6.05	24	194	34	26	8.38	0.25	2.20	3.34	0.36	2.20
Pond	6410	5.74	473	484	94	5580	254.40	40.77	23.64	831.40	268.31	602.88
Pit	4240	3.02	339	1884	346	3236	302.37	126.13	16.81	268.74	192.55	304.65
Gypsum	5390	10.64	<3	30	4	3340	379.88	<0.005	44.62	7.15	<0.005	1330.09

Table 3
Analysis results of ice samples, relevant parameters shown.

	Conductivity	pH	COD	Color	Turbidity	SO_4	Ca	Fe	K	Mg	Mn	Na
	(µS/cm)		(mg/L)	(PtCo)	(FTU)	(mg/L)	(mg/L)	(mg/L)	(mg/L)	(mg/L)	(mg/L)	(mg/L)
Lake	2.54	5.55	<3	2	1	<1	0.05	<0.005	0.98	0.02	<0.005	0.68
Peat I	4.41	5.83	7	55	10	<1	0.35	0.03	0.79	0.12	<0.005	0.42
Peat II	24.4	6.05	10	80	14	7.7	2.54	0.02	0.70	0.88	0.01	0.49
Pond	1083	5.75	55	393	68	694	63.53	0.01	2.41	76.50	22.32	54.47
Pit	575	3.61	45	176	31	316	34.73	6.81	1.89	19.33	13.33	23.42
Gypsum	1259	6.60	<3	25	4	727	214.79	0.03	3.23	3.26	0.10	101.65

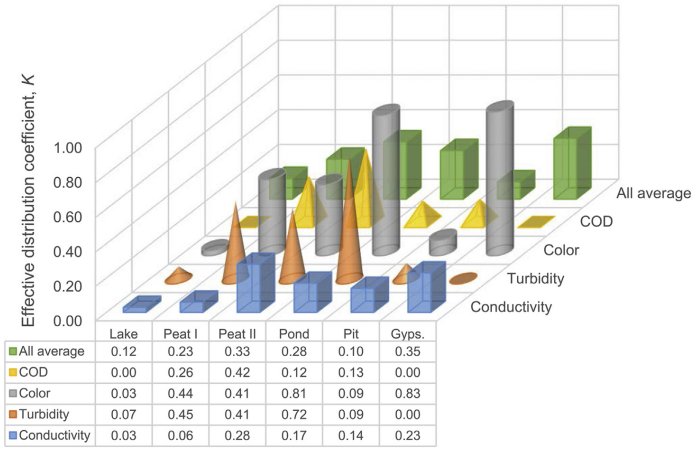

Fig. 8. Effective distribution coefficient K determined by organic (COD) and physical (color, turbidity, conductivity) characteristics and calculated average of all constituents for all sites. (For interpretation of the references to color in this figure legend, the reader is referred to the Web version of this article.)

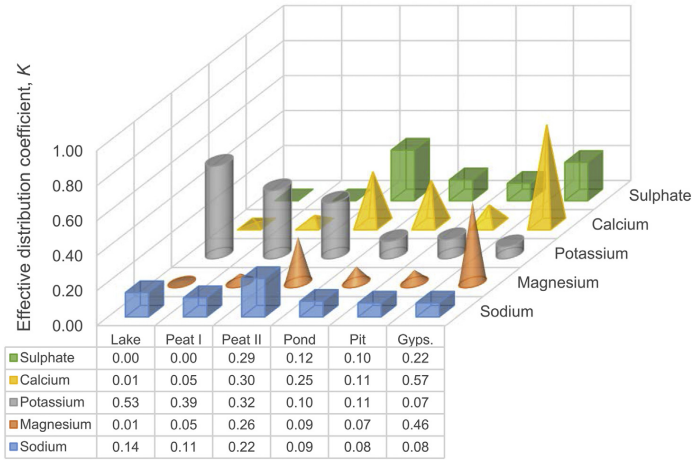

Fig. 9. Effective distribution coefficient *K*, determined by inorganic characteristics: sulphate, calcium, potassium, magnesium and sodium for all sites.

significant scatter in strength – both between some of the layers and between different samples taken from the same ice layer right next to the previous sample. To avoid contamination, the ice samples for impurity tests could not be taken directly from ice samples for the strength tests. This means that there will inevitably be some measurement uncertainty, as the impurity content of the ice varies. Thus, mean impurities are compared with mean strengths. The plotting of the mean impurity values by layers vs. mean strength values by layers, or the plotting of individual strength values vs. layer per average impurity values did not show a significant relation (see Supplementary material, Fig. A.1, A.2 and A.3). This is reflected in the analysis of the ice strength as a function of various impurities: utilizing the mean values for each of the six sample sites, several meaningful mathematical relationships were found. When the comparison was done on a mean layer by layer, the values for R^2 (the coefficient of determination) decreased. Only mathematically meaningful relationships are presented here, as the quantities of different constituents in samples vary on a wide scale (a 1000 times from μg/L to mg/L). Elements with relatively small concentrations can be assumed to have a negligible effect on strength.

The average strength and average impurity values for all relevant samples of a test site (six in total) were analyzed. These calculations can be considered the most reliable, as the measurement uncertainty described earlier can be eliminated, but then we have a quite low $N = 6$. For the flexural strength, meaningful potential relationships were found between strength and calcium, magnesium, sodium and sulphate (see Fig. 10a). Of these, the strongest R^2 with flexural strength was found for calcium ($R^2 = 0.92$). A potential relationship was found between strength and color as well as turbidity, but with COD, R^2 is quite low (see Fig. 11). For the compressive strength, the results were different, providing meaningful results for sodium ($R^2 = 0.824$), sulphate ($R^2 = 0.813$), calcium ($R^2 = 0.669$) and magnesium ($R^2 = 0.638$) (see Fig. 10b).

The most promising single relationship to ice strength as a function of impurity was found to be with conductivity, which can be considered an overall metavariable for other impurities and was shown to correlate strongly with many pollutants. The relationship

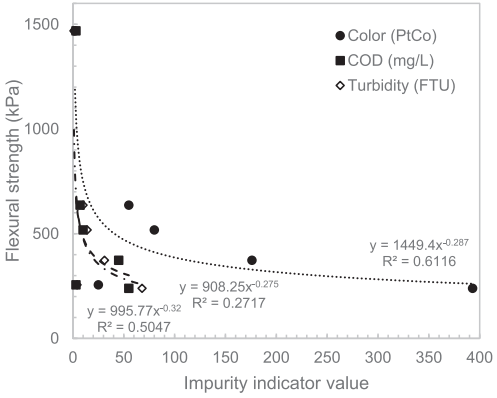

Fig. 11. Mean flexural strength values of test sites as a function of mean color, turbidity and COD values.

between conductivity and ice strength is well modelled with $R^2 > 0.85$ (with equation $y = 1231.2 \cdot x^{-0.221}$) for the mean flexural strength and $R^2 > 0.72$ (with equation $y = 1872.7 \cdot x^{-0.203}$) for the compressive strength (Fig. 12). The R^2 values were even better (0.91 and 0.83) when excluding the freshwater lake ice samples, which barely contain any impurities (Supplementary material, Fig. A.4 and A.5).

Conductivity measurement is based on the conducted electric current due to ionic transportation in a solution; the more concentrated the ionic solution is, the higher the electrical conductivity value is. Based on analyses of the present research, electrical conductivity correlates strongly ($R^2 = 0.9899$) with total ionic concentration, as expected, when all analyzed ionic concentrations for ice samples are simply summarized ($N = 14$) (see Supplementary material, Fig. A.6).

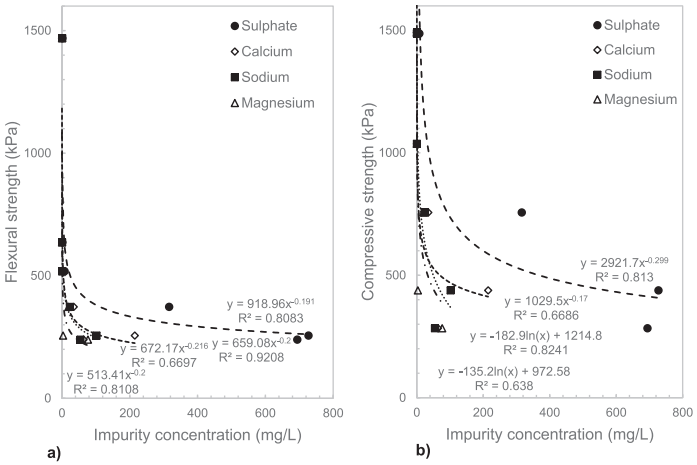

Fig. 10. Mean (a) flexural and (b) compressive strength values of test sites as a function of mean sulphate, calcium, sodium and magnesium concentrations.

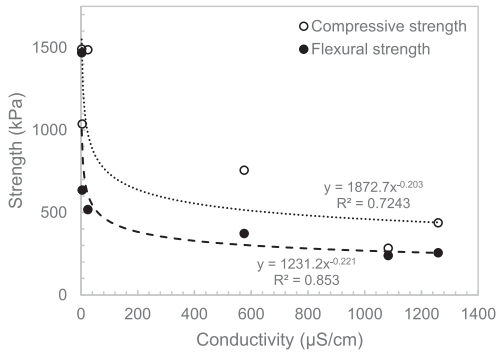

Fig. 12. Mean flexural strength and compressive strength as a function of mean conductivity.

Electrical conductivity is a commonly used water quality indicator in environmental analysis. The conductivity of water is used to estimate the concentration of total dissolved solids (TDS) where the correlating constant numeric value depends on the type of water, i.e. is the ratio of organic and inorganic solid content. In agricultural irrigation, the suitability of effluent from a wastewater treatment plant is determined by applying TDS based on electrical conductivity (Tchobanoglous et al., 2003). The salinity of seawater has been determined by conductivity measurement (see e.g. Timco and Weeks, 2010). Leppäranta (2015) gives a direct method for salinity calculation with lake waters by estimating the dissolved matter concentration by multiplying the conductivity value directly.

Within an electrolyte solution, conductivity can be calculated if all ionic concentrations in the solution are known. Natural or waste waters contain various impurities and the relation of conductivity and concentration is much more complicated. The methods for such calculations have been studied with a comprehensive range of different water types from ground water to mine water and with wide-ranging analysis (McCleskey et al., 2012; Marandi et al., 2013). As a correlation between the electrical conductivity and strength of ice was found, it is of interest to explore the potential of using this easy and quick measurement method further in the evaluation of ice strength.

3.6. Emerged remarks

As the ice layers were grown under non-controlled conditions presented above, the ice layer samples were not homogenous and showed variation between layers and between various layer samples, as was expected. The ice layers exhibited clearly different degrees of transparency and ice structures (e.g. bubbles). In lake ice, there were layers with large bubbles, whereas peatland ice showed brownish middle or top layers and the mine site samples had layers practically detached (fractured) from one another. Due to this, a limitation of the study is the calculation of mean ice flexural and compressive strength, which is calculated here as a pure average of the samples in the ice beams that were cut horizontally. There are methods for calculating the flexural strength for composite beams that could be utilized here. However, these methods should firstly be validated for ice: one of the main open questions is whether the ice in question should be treated as a composite or as loose layers.

The problem of variance in flexural strength in-situ measurements has been demonstrated in other experiments, such as with first year sea ice brine content (Timco and Weeks, 2010). Thus, this variation could be expected. Using the mean strengths and mean impurity values yields much better results, as some of the measurement uncertainty, such as the effect of temperature and fractures or micro cracks inside the ice layer, can be diminished. The results were unexpectedly positive for the mean values despite several limitations. Variation in layers could be investigated more in depth by more controlled experiments with samples of a wide range including also accurate ice crystal structure observations.

In this study, conductivity showed to be the best parameter explaining and comparing the quality of ice or water from different water sources. Lake ice was clearly the cleanest (2.54 µS/cm) and mine pond water the most contaminated (6410 µS/cm). However, the results show that other factors also affect the ice strength. None of these determined constituents can really explain as significant a difference in ice strength as was noticed between lake ice and peatland ice. The average flexural strength of peatland ice showed to be 57–65% smaller than the strength of freshwater lake ice. Nevertheless, a notable difference can be found in color and turbidity, as peatland ice looked partly very colorful and opaque. This can be due to humus and other organic matters which were determined here based on COD analyses only. It would be interesting and important to conduct similar research with wastewaters containing more organic constituents to be better able to define the combined effect of different types of impurities on ice structure and mechanical strength.

4. Conclusions

- The results highlight how much ice is weakened by the presence of impurities in ice: the mean flexural strength value decreased from 1450 kPa to 250 kPa between freshwater lake ice and the more impure ice from a mining site. This is important from the perspective of ice removal: pure ice is quite strong, whereas purified ice still containing some impurities can be broken easily with less force and energy. The results presented here can be utilized towards evaluating how much energy would be needed to break the ice formed from wastewater.
- A strong relationship between mean flexural strength and ice impurity was found. This relationship is surprisingly well modelled with a single variable, electrical conductivity, with $R^2 > 0.8$. This easy measurement may prove to be a feasible parameter in controlling ice harvesting operations.
- The natural freezing of wastewater systems was proved to achieve a 65–90% separation efficiency with different wastewater concentrations. In this study, the purity of ice (water) of the mining site was at a very good level and could also fill the requirements of the environmental permit. When the method is utilized in a designed wastewater treatment process, the efficiency can be expected to be much higher. Therefore, the natural freezing method is applicable to practice in wastewater purification.

The results obtained in this research were consistent with the hypothesis of correlation between impurity and strength: the purer the naturally frozen ice is, the harder it is to break mechanically. This research also showed that the natural freeze separation will work with wide-scale concentrations of wastewaters. This poses challenges in freeze separation process design and optimization. As the production of extremely pure ice will consume more energy in harvesting, finding the optimal thickness and sufficient purity of ice for harvesting operations will be essential in future studies.

Acknowledgements

The research was funded by the Academy of Finland (project no. 285065, 286184 and 285064). The authors would like to thank Jarmo Reunanen, M.Sc. (Tech.), Terrafame Ltd., and Pekka Kuokkanen, M.Sc. (Tech.), Vapo Ltd., for their collaboration and providing access to the experiment sites. The contribution of Maaret Paakkunainen, D.Sc. (Tech.), during the experimental work is also acknowledged.

Appendix A. Supplementary data

Supplementary data related to this article can be found at https://doi.org/10.1016/j.watres.2018.08.063.

References

Akcil, A., Koldas, S., 2006. Acid Mine Drainage (AMD): causes, treatment and case studies. J. Clean. Prod. 14 (12), 1139–1145.
Babel, S., Kurniawan, T.A., 2003. Low-cost adsorbents for heavy metals uptake from contaminated water: a review. J. Hazard Mater. 97 (1), 219–243.
Bogdan, A., Molina, J., 2010. Aqueous aerosol may build up an elevated upper tropospheric ice supersaturation and form mixed-phase particles after freezing. J. Phys. Chem. A 114, 2821–2829.
Bogdan, A., Molina, J., 2017. Physical chemistry of the freezing process of atmospheric aqueous drops. J. Phys. Chem. A 121 (16), 3109–3116.
Bogdan, A., Molina, M.J., Tenhu, H., Bertel, E., Bogdan, N., Loerting, T., 2014. Visualization of freezing process in situ upon cooling and warming of aqueous solutions. Sci. Rep. 4 (7414).
Borland, S., 1988. The growth of EG/AD/S model ice in a small tank. OMAE 1988 Houston. In: Proceedings of the Seventh International Conference on Offshore Mechanics and Arctic Engineering, vol. 4. Arctic engineering and technology, Houston, Texas, pp. 47–53. February 7-12, 1988.
Fu, F., Wang, Q., 2011. Removal of heavy metal ions from wastewaters: a review. J. Environ. Manag. 92, 407–418.
García, V., Häyrynen, P., Landaburu-Aguirre, J., Pirilä, M., Keiski, R.L., Urtiaga, A., 2014. Purification techniques for the recovery of valuable compounds from acid mine drainage and cyanide tailings: application of green engineering principles. J. Chem. Technol. Biotechnol. 89 (6), 803–813.
Hasan, M., Louhi-Kultanen, M., 2015. Ice growth kinetics modeling of air-cooled layer crystallization from sodium sulfate solutions. Chem. Eng. Sci. 133, 44–53.
Hasan, M., Rotich, N., John, M., Louhi-Kultanen, M., 2017. Salt recovery from wastewater by air-cooled eutectic freeze crystallization. Chem. Eng. J. 326, 192–200.
Hirayama, K.-I., 1983a. Experience with urea doped ice in the CRREL test basin. In: POAC'83, Helsinki. Proceedings of the 7th Port and Ocean Engineering under Arctic Conditions Conference. Technical Research Center of Finland in Helsinki, pp. 788–801. April 5-9, 1983.
Hirayama, K.-I., 1983b. Properties of Urea-doped Ice in the CRREL Test Basin. CRREL Report 83-8. U.S. Army Engineer Division, Massachusetts, U.S.A.
Kuokkanen, P., 2017. Vapo Ltd. Personal Communications discussions during field measurements in March 8-9, 2017.
Kurniawan, T.A., Chan, G.Y., Lo, W.H., Babel, S., 2006. Physico–chemical treatment techniques for wastewater laden with heavy metals. Chem. Eng. J. 118 (1), 83–98.
Lehmus, E., 1988. The properties of EG/AD-model ice in VTT ice basin. In: Proceedings of Polartech '88. International Conference on Technology for Polar Areas, the Norwegian Institute of Technology, Trondheim, Norway, 15-17 June 1988, vol. 2, pp. 661–668.
Leppäranta, M., 2015. Freezing of Lakes and the Evolution of Their Ice Cover. Springer Berlin Heidelberg.
Light, B., Maykut, G.A., Grenfell, T.C., 2003. Effects of temperature on the microstructure of first-year arctic sea ice. J. Geophys. Res.: Oceans 108 (C2), 3051.
Lorain, O., Thiebaud, P., Badorc, E., Aurelle, Y., 2001. Potential of freezing in wastewater treatment: soluble pollutant applications. Water Res. 35 (2), 541–547.
Marandi, A., Polikarpus, M., Jõeleht, A., 2013. A new approach for describing the relationship between electrical conductivity and major anion concentration in natural waters. Appl. Geochem. 38, 103–109.
McCleskey, R.B., Nordstrom, D.K., Ryan, J.N., Ball, J.W., 2012. A new method of calculating electrical conductivity with applications to natural waters. Geochem. Cosmochim. Acta 77, 369–382.
Randall, D.G., Nathoo, J., Lewis, A.E., 2011. A case study for treating a reverse osmosis brine using Eutectic Freeze Crystallization - approaching a zero waste process. Desalination 266 (1), 256–262.
Sääksjärvi, E., Reinikainen, S.-P., Louhi-Kultanen, M., 2016. Assessment of water quality in the vicinity of peat extraction sites: the case of Pien-Saimaa, Finland. Water Environ. J. 30 (1–2), 157–166.
Shirai, Y., Wakisaka, M., Miyawaki, O., Sakashita, S., 1998. Conditions of producing an ice layer with high purity for freeze wastewater treatment. J. Food Eng. 38 (3), 297–308.
Shirai, Y., Wakisaka, M., Miyawaki, O., Sakashita, S., 1999. Effect of seed ice on formation of tube ice with high purity for a freeze wastewater treatment system with a bubble-flow circulator. Water Res. 33 (5), 1325–1329.
Suominen, M., Karhunen, J., Bekker, A., Kujala, P., Elo, M., Enlund, H., Saarinen, S., 2013. Full-scale measurements on board PSRV S.A. Agulhas II in the Baltic sea. In: Proceedings of the 22nd International Conference, Port and Ocean Engineering under Arctic Conditions (POAC'13), Espoo, Finland, June 9-13, 2013.
Tchobanoglous, G., Burton, F.L., Stensel, D.H., 2003. Wastewater Engineering: Treatment and Reuse, fourth ed. McGraw-Hill, New York.
Terrafame Ltd, 2018. Annual Report 2017. Responsibility (Accessed 17 May 2018). https://www.annualreport2017.terrafame.fi/responsibility-2/chief-sustainability-officers-review.html.
Timco, G., 1981. Flexural strength of ice grown from chemically impure melts. Cold Reg. Sci. Technol. 4 (2), 81–92.
Timco, G., O'Brien, S., 1994. Flexural strength equation for sea ice. Cold Reg. Sci. Technol. 22, 285–298.
Timco, G., Weeks, W., 2010. A review of the engineering properties of sea ice. Cold Reg. Sci. Technol. 60 (2), 107–129.

Publication IV

John, M., Choudhury, T., Filimonov, R., Kurvinen, E., Saeed, M., Mikkola, A., Mänttäri, M., and Louhi-Kultanen, M.
Impurity separation efficiency of multi-component wastewater in a pilot-scale freeze crystallizer

Reprinted with permission from
Separation and Purification Technology
Vol 236, 116271, 2020

Separation and Purification Technology 236 (2020) 116271

Contents lists available at ScienceDirect

Separation and Purification Technology

journal homepage: www.elsevier.com/locate/seppur

Impurity separation efficiency of multi-component wastewater in a pilot-scale freeze crystallizer

Miia John[a,*], Tuhin Choudhury[b], Roman Filimonov[c], Emil Kurvinen[b], Muhammad Saeed[a], Aki Mikkola[b], Mika Mänttäri[a], Marjatta Louhi-Kultanen[d]

[a] Department of Separation and Purification Technology, LUT School of Engineering Science, LUT University, P.O. Box 20, FI-53850 Lappeenranta, Finland
[b] Department of Mechanical Engineering, LUT School of Energy Systems, LUT University, P.O. Box 20, FI-53850 Lappeenranta, Finland
[c] Department of Computational and Process Engineering, LUT School of Engineering Science, LUT University, P.O. Box 20, FI-53850 Lappeenranta, Finland
[d] Department of Chemical and Metallurgical Engineering, School of Chemical Engineering, Aalto University, P.O. Box 16100, FI-00076 Aalto, Finland

ARTICLE INFO

Keywords:
Ice purity
Freeze crystallization
Purification efficiency
Wastewater treatment

ABSTRACT

New directions in wastewater treatment consider not only the adequate purification efficiencies but also water and material recovery for recycling and reuse. Freeze crystallization offers the potential for the simultaneous separation of water (ice) and material (i.e., salts and nutrients) from wastewater using a single wastewater purification process. However, the impurity-separation performance of freeze crystallization applied to multi-component wastewaters is still unclear, particularly for industrial or municipal scales.

In this study, a prototype was developed to demonstrate the application of freeze crystallization to wastewater purification on the industrial scale. This freeze crystallizer, a 120 L jacketed vessel equipped with stirring and ice scraping mechanisms, produced relatively large (500 μm) ice crystals, primarily in water suspension. To evaluate the purification efficiencies of the prototype system, a comprehensive number of water-quality indicators were measured following the purification of highly concentrated landfill leachates. The prototype system achieved a > 95% average impurity removal efficiency for both organic and inorganic matter, including heavy metals. This excellent separation ability, given the variety of impurities present in the leachates, shows the non-selective nature of freeze separation for wastewater treatment. These outcomes represent an important step forward in scaling up and developing the full scale freeze purification process for wastewaters.

1. Introduction

Conventional wastewater treatment systems combine a number of different purification sub-processes to make effluent clean enough to be returned to the environment. Because of urban living and industrial activities, variegated impurities accumulate in waters forming dilute but complex aqueous solutions. Then, the wastewaters are drained and piped long distances to wastewater treatment plants. There, the physical, chemical and biological processes play their unique roles in the purification process with more advanced techniques applied in even more limited operating environments. The complexity of these systems makes it difficult to maintain reasonable energy consumption levels and operating costs. Reducing the overall volume of water being transferred and/or treating the wastewater nearer to its source could help. Moreover, it is becoming increasingly important to address industrial effluents that contain toxics, heavy metals, or other harmful substances, and urban origin wastewaters that contain emerging micropollutants, with more advanced water purification methods.

According to our previous research [1] and the results obtained by Erlbeck et al. [2], Yin et al. [3] and Williams et al. [4], freeze crystallization has many of the attributes needed for efficient and cost effective wastewater treatment. Environmental friendliness is a key benefit, because the freezing process needs no added chemicals, no more waste is generated (as filter media), and toxic waters can be treated. In arctic areas, energy efficiencies can even be higher if the colder temperatures in those environments are properly exploited. In addition to cost savings, the lower operating temperatures associated with freeze crystallization can result in substantially less corrosion. In this study, however, purification efficiencies and the theorized non-selective nature of impurity separation are of interest. The high separation ability may enable better water and material recovery and recycling in the future. In addition, by freeze crystallization it is possible to reduce the pure water quantity of wastewater concurrently with the wastewater purification process [5].

* Corresponding author.
E-mail address: miia.john@lut.fi (M. John).

https://doi.org/10.1016/j.seppur.2019.116271
Received 12 July 2019; Received in revised form 16 October 2019; Accepted 30 October 2019
Available online 05 November 2019
1383-5866/

Existing freeze crystallization methods in wastewater treatment can be divided into three main categories: ice growth in a layer, droplet (spray) freezing, and ice growth in suspension. This study focuses on the latter and in particular on the suspension freeze crystallizer. Bogdan and Molina [6] studied the forming of mixed–phase particles from solution droplets during freezing and observed an ice core forming with a freeze-concentrated solution coating. Similarly, when ice crystallization takes place in an aqueous solution, the formed ice naturally repels impurities leaving a remaining liquid with a concentration of impurities. In a suspension freeze crystallizer, the formed ice particles are dispersed throughout the fluid in the suspension of the mother liquid. The transactions between growing ice crystals and concentrated solution, i.e., how impurities adhere to the ice crystal surface when crystals are forming and floating inside the liquid and how easily impurities are detached during ice separation, determine total impurity removal efficiencies [7,8].

Previous research concerning suspension freeze crystallizers has often been performed using model or artificial waters instead of real wastewaters and mostly in the laboratory. Moreover, these experiments usually utilize eutectic freeze crystallization (EFC), and they focus more on investigating process parameters and crystal size than on examining purification efficiencies in terms of ice purity [1,9,10]. Experiments conducted on a larger scale are more often carried out using the EFC technique and with industrial effluents or brines as concluded from reviews of freeze crystallization for desalination [3] and reverse osmosis brine treatments [11]. For instance, Rodriguez Pascual et al. [12] and Van Spronsen et al. [13] conducted EFC-tests with scraped and cooled wall crystallizers, volumes of 130 L and 180 L, respectively. Clear purification efficiencies by ice purity were not presented, as the study was more focused on process control, heat transfer, and carbonate salts production from specific industrial waste solutions.

Suspension freeze crystallization experiments conducted with real wastewater that include purification efficiency studies or extensive impurity analyses are rare. Chang et al. [8] studied freeze desalination by analyzing the major ions from seawater: sodium, magnesium, calcium, and potassium. Their focus was on the salinity limits of potable water so clear impurity removal efficiencies were not determined. Similarly, Erlbeck et al. [2] studied freeze desalination with slightly wider analysis (anions chloride and sulfate in addition) using the Atlantic Ocean seawater and results were presented by concentrations (mg/L) as well. In most studies, the ice formed in wastewater is analyzed using one or two indicators. For instance, Yin et al. [3] and Feng et al. [14] presented a chemical oxygen demand (COD) removal efficiency above 90% with wastewaters from the pharmaceutical industry and waste cutting fluid from a machinery factory, respectively. Similarly, the 98% ice purity from EFC used to treat textile wastewaters was presented in a color and sodium analysis indicating the main impurity, sodium sulfate [15]. Slightly wider analyses with some cation and anion concentrations were conducted via EFC tests with reverse osmosis brine by Randall et al. [10]. However, the purities of the produced sulfate salts and not the clear removal efficiencies were presented. The scarcity of published research where actual wastewaters are treated by freeze crystallization in a reactor might be the result of the complex nature of wastewater matrices, i.e. a multi-component mixture of impurities [16].

The research reported here demonstrates how well the landfill leachate wastewater was purified in the newly developed freeze crystallizer prototype. In a broader context, the objectives were to establish how well the freeze crystallization method separates all types of wastewater impurities (organic and inorganic, soluble and insoluble) and to demonstrate, through extensive analysis, the non-selective nature of the freezing method. The landfill leachate was selected for testing, because it contains a wide variety of impurities.

2. Pilot crystallizer design

Important design basis requirements for the wastewater freeze crystallizer included high separation performance and ease of operation. To ensure mobility, another requirement was to keep the reactor size small enough to accommodate installation in an intermodal container. Proving the freeze crystallization process in the resulting reactor was the basis for all design choices. A process that produces larger ice crystal sizes in lower quantities was targeted to minimize overall ice crystal surface area and, as a result, minimize the percentage of impurities adhering to crystal surfaces [7]. With less contamination, the separation of solid ice from the ice-water slurry is more effective and results in less washing needed. The main driving force in freeze crystallization is temperature difference (ΔT) between the water in the reactor and the coolant [1]. Therefore, the ability to control the water temperature during the crystallization process was considered especially important to process design. Stirring was introduced to keep the water mixed, which improves heat transfer and temperature equalization. Simplistically, stirring directly affects supersaturation, ice nucleation, ice crystal growth, and ultimately ice crystal size [17]. Encrustation, ice scaling on the cooling wall surface, is undesirable for the process; however, the freeze crystallizer prototype was designed with a scraping assembly to prevent the forming of ice scale.

2.1. Freeze crystallizer

Precooling the wastewater input to the freeze crystallization reactor minimizes the cooling load required within the reactor vessel and allows the use of a conventional jacketed vessel even though heat transfer out through the jacketed walls is reduced. Fig. 1 shows the reactor model of the freeze crystallizer used in this study for impurity separation. The water capacity of the vessel is 120 L excluding the non-jacketed conical volume at the base. The jacketed vessel is approximately 1080 mm in height, has an inner diameter of 400 mm, and an outer diameter of 450 mm. Wastewater enters the vessel via an inlet located at the top head of the reactor. The ice slurry outlet is at the top of the vessel as well. Emptying of the vessel, and sampling of the concentrated water if needed, can be accomplished through the pinch valve with a manual actuator installed at the bottom of the vessel.

The crystallizer operates on the principle of indirect contact freezing. The coolant is pumped into the jacket through the coolant inlet at the bottom (Fig. 1) and is fed out from the top of the jacket. The

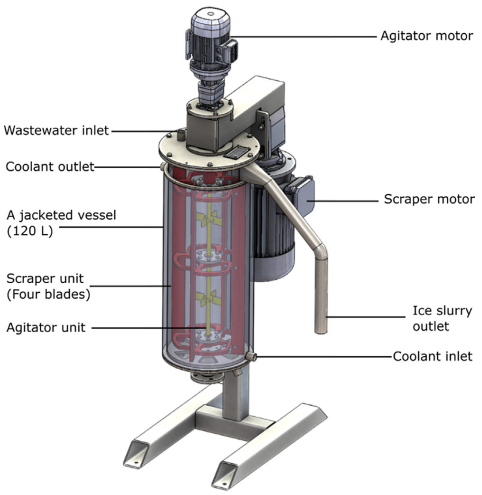

Fig. 1. Pilot-scale reactor and its main components.

total amount of coolant, including the pipe and reactor jacket volumes, is 60 L (29 L in the reactor jacket). Because the outer jacket wall is thermally insulated, the flow through of coolant in the jacket induces heat transfer by conduction from the wastewater through the jacket wall to the coolant. The wall comes directly into contact with the coolant; therefore, it induces a local high temperature difference between the inner wall surface of the reactor and the water being cooled. As a result, ice crystals tend to form and adhere to the cold surface of the wall, i.e. ice scaling occurs instead of forming ice crystals in the suspension of the water. Usually, it is difficult to prevent ice scaling or to remove the formed ice layer from the surface of the wall without adding a scraping mechanism [13]. Furthermore, as the thickness of ice layer increases, it begins behaving like thermal insulation due to the low thermal conductivity of ice, 2.2 W/(m·K) at 0 K [18]. This leads to a reduction of overall heat transfer coefficient between the coolant and water, which works against any further wastewater cooling. The scraping mechanism eliminates the problem by mechanically removing the ice layer before it grows overly thick. Our previous studies [19,20] concerning the ice growing in layers, showed that the purity of the ice layer correlates with the mechanical strength of ice; the purer the formed ice layer, the more force needed to break the ice. Consequently, a scraper operating at high torque is necessary to ensure sufficient scraping force to maintain optimum heat transfer and maximum ice production.

Notwithstanding incorporation of the scraping mechanism, the rate of cooling of the wastewater remains uneven throughout the solution in the reactor. Firstly, the radial distribution of cooling is higher near the surface of the wall than at the center of the vessel. Secondly, the surface close to the inlet point of the coolant is subjected to the maximum amount of cooling. This uneven radial and vertical cooling can be avoided by installing an agitator inside the reactor. By enhancing liquid circulation, the cooling rate of the solution can be improved and a more uniform temperature distribution inside the crystallizer can be achieved [1,21]. The configuration of the agitator impeller was determined using computational fluid dynamics (CFD) modeling (see Supplementary material, CFD simulations). The present reactor employs a dual impeller configuration: two 4-flat-blade disk type radial flow impellers installed equidistantly from the scraper discs (Fig. 2a). The impeller diameter is 150 mm (~0.37 · diameter of the reactor), the blade length is 50 mm, the blade width is 40 mm, and the disk diameter is 55 mm. The agitator was connected to a 1.1 kW motor via a gear-box with a 2.8 gear ratio (BONF C122P-2.8 P90 B3). The axle assembly consists of a nested scraper and agitator axles with mounted bearings at the bottom of the vessel.

The scraper consists of four blades, which are bolted to three equally spaced discs along the length of the reactor (Fig. 2a and b). The short hollow shaft at the top of the scraper (Fig. 2a) connects to a 2.2 kW variable speed motor via a gear-box with a 72.9 gear ratio (Fig. 1). The gear-box provides the required torque (here maximally 800 Nm) while varying the scraper speed between 0 and 20 rpm. With an increase in ice scaling on the walls, torque requirement increases, which is automatically facilitated by the gear-box. Furthermore, based on a study by Nixon et al. [22] on general improvements to an ice scraping edge, a clearance angle of 5° between the cutting edge of the blade and the ice surface results in the least amount of force needed for scraping. This particular feature is incorporated on the scraping edge of the blades, as shown in Fig. 2b, for efficient ice removal.

The selection of material for the reactor vessel and the auxiliary subassemblies such as the scraper and agitator is another challenging aspect of crystallization reactor design. The reactor requires a material that has high thermal conductivity, such as copper. However, the material must be less reactive to acids or other compounds that might be present in the wastewater. Therefore, AISI 316 grade of stainless steel is considered a suitable alternative. The stainless steel is also used for the scraper and the agitator as it provides the necessary sturdiness for the structure without compromising on heat transfer.

2.2. Cooling unit

The custom-made cooling device, with a maximum cooling power of 15 kW, comprises a refrigeration unit with a R-134a refrigerant cycle assembled with standard parts. The unit is responsible for circulating monopropylene glycol coolant to the jacket of the reactor with automatic flow control at a minimum flow rate of 10 L/min to a maximum of 60 L/min. The cooling unit is operated and controlled by a Siemens Simatic HMI. The glycol coolant temperature can be preset to any value in the range of −25 °C to 25 °C with an accuracy of 0.01 °C. The nominal coolant temperature is set from 1 to 3 °C below the freezing point temperature of the wastewater being treated. An immersion heater was added to the cooling loop for use in emergency cases, such as the scraper jamming in the ice layer or the water in the reactor freezing.

3. Materials and methods

3.1. Wastewater

Freeze crystallization testing was carried out using landfill leachate

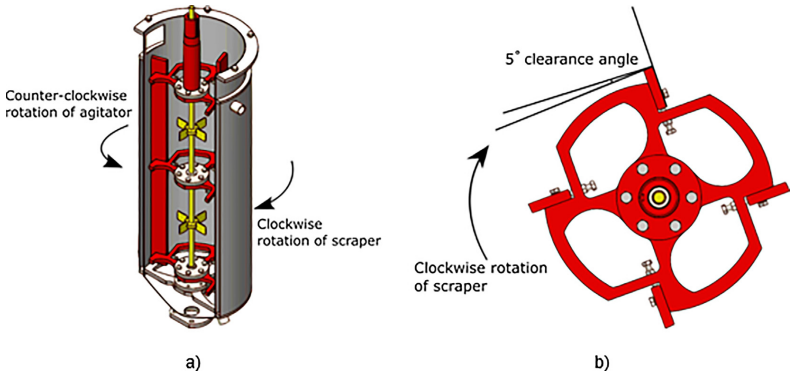

Fig. 2. Section view of the reactor; (a) the configuration of the scraper and the agitator, (b) the scraper-agitator sub-assembly showing 5° clearance angle for the scraping blade.

wastewater taken from the Kukkuroinmäki landfill (Lappeenranta, Finland). The landfill serves as a waste disposal site for non-recyclable waste fractions, and it is situated next to the regional waste management center of Etelä-Karjalan Jätehuolto Oy. Wastewater quality is regularly monitored in compliance with environmental permit regulations. Test wastewater was collected by pumping water from the tank collecting the downward percolation water (due to the precipitation) from the ordinary dry waste bank. Accordingly, the leachate contains constituents dissolved out from the soil fillings and waste materials. The water for the tests was collected in the winter of 2018 when the volume of pumped leachate from the bank is exceptionally low, ~1175 m^3 in a month, as the variation of flow can be 1000–6300 m^3/month. This resulted in an atypically high concentration of impurities in the leachate. The collected water was transported and stored in 200 L polyethylene plastic barrels and preserved in a cold room at 4 °C before use in the experiments.

3.2. Experimental setup

The freeze separation experiments were conducted with the pilot-scale crystallizer and the cooling unit presented above (Section 2.) and in Fig. 3. The process parameters for wastewater freezing experiments were chosen based on the preliminary experiments. When the new reactor was initiated, the freezing experiments were conducted using tap water, model sodium chloride solutions and landfill leachate as well. As a result of those tests, it was found that the proper ice generated at the operating temperature of −3 °C and high separation efficiency, > 95%, was achieved. Since some challenges with the startup of new equipment were faced, as expected, the functional limits for the scraper and agitator were assessed as well. The minimum rotational speeds were found to be 5 rpm and 100 rpm, respectively, since the use of lower speeds induced an overheating of air-cooled motors. In turn, mechanical effects like increased vibration were found to limit the use of higher rotational speeds. Thus, moderate but different scraper rotational speeds

Fig. 3. Freeze crystallizer and cooling unit in the testing environment.

Table 1
Experimental conditions (DoE) in freeze crystallization tests.

Test	T	ω, scraper	ω, agitator
	(°C)	(rpm)	(rpm)
Series C1: Ice seeding at 0 to −0.06 °C			
A	−3.0	7	150
B	−3.0	7	200
C	−3.0	7	250
D	−3.0	10	250
E	−3.0	10	150
Series C2: Ice seeding at −0.4 °C			
F	−3.0	7	150
G	−3.0	7	200
H	−3.0	7	250
I	−3.0	10	250
J	−3.0	10	150

of 7 and 10 rpm and agitator rotational speeds of 150, 200 and 250 rpm were chosen for experimental comparison. The frequency converters (1.1 kW and 2.2 kW) were used to control the rotational speed of the agitator and scraper motors (respectively) as well for the control of the direction of rotation. In these experiments, the agitator was rotating anti-clockwise and the scraper clockwise. Table 1 presents the Design of Experiments (DoE) which shows the different scraper and agitator rotational speed combinations used in these tests.

In this study, the freeze crystallization process was operated as a batch process with the residence time of 60 min in every test. The time was counted from the start point of freezing, as the freezing point temperature was reached and ice crystals began to form. The operating temperature (T) for the circulating coolant was −3.0 °C for every test. This derived the temperature difference (ΔT) between coolant and wastewater to be close to 3 °C, as the freezing point depression of the wastewater was measured to be moderate, 0.1 °C. The effect of undercooling on freezing was studied by choosing two different ice seeding (i.e., adding of some ice crystals) temperatures, as shown in Table 1. First, the seeding temperature with series C1 was set close to the freezing point temperature −0.06 °C (~0 °C). With series C2, the wastewater was let to undercool slightly and seeds were added at −0.4 °C.

The temperature of the water was measured at the bottom of the reactor. A PT 100 sensor (accuracy ± 0.015 °C, resolution 0.001 °C) was connected with a Pico PT-104 Data logger to a PC. The PicoLog software was used for data logging with a 10 s detecting interval as well as online temperature observation on screen during the freezing process. The ice-crystal growth process within the crystallizer was observed visually and by video camera. A bulk endoscope camera YPC110 (resolution 1600 × 1200, diameter 8 mm, 30 FPS and FOV 70°) was installed on the top of the reactor. An external lamp was used while observing the formed crystals inside the reactor.

3.3. Experimental procedure

A 120 kg batch of well-stirred wastewater was pumped from the barrel container into the crystallizer through the inlet. The wastewater was stored in a cold room, so it had already been precooled to ~4 °C. The water was further cooled via refrigeration and coolant circulation through the jacket by setting the coolant temperature to −3 °C via the control unit of the cooling device. The process parameters, agitator rotational speed and scraper rotational speed, were set according to the DoE. These settings were kept constant. Ice seeding was performed at a predefined temperature. It was implemented manually by dropping a few ice grains into the water through the inspection hole in the reactor cover. The primary tests showed that the number of ice seeds needed is low, ≪0.02% of water volume.

Prior to each freezing test, a sample of the initial wastewater was collected and stored. Immediately after each freeze crystallization test

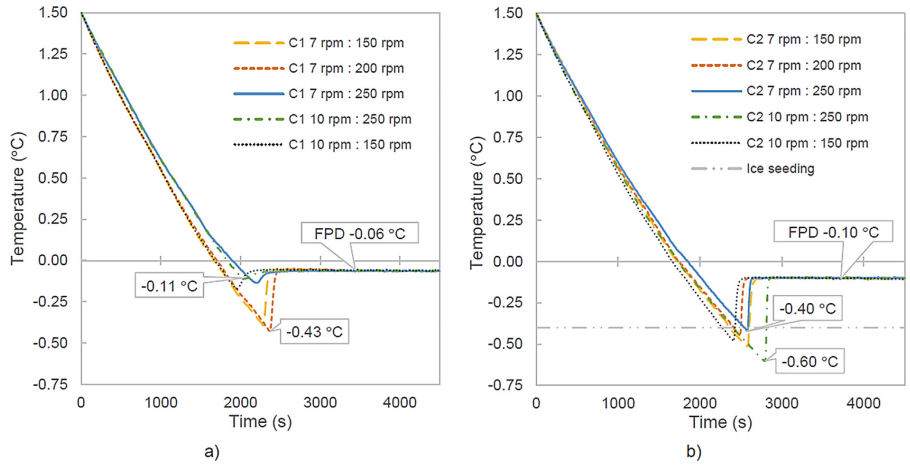

Fig. 4. The cooling curves of freezing processes with different test conditions observed for 75 min: (a) Series C1, the ice seeding at ~0 to −0.06 °C and (b) Series C2, the ice seeding during the undercooling at −0.4 °C.

with a residence time of 60 min, the agitator and the scraper were turned off allowing ice to float on the wastewater surface. Several small samples were collected through the top part of the reactor using a small sieve-like sampler (skimmer tool) and combined to make up each sample of formed ice. The collected ice crystals were placed in a 150 mL PP-plastic funnel (with a perforated plate) to drain the excess water. Finally, the samples of "unwashed ice" were combined. For the sample of "washed ice", the ice crystals were washed three times by filling the funnel with 30 mL cooled tap water (~0 °C) to form an ice-water suspension, which was then mixed and drained. Because the intention was to simulate realistic process conditions, no vacuum filtration was used to ensure the slow release and dissolution of the impurities attached to the ice crystals. Some natural melting of the ice also contributed to impurity detachment. The ice and wastewater samples were stored in tightly closed 250 mL PE-plastic bottles in a freeze room at −18 °C. Before chemical analysis, the melted ice samples and stored initial wastewater samples were warmed to room temperature.

3.4. Chemical analyses

The initial wastewater and produced unwashed and washed ice samples were analyzed using common water quality measures and methods. A Consort C3040 Multi-parameter analyzer was used to measure pH and electrical conductivity (EC, mS/cm) using a probe with cell constant 1.0 1/cm and range 0.001–100 mS/cm. A HACH DR/2000 spectrophotometer was used to determine chemical oxygen demand (COD, mg/L) via the dichromate oxidation method using 0–150 ± 2.7 mg/L (420 nm) and 0–1500 ± 14 mg/L (620 nm) Spectroquant COD reaction cell test tubes. The same spectrophotometer was used to measure turbidity (FTU) and apparent color (PtCo) via the colorimetric method (450 nm, 455 nm). Total phosphorus (TP, mg/L) of a small number of samples was analyzed using a Merck Spectroquant Nova 60 photometer and photometric test kits for phosphorous.

A wider range of elements was analyzed to investigate the non-selective nature of freeze separation. The concentrations (mg/L) of total organic carbon (TOC), total carbon (TC), inorganic carbon (IC), and total nitrogen (TN) were analyzed with a Shimadzu TOC-L analyzer using the Combustion Catalytic Oxidation/Non-Dispersive Infrared Detection method (detection limit for TC and IC 4 µg/L, for TN 5 µg/L). In total, 25 elements; Au, Ag, Al, As, Bi, Ca, Cd, Co, Cu, Cr, Fe, Hg, K, Mg, Mn, Mo, Na, Ni, Pb, Sb, Se, Te, U, V, and Zn; were analyzed using an Agilent 7700 ICP-MS inductively coupled plasma mass spectrometer. For analysis, the samples were syringed with 0.45 µm pore size cellulose acetate membrane filters. Samples for ICP analyses were diluted with an acid solution (1% HCl, 1% HNO_3). The samples apparently containing a lot of suspended solids were centrifuged at 3000 rpm for 5 min before dilution for the ICP analyses.

4. Results and discussion

4.1. Freezing process

Based on acoustic and visual observations made during the experiments, ice growth in the water suspension occurred first followed by ice-scaling layer growth. The scraping sound made as the scraper blades shaved the ice layer from the wall was very clearly perceptible. Based on the initiation of that sound, the freezing time it took to reach 2 mm ice thickness on the cooling wall surface (at some part of the wall) was about 50 min with the process parameters used.

The ice mass production goal was 10 kg/h, i.e., 83 kg/(h·m^3). The result after an hour of residence time was 11–12 kg, which was determined by measuring the masses of concentrated water and/or the ice. Accordingly, the mean ice growth rate calculated by measuring total ice mass yield and freezing time was 96 kg/(h·m^3), i.e., 27 g/(s·m^3). This ice mass production rate is similar to results presented in previous studies though with a continuous crystallization process. For instance, Rodriguez Pascual et al. [12] reported 25.6–42 g/(s·m^3) ice production in a cooled wall EFC crystallizer with scraping. The volume of their system, for a sodium carbonate solution, was 130 L. Van der Ham et al. [23] reported 79 kg/(h·m^3) ice production in a cooled disk column crystallizer.

In the present study, since the temperature difference between coolant and water was kept at about −3 °C for every test, there was no clear evidence for how the process parameters used affected ice production. It seemed that agitator intensity did influence the onset of ice scaling, but this could not be verified explicitly.

From the temperature measurements, a cooling curve can be drawn and the basic thermodynamics of the freezing process can be clearly presented. Fig. 4 presents the cooling curves (the temperature as a function of time) of the two series C1 and C2, each with different test

conditions, measured during the period close the freezing temperatures when water temperatures were < 1.5 °C. The average cooling rate for all experiments was 0.052 °C/min. Because cooling was linear as a function of the − 3 °C coolant temperature difference (the main driving force), no significant changes between the slopes can be seen. One minor divergence was seen when a higher 250 rpm stirring speed resulted in lower cooling rates, 0.047–0.049 °C/min, in three tests out of four. However, one test gave no clear indication of a stirring effect. Therefore, a clear conclusion regarding this effect could not be made.

Even though temperature differences were small, test results showed that freezing point depression (FPD) temperatures were a function of impurity concentration. By comparing FPDs, the different compositions of the leachate samples in barrels were evident. In the series C1 tests, the average conductivity of the raw feed water was 5.31 mS/cm and the FPD temperature was − 0.06 °C (Fig. 4a). In the series C2 tests, conductivity was a higher 6.32 mS/cm and FPD temperature was a lower − 0.10 °C (Fig. 4b). This is likely because of the water sampling procedure in which water was pumped out of the tank in the landfill. The leachate may have been concentrated in layers in the tank.

Between the series C1 and C2 tests, clear undercooling temperature differences were observed as expected. These differences were coincident with the timing of ice seeding. However, no reasonable explanation for how seeding influenced undercooling or the duration of the induction period could be determined. In this study, the induction period was determined as a delay time between ice seeding and the time when freezing point temperature was reached. These times varied between 500 and 1670 s with the series C1 tests and 130 – 500 s with the series C2 tests. The variability is more apparent in series C1, Fig. 4a, where the undercooling (and therefore the induction time too) is strong (~ − 0.4 °C) in two tests and lower in three other tests. The reason might be explained by slow response time of cooling operation and control, or unsuccessful seeding time (with two first series C1 tests). If seed ice is added too soon, it melts and undercooling continues. On the other hand, because wastewater contains many impurities, slight or moderate undercooling can induce spontaneous ice nucleation. In this case, ice seeding may not be needed at all.

Median ice crystal size is difficult to measure. In this study, the ice crystal size was visually observed. Microscopic observation (image analysis) using an Olympus BH2-UMA was also used to support the visual observations (Fig. 5a). No clear differences in ice crystal growth (form, size, quantity) resulting from the different processes were apparent. Seeding at close to − 0.06 °C (practically near to 0 °C) and seeding at − 0.4 °C, formed very irregular and mainly thin plate-shaped ice crystals. The agglomeration of individual ice crystals (forming ice clusters by gathering single crystals together and forming larger crystals) was not detected. Although, this does not exclude the possibility of agglomeration. Shirai et al. [7] discovered that this type of formation had a substantial effect on ice crystal size for longer, one to two hours, residence times. However, Ostwald ripening, when smallest ice crystals melt and larger ice crystals grow further to form bigger crystals, may have possibly taken place - deduced from the crystal size [9,24].

For the most part, the crystals were relatively large, even > 500 µm, as shown in Fig. 5, when compared with previous studies. For instance, Van der Ham et al. [23] and Chivavava et al. [9] each produced smaller than 150 µm ice crystals. Washing the ice did not result in a significant crystal size shrinkage effect either (Fig. 5b). To thoroughly evaluate crystal size distribution or ice crystal size evolution during the freezing process, an on-line measurement should have been used. It was also not possible to evaluate the effects on nucleation or ice crystal size of collision, the shear stresses of large crystals, stirring tip speed, or local micro mixing of the scraper [17].

4.2. Separation efficiency

The landfill leachate, used as feed water in this study, proved to contain many compounds in high concentrations at the time of collection. The leachates were similar to high-strength untreated domestic wastewaters, particularly in chemical oxygen demand (COD) and total nitrogen (TN) concentrations [25]. The COD/TOC ratio was 4.6–5.3, which indicates that the wastewater contained a lot of organics other than carbon, e.g., nitrogen, phosphorus, or sulphur as well. However, the total phosphorus concentration was low (1.1 – 1.6 mg/L).

On the contrary, the high electrical conductivities measured, 5.3–6.3 mS/cm, indicate high ionic inorganics content. The density of the landfill leachate was close to that of water. The calculated average results of the analyzed water quality indicators for both test series (and containers) are presented in Table 2. Even though the leachate was collected at the same time, the water content differed in the different storage containers used in the test series. The tested water was slightly alkaline, being very suitable for device structure materials. The detailed, relevant results of measurements and analyses in this study for wastewater, washed ice, and unwashed ice samples are shown in the supplementary material (Supplementary material, Table A.1–A.4). Several analyzed elements are not presented in the results due to the very low concentrations under the detection limits of the method used.

The separation (purification) efficiency of the freeze crystallization can be evaluated by determining the impurity reduction due to the process. Conversely, the effective distribution coefficient K indicates the relative part of the impurity quantity remaining in the ice and is calculated by $K = C_i/C_w$, where C_i is the concentration (mg/L) or other measuring value of the substance or the element in melted ice, and C_w is the concentration of the substance or the element in the initial wastewater. Fig. 6 shows the calculated average effective distribution coefficient K results for water quality measures COD, EC, color, and turbidity as well as carbon TOC, TC, IC, and nitrogen TN content, for both washed ice and unwashed ice samples. The purification was found to be more efficient with the series C2 tests (Fig. 6b), which were conducted with a higher degree of undercooling. The washed ice of series C1 showed an average efficiency for all these quality measures of 0.110 (89.0%), whereas the series C2 showed 0.027 (97.3%). The variation in the efficiency results between the different tests was also more extensive with the series C1 tests (A to E) than with the series C2 tests (F to J). The freeze separation process was better balanced when a slight undercooling affected the nucleation.

Ice washing was found to be of critical importance in ice sample handling - as expected based on the previous research by Lemmer et al. [5], Randall et al. [10,15], and Chang et al. [8]. Even though this study did no focus on the washing procedure as such, Fig. 6a and b clearly show the difference between washed and unwashed ice in effective distribution coefficient results. Without washing, the degree of $K = 0.50$ (50%) in efficiency is hardly achievable. Binding conclusions about the ice purity produced cannot be made based only on analyzing the results of the unwashed ice samples. Even though the impurities seemed to be very unequally distributed on the ice crystal surfaces, the effective separation distribution K will be leveled out by washing. Unfortunately, using tap water in ice washing resulted in copper Cu and zinc Zn contamination. The unexpectedly poor water quality from the used tap was only revealed after analysis (Supplementary material, Table A5) and the affected results were excluded. Furthermore, silver Ag, bismuth Bi, and lead Pb contamination occurred as well. However, these elements were present in such low concentrations that they are not covered in the results. The influence of ice polishing (e.g., washing) on the complete purification efficiency evaluation with wastewater would be worth detailed experimental research in the future. In terms of economy, alternative post-treatment methods other than ice washing should be considered as well. For instance, Erlbeck et al. [26] reported recently favorable results in the separation performance of salt solutions treated by a newly designed crystallizer. The process plant incorporates a screw conveyor for ice pressing which brings about the efficient separation of pure ice from an ice/brine mixture.

The separation and purification results for the various elements in

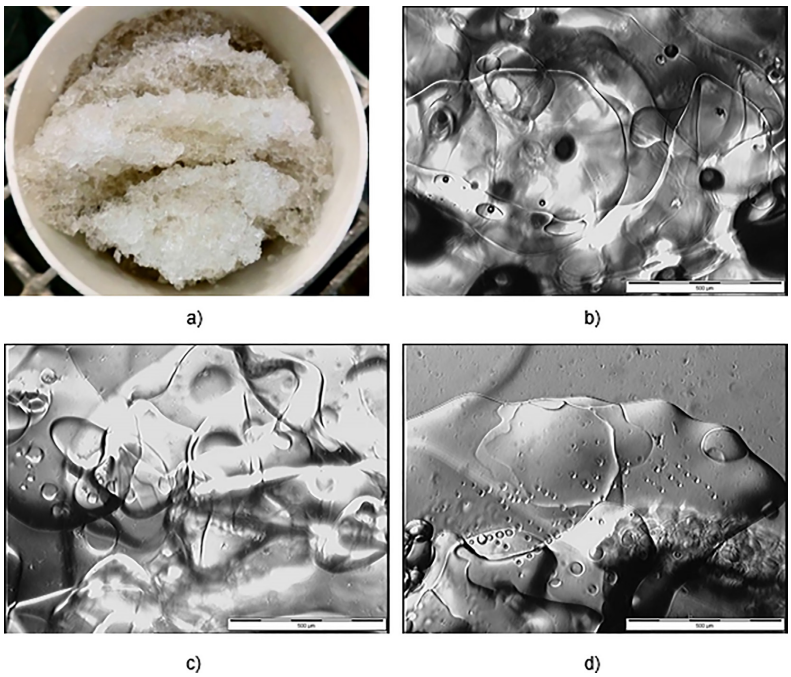

Fig. 5. The characteristics of formed ice crystals; (a) unwashed ice crystals from the series C2 tests formed with an agitator speed of 7 rpm, a scraper speed of 150 rpm, and an ice seeding temperature of −0.4 °C; and the microscopic characteristics of; (b) washed ice after 60 min; (c) unwashed ice after 30 min; and (d) unwashed ice after 60 min residence time (bar scale 500 µm in the picture, magnification 5x).

Table 2
Analyzed results of the initial wastewater (landfill leachate) content averagely in test series.

Test	pH	COD	Conductivity	Color	Turbidity	TOC	TN	TP
		(mg/L)	(mS/cm)	(PtCo)	(FTU)	(mg C/L)	(mg N/L)	(mg P/L)
Series C1	8.31	811	5.313	1140	278	154	169	1.60
Series C2	7.97	829	6.323	1616	313	180	224	1.10

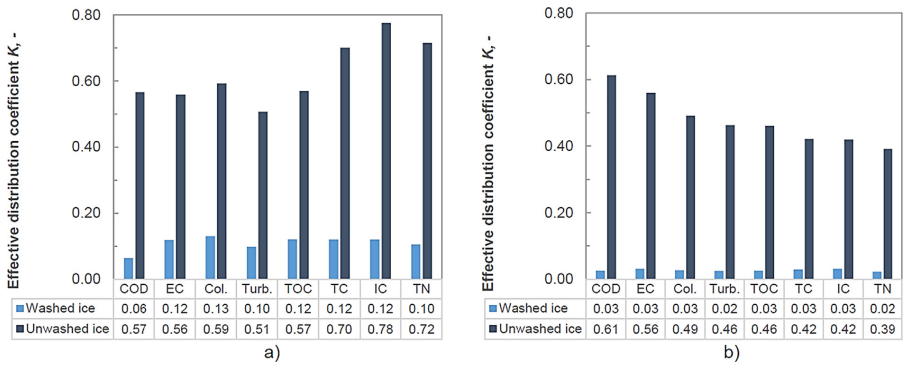

Fig. 6. Average results of test series a) C1 and b) C2 – Determined effective distribution efficiency *K* of chemical oxygen demand COD, electric conductivity EC, color (Col.), turbidity (Turb.), total organic carbon TOC, total carbon TC, inorganic carbon IC, and total nitrogen TN.

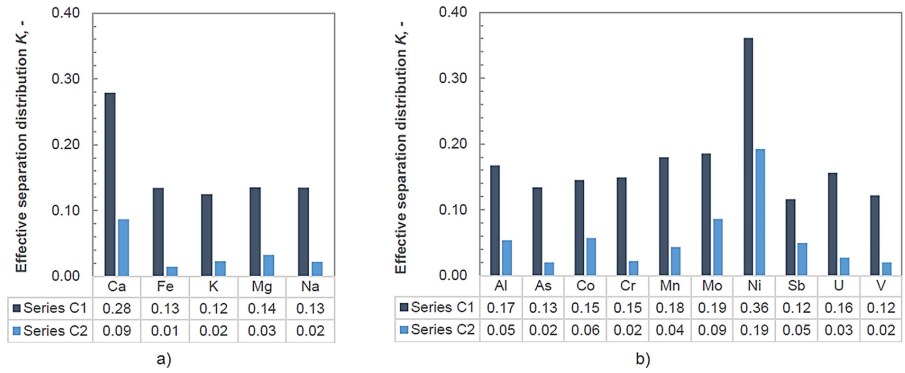

Fig. 7. Average results of test series showing the effective distribution efficiency *K* of various elements with (a) higher concentrations (> 1.5 mg/ L to 690 mg/L) and (b) lower concentrations (< 0.5 mg/L) in initial wastewater.

the leachates are in line with the water quality results presented above. Because the elemental concentrations of the wastewaters studied vary greatly, from ppb to ppm, the effective separation distribution *K* results are presented in two different figures (Fig. 7a and b) sorted by a concentration scale and shown here only with washed ice samples. The average *K* values of all elements were 0.168 (83%) for series C1 and a much better 0.050 (95%) for series C2. However, there was no significant difference in the average *K* values for the elements between the high and low concentrations - the efficiencies were equivalent. The *K* values of calcium Ca and nickel Ni were quite different (almost double) from the average *K* values. This is probably the result of contamination during analysis or from the steel structures and not a function of freezing process characteristics. Of the analyzed elements, the sodium Na (> 600 mg/L) and potassium K (< 210 mg/L) concentrations were found to be highest in the initial wastewaters. Regardless, the average purification efficiencies were high in series C2: 97.8% and 97.7%, respectively. In conclusion, the freeze crystallizer separated all analyzed impurities of landfill leachate with fairly equal efficiency in similar process conditions.

Even though the timing of ice seeding by slightly undercooling was found to have an effect on separation efficiency, the other process parameters did not have an obvious effect. The agitator rotational speed (150, 200, or 250 rpm), scraper rotational speed (7 or 10 rpm) or a combination of these did not influence separation efficiency. The effect of the operating (i.e., freezing) temperature was not studied here, because the temperature used here was selected based on previous tests with model solutions to ensure controlled ice formation. Freezing in different temperatures and varying the other parameters across a broader should also be investigated to find limits and limitations for the freeze crystallizer. The optimization of operation temperature and its influence on purification efficiency should also be more closely examined. The −3 °C operation temperature is relatively low. It represents the maximal nominal coolant temperature. Better total energy efficiency is likely achievable at higher freezing temperatures, however, ice production would decrease.

It is difficult to compare the purification efficiencies seen in the study with those achieved in previous large-scale freeze crystallization research studies, because of the significant variations in experiment setups, used water quality (seawater, industrial and model water etc.), reactor size, and the undefined tip speeds of stirring. Moreover, previous studies concern mostly eutectic freeze crystallization, and the analyses of impurities focused on salt recovery [12,13]. Previous laboratory-scale studies have mostly resulted in similar purification efficiencies (> 95%). For instance, Yin et al. [3] reported a 70–90% COD removal efficiency with highly concentrated pharmaceutical industrial wastewater in a 500 mL suspension crystallizer with an optimal 300 rpm stirring speed at −6 °C. Eutectic freeze crystallization using a cascading concentrating process for textile wastewater treatment was investigated by Randall et al. [15] with a 1.5 L jacketed crystallizer, a 350 rpm stirring speed, and a 5 °C temperature difference (ΔT). The 98% ice purity was determined based on sodium concentration and color.

The legislation and norms for wastewater treatment and the requirements for sufficient purification efficiencies are complicated and vary globally. In Finland, for instance, the environmental impact of a wastewater treatment plant is assessed site-specifically based on the Environmental Protection Act and the Water Act. This means that every plant has a specific environmental permit defining the limits for emissions. These limits are more often significantly stricter than is regulated by the direct law (Government decree on Urban Waste Water Treatment 888/2006, Ministry of Environment, Finland), and they will become even more stringent in the future. For that reason, it is difficult to determine if the purification efficiencies achieved via freeze crystallization in this study will be sufficient to satisfy future purification requirements. However, purification efficiencies of over 95% for wastewaters with a great variety of impurities have now been achieved using a novel apparatus. Further development of the equipment and the processes should provide even higher purity levels.

5. Conclusions

This study introduced a wastewater purification process based on the freeze crystallization. The prototype crystallizer employs a 120 L jacketed vessel equipped with an agitator and an ice scraper. The design of the freeze crystallizer and the up scaling of a freeze separation process proved successful. An average ice mass production of 96 kg/(h·m^3) was achieved using fixed process conditions and the residence time of 60 min. Most of the ice formed in suspension in the water since ice scale began to form on the cooling wall surface only after 50 min freezing time. The formed ice crystals were relatively large, ~500 µm, which can be seen as an indicator of ice crystal ripening during the process.

The wastewater treatment device purified highly concentrated landfill leachate with appropriate efficiency. With ice washing, average purification efficiencies were > 95 – 97%. Without washing, efficiencies of barely 50% were attained. The purification efficiency analyses considered organics (COD, TOC, TN), inorganics (IC, conductivity), and elements such as heavy metals. For the future research, the development and testing of the continuous freeze crystallization

process to improve energy efficiency with suitable sub-processes, such as precooling, cold heat recovery, and recycling, as well as the study and development of ice crystal polishing techniques could be considered. Also, testing the crystallizer as an EFC process with salt and nutrient recovery would be of interest.

Declaration of Competing Interest

The authors declare that they have no known competing financial interests or personal relationships that could have appeared to influence the work reported in this paper.

Acknowledgements

The research was funded by the Business Finland, project no. 4591/31/2016. The authors wish to thank Heidi Oksman-Takalo and Sami Huotari, Etelä-Karjalan Jätehuolto Oy, and Hannu Pesonen, Lakeuden Kylmätekniikka Oy, for their collaboration. The authors wish to acknowledge CSC-IT Center for Science, Finland, for providing computational resources. The contributions of Tuomas Nevalainen, Mikko Huhtanen, Toni Kangasmäki and Scott Semken as well as the earlier contribution of Mehdi Hasan during the project are greatly acknowledged.

Appendix A. Supplementary material

Supplementary data to this article can be found online at https://doi.org/10.1016/j.seppur.2019.116271.

References

[1] M. Hasan, R. Filimonov, J. Chivavava, J. Sorvari, M. Louhi-Kultanen, A. Lewis, Ice growth on the cooling surface in a jacketed and stirred eutectic freeze crystallizer of aqueous Na2SO4 solutions, Sep. Purif. Technol. 175 (2017) 512–526, https://doi.org/10.1016/j.seppur.2016.10.014.

[2] L. Erlbeck, M. Rädle, R. Nessel, F. Illner, W. Müller, K. Rudolph, T. Kunz, F.-J. Methner, Investigation of the depletion of ions through freeze desalination, Desalination 407 (2017) 93–102, https://doi.org/10.1016/j.desal.2016.12.009.

[3] Y. Yin, Y. Yang, M. de Lourdes Mendoza, S. Zhai, W.L. Feng, Y. Wang, M. Gu, L. Cai, L. Zhang, Progressive freezing and suspension crystallization methods for tetrahydrofuran recovery from Grignard reagent wastewater, J. Clean. Prod. 144 (2017) 180–186, https://doi.org/10.1016/j.jclepro.2017.01.012.

[4] P.M. Williams, M. Ahmad, B.S. Connolly, D.L. Oatley-Radcliffe, Technology for freeze concentration in the desalination industry, Desalination 356 (2015) 314–327, https://doi.org/10.1016/j.desal.2014.10.023.

[5] S. Lemmer, R. Klomp, R. Ruemekorf, R. Scholz, Preconcentration of wastewater through the Niro freeze concentration process, Chem. Eng. Technol. 24 (5) (2001) 485–488, https://doi.org/10.1002/1521-4125(200105)24:5<485::AID-CEAT485>3.0.CO;2-H.

[6] A. Bogdan, J. Molina, Physical chemistry of the freezing process of atmospheric aqueous drops, J. Phys. Chem. A 121 (16) (2017) 3109–3116, https://doi.org/10.1021/acs.jpca.7b02571.

[7] Y. Shirai, T. Sugimoto, M. Hashimoto, K. Nakanishi, R. Matsuno, Mechanism of ice growth in a batch crystallizer with an external cooler for freeze concentration, Agr. Biol. Chem. 51 (9) (1987) 2359–2366, https://doi.org/10.1080/00021369.1987.10868410.

[8] J. Chang, J. Zuo, K.-J. Lu, T.-S. Chung, Freeze desalination of seawater using LNG cold energy, Water Res. 102 (2016) 282–293, https://doi.org/10.1016/j.watres.2016.06.046.

[9] J. Chivavava, M. Rodriguez Pascual, A.E. Lewis, Effect of operating conditions on ice characteristics in continuous eutectic freeze crystallization, Chem. Eng. Technol. 37 (8) (2014) 1314–1320, https://doi.org/10.1002/ceat.201400094.

[10] D.G. Randall, J. Nathoo, A.E. Lewis, A case study for treating a reverse osmosis brine using Eutectic Freeze Crystallization- approaching a zero waste process, Desalination 266 (1–3) (2011) 256–262, https://doi.org/10.1016/j.desal.2010.08.034.

[11] D.G. Randall, J. Nathoo, A succinct review of the treatment of Reverse Osmosis brines using Freeze Crystallization, J. Water Proc. Eng. 8 (2015) 186–194, https://doi.org/10.1016/j.jwpe.2015.10.005.

[12] M. Rodriguez Pascual, F.E. Genceli, D.O. Trambitas, H. Evers, J. Van Spronsen, G.J. Witkamp, A novel scraped cooled wall crystallizer: Recovery of sodium carbonate and ice from an industrial aqueous solution by eutectic freeze crystallization, Chem. Eng. Res. Des. 88 (9) (2010) 1252–1258, https://doi.org/10.1016/j.cherd.2009.07.015.

[13] J. Van Spronsen, M. Rodriguez Pascual, F.E. Genceli, D.O. Trambitas, H. Evers, G.J. Witkamp, Eutectic freeze crystallization from the ternary Na2CO3–NaHCO3–H2O system: A novel scraped wall crystallizer for the recovery of soda from an industrial aqueous stream, Chem. Eng. Res. Des. 88 (9) (2010) 1259–1263, https://doi.org/10.1016/j.cherd.2009.09.012.

[14] W. Feng, Y. Yin, M. De Lourdes Mendoza, L. Wang, P. Chen, Y. Liu, L. Cai, L. Zhang, Oil recovery from waste cutting fluid via the combination of suspension crystallization and freeze-thaw processes, J. Clean. Prod. 172 (2018) 481–487, https://doi.org/10.1016/j.jclepro.2017.09.281.

[15] D.G. Randall, C. Zinn, A.E. Lewis, Treatment of textile wastewaters using Eutectic Freeze Crystallization, Water Sci. Technol. 70 (4) (2014) 736–741, https://doi.org/10.2166/wst.2014.289.

[16] O. Lorain, P. Thiebaud, E. Badorc, Y. Aurelle, Potential of freezing in wastewater treatment: soluble pollutant applications, Water Res. 35 (2) (2001) 541–547, https://doi.org/10.1016/S0043-1354(00)00287-6.

[17] A. Mersmann, Crystallization Technology Handbook, second ed., Dekker, New York, 2001.

[18] J.R. Rumble (Ed.), CRC Handbook of Chemistry and Physics, 99th ed., CRC Press/Taylor & Francis, Boca Raton, FL, Internet Version, 2018.

[19] M. John, M. Suominen, O.-V. Sormunen, M. Hasan, E. Kurvinen, P. Kujala, A. Mikkola, M. Louhi-Kultanen, Purity and mechanical strength of naturally frozen ice in wastewater basins, Water Res. 145 (2018) 418–428, https://doi.org/10.1016/j.watres.2018.08.063.

[20] M. John, M. Suominen, E. Kurvinen, O.-V. Sormunen, M. Hasan, P. Kujala, A. Mikkola, M. Louhi-Kultanen, Separation efficiency and ice strength properties in simulated natural freezing of aqueous solutions, Cold Reg. Sci. Technol. 158 (2019) 18–29, https://doi.org/10.1016/j.coldregions.2018.11.006.

[21] S. Palosaari, M. Louhi-Kultanen, Z. Sha, Industrial Crystallization, in: A.S. Mujumdar (Ed.), Handbook of industrial drying, fourth ed., CRC Press Inc., 2014, pp. 1271–1290.

[22] W.A. Nixon, T.J. Gawronski, A.E. Whelan, Development of a model for the ice scraping process, IIHR Technical Report No. 383, Iowa Inst. Hydraulic Res. (1996).

[23] F. Van der Ham, M.M. Seckler, G.J. Witkamp, Eutectic freeze crystallization in a new apparatus: the cooled disk column crystallizer, Chem. Eng. Process.: Process Intensif. 43 (2) (2004) 161–167, https://doi.org/10.1016/S0255-2701(03)00018-7.

[24] A.S. Myerson, Handbook of industrial crystallization, second ed., Butterworth Heinemann, Boston (MA), 2002.

[25] G. Tchobanoglous, F.L. Burton, D.H. Stensel, Wastewater engineering: Treatment and reuse, fourth ed., McGraw-Hill, New York, 2003.

[26] L. Erlbeck, D. Wössner, K. Schlachter, T. Kunz, F.-J. Methner, M. Rädle, Investigation of a novel scraped surface crystallizer with included ice-pressing section as new purification technology, Sep. Purif. Technol. 228 (2019) 115748, https://doi.org/10.1016/j.seppur.2019.115748.

ACTA UNIVERSITATIS LAPPEENRANTAENSIS

868. SAVCHENKO, DMITRII. Testing microservice applications. 2019. Diss.

869. KARHU, MIIKKA. On weldability of thick section austenitic stainless steel using laser processes. 2019. Diss.

870. KUPARINEN, KATJA. Transforming the chemical pulp industry – From an emitter to a source of negative CO2 emissions. 2019. Diss.

871. HUJALA, ELINA. Quantification of large steam bubble oscillations and chugging using image analysis. 2019. Diss.

872. ZHIDCHENKO, VICTOR. Methods for lifecycle support of hydraulically actuated mobile working machines using IoT and digital twin concepts. 2019. Diss.

873. EGOROV, DMITRY. Ferrite permanent magnet hysteresis loss in rotating electrical machinery. 2019. Diss.

874. PALMER, CAROLIN. Psychological aspects of entrepreneurship – How personality and cognitive abilities influence leadership. 2019. Diss.

875. TALÁSEK, TOMÁS. The linguistic approximation of fuzzy models outputs. 2019. Diss.

876. LAHDENPERÄ, ESKO. Mass transfer modeling in slow-release dissolution and in reactive extraction using experimental verification. 2019. Diss.

877. GRÜNENWALD, STEFAN. High power fiber laser welding of thick section materials - Process performance and weld properties. 2019. Diss.

878. NARAYANAN, ARUN. Renewable-energy-based single and community microgrids integrated with electricity markets. 2019. Diss.

879. JAATINEN, PEKKO. Design and control of a permanent magnet bearingless machine. 2019. Diss.

880. HILTUNEN, JANI. Improving the DC-DC power conversion efficiency in a solid oxide fuel cell system. 2019. Diss.

881. RAHIKAINEN, JARKKO. On the dynamic simulation of coupled multibody and hydraulic systems for real-time applications. 2019. Diss.

882. ALAPERÄ, ILARI. Grid support by battery energy storage system secondary applications. 2019. Diss.

883. TYKKYLÄINEN, SAILA. Growth for the common good? Social enterprises' growth process. 2019. Diss.

884. TUOMISALO, TEEMU. Learning and entrepreneurial opportunity development within a Finnish telecommunication International Venture. 2019. Diss.

885. OYEDEJI, SHOLA. Software sustainability by design. 2019. Diss.

886. HUTTUNEN, MANU. Optimizing the specific energy consumption of vacuum filtration. 2019. Diss.

887. LIIKANEN, MIIA. Identifying the influence of an operational environment on environmental impacts of waste management. 2019. Diss.

888. RANTALA, TERO. Operational level performance measurement in university-industry collaboration. 2019. Diss.

889. LAUKKANEN, MINTTU. Sustainable business models for advancing system-level sustainability. 2019. Diss.

890. LOHRMANN, CHRISTOPH. Heuristic similarity- and distance-based supervised feature selection methods. 2019. Diss.

891. ABDULLAH, UMMI. Novel methods for assessing and improving usability of a remote-operated off-road vehicle interface. 2019. Diss.

892. PÖLLÄNEN, ILKKA. The efficiency and damage control of a recovery boiler. 2019. Diss.

893. HEKMATMANESH, AMIN. Investigation of EEG signal processing for rehabilitation robot control. 2019. Diss.

894. HARMOKIVI-SALORANTA, PAULA. Käyttäjät liikuntapalvelujen kehittäjinä - Käyttäjälähtöisessä palveluinnovaatioprosessissa käyttäjien tuottama tieto tutkimuksen kohteena. 2020. Diss.

895. BERGMAN, JUKKA-PEKKA. Managerial cognitive structures, strategy frames, collective strategy frame and their implications for the firms. 2020. Diss.

896. POLUEKTOV, ANTON. Application of software-defined radio for power-line-communication-based monitoring. 2020. Diss.

897. JÄRVISALO, HEIKKI. Applicability of GaN high electron mobility transistors in a high-speed drive system. 2020. Diss.

898. KOPONEN, JOONAS. Energy efficient hydrogen production by water electrolysis. 2020. Diss.

899. MAMELKINA, MARIA. Treatment of mining waters by electrocoagulation. 2020. Diss.

900. AMBAT, INDU. Application of diverse feedstocks for biodiesel production using catalytic technology. 2020. Diss.

901. LAAPIO-RAPI, EMILIA. Sairaanhoitajien rajatun lääkkeenmääräämistoiminnan tuottavuuden, tehokkuuden ja kustannusvaikuttavuuden arviointi perusterveydenhuollon avohoidon palveluprosessissa. 2020. Diss.

902. DI, CHONG. Modeling and analysis of a high-speed solid-rotor induction machine. 2020. Diss.

903. AROLA, KIMMO. Enhanced micropollutant removal and nutrient recovery in municipal wastewater treatment. 2020. Diss.

904. RAHIMPOUR GOLROUDBARY, SAEED. Sustainable recycling of critical materials. 2020. Diss.

905. BURGOS CASTILLO, RUTELY CONCEPCION. Fenton chemistry beyond remediating wastewater and producing cleaner water. 2020. Diss.

LUT University

ISBN 978-952-335-515-6
ISBN 978-952-335-516-3 (PDF)
ISSN-L 1456-4491
ISSN 1456-4491
Lappeenranta 2020